INVESTIGATION OF SLURRY EROSION IN PIPELINE MATERIALS

A Dissertation

submitted in partial fulfillment of the requirements for the award of degree of

Master of Engineering

In

Thermal Engineering

Submitted by

PRABHJOT SINGH

(ROLL NO. 801283029)

Under the guidance of

MR. SATISH KUMAR

(ASSISTANT PROFESSOR)

MECHANICAL ENGINEERING DEPARTMENT

THAPAR UNIVERSITY, PATIALA – 147004

JULY 2014

CERTIFICATE

I hereby declare that the thesis entitled "**Investigation of Slurry Erosion in Pipeline Materials**" is an authentic record of my study carried out as requirements for the award of the degree of **Master of Engineering** in **Thermal Engineering** at **Thapar University, Patiala** under the supervision of **Mr. Satish Kumar**, Assistant Professor, Mechanical Engineering Department, Thapar University, Patiala during July, 2012 to July, 2014. The matter embodied in this report has not been submitted in partial or full to any other university or institute for the award of any degree.

Date: 18 July 2014

Prabhjot Singh
(Roll No. - 801283029)

It is certified that the above statement made by the student is correct to the best of my/our knowledge and belief.

Mr. Satish Kumar
Mechanical Engineering Department
Thapar University, Patiala - 147004

Countersigned by

Dr. Ajay Batish
Professor & Head
Mechanical Engineering Department
Thapar University, Patiala - 147004

Dr. S.K. Mohapatra
Dean of Academic Affairs
Thapar University, Patiala - 147004

ACKNOWLEDGEMENT

First of all, I would like to express my gratitude to **Mr Satish Kumar**, Assistant Professor, Mechanical Engineering Department, Thapar University, Patiala for his patience guidance and support throughout this report. I am truly very fortunate to have the opportunity to work with him. I found his guidance to be extremely valuable.

I also express my special thanks to **Dr. Ajay Batish,** Professor and Head, Mechanical Engineering Department, **Dr. S.K Mohapatra,** Sr. Professor, Mechanical Engineering Department, and Dean Academic Affair, Thapar University Patiala for providing me opportunity to conduct this work and bring it out in present form.

Last but not the least; I want to convey my heartiest gratitude to my parents and my friends for their immeasurable love, support and encouragement.

Prabhjot Singh

Prabhjot Singh

ABSTRACT

Erosion wear is very serious problem in slurry pipelines specifically in thermal power plants. Wear of the pipelines results in loss of capital money due to failure and frequent replacement of pipelines. According to FAU-2012, 88 thermal power plants in India with installed capacity of 80458MW, consume 407.61 million tonne of coal (lignite based) every year. Huge amount of bottom ash is produced every year in these thermal power plants and this is transported to ash ponds mainly through mild steel piping system. Literature survey of various researchers shows the high erosion wear of mild steel pipeline material with bottom ash slurry.

In the view of above, author is motivated to study erosion wear behavior of different general purpose materials and coatings. Erosion wear of WC-12Co and Ni-20Cr_2O3 coated and uncoated Mild steel, SS 304 and SS 202 materials is evaluated by using slurry pot tester with bottom ash slurry. High velocity oxy-fuel process is used for the coating. Erosion wear at four different speeds 500rpm, 800rpm, 1100rpm and 1400rpm is evaluated at 25% and 45% slurry concentrations with 90min and 180min experimental study. Erosion wear increases with increase in slurry concentration and speed, it is noticed that at low speeds (500rpm to 800rpm) rate of erosion wear is more as compared to higher speeds(1100rpm to 1400rpm). The speed exponent and concentration exponent are also calculated and are in good agreement with previous research works, experimental results are also investigated with taguchi approach so as to evaluate the influence of speed, concentration and time parameters on the erosion wear of the materials and it is found that influence (percentage) of speed is more on erosion wear and is followed by time and concentration parameters.

CONTENTS

LIST OF FIGURES

LIST OF TABLES

NOMENCLEATURE

a.u.	Arbitrary unit
C_w	Concentration by weight
C.F	Correction factor
d_e	Erodent particle diameter
d_{50}	Median particle diameter, (μm)
E_w	Erosion wear
F	Variance ratio
g/min	Gram per minute
H_v	Vickers microhardness
LPM	Liter per minute
L/cm^2	Liter per centimeter square
m_e	Mass of erodent striking per unit time with target material
MSD	Mean square deviation
N_{ep}	Number of erodent particles striking per unit time with target material
P	Percentage contribution
RPM	Revolutions per minute
R_a	Arithmetic mean roughness value
S_p	Pure sum of squares
S/N_{ratio}	Signal to noise ratio
S	Sum of squares
ρ_e	Density of erodent particles
V	Speed (rpm)

CHAPTER 1

INTRODUCTION

Solid particle erosion is a major concern in the coal ash slurry transport through pipelines. Entrained solids such as sand particles in the coal ash slurry impinge the inside surfaces of pump, pipes, fittings, valves and other system components, causing erosion-abrasion wear and eventual failure of these devices. Most of the fluid/slurry transport systems contain useful components that are susceptible to erosion/failure by solid particles suspended in the slurry. This phenomenon can be extremely expensive for the life of pipelines or even may require frequent replacement of components due to the failure of the system.

1.1 WEAR

There are several precise ways for the description of wear. However, for engineering purposes the following method of wear description may contain the essential elements:

- Wear is damage to a particular surface due to the contact of it with another substance/particle as a result of relative motion with respect to another substance/particle. One key point is that it is not merely loss of material from the surface it can be a serious damage However, loss of material from the surface is definitely one way in which that particular surface can experience wear.

- Wear is a system phenomenon or characteristic; wear is not a property of materials. in different wear situations/atmospheres materials wear differently, and also different materials may wear out differently in the same situation/atmosphere. Therefore, it is necessary to characterize and investigate a number of different parameters responsible for wear, and not simply the worn out surface.

1.2 TYPES OF WEAR

There are several categories of wear but mainly wear is generally classified into following main categories:

- Abrasion Wear
- Adhesion Wear
- Corrosion Wear
- Erosion Wear
- Fatigue Wear

The various types of wear, with recognised symptoms and appearance of the worn out surfaces are given below.

Types of Wear	Symptoms	Appearance of the worn out surface
Abrasive	cut out by abrasive particles presence of clean furrows	Groves
Adhesive	Metal transfer from surface is a prime Symptom	Torn out, catering and seizure surfaces
Corrosion	Presence of metal corrosion constituents	Depressions or rough pits
Erosion	**Presence of hard abrasive particles in the fast moving slurry/fluid and short abrasion furrows**	**Troughs and waves**
Fatigue	Presence of surface and sub surface cracks in mating surfaces accompanied by pits and spalls	Sharp and short angular edges around pits

Table 1.1: types of wear, wear symptoms and appearance of worn-out surfaces

1.2.1 Abrasive Wear - Abrasive wear occurs when a hard material flows over the surface of relatively less hard material and cause the removal of the material from the less hard surface and leaving hard particles of debris between the two mating surfaces, mainly this type of wear occurs under two conditions: Three body wear and two body wear. Following are the further categories of the abrasion wear.

- Gouging

- Polishing
- Scratching

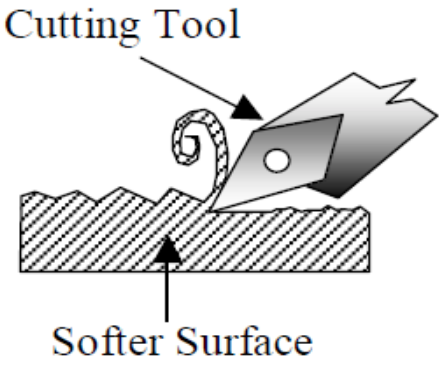

Fig. 1.1: Abrasive wear mechanism

1.2.2 Adhesive Wear - it is often known as galling or scuffing, in this type of wear interfacial adhesive junctions lock gets developed together as under high pressure, two mating surfaces slide across each other. Between two mating surfaces in the absence of required lubricants, asperities gets cold-weld together or else may the junctions shear off each other and form new junctions gets formed. This wear mechanism is very harmful that not only destroys the mating sliding surfaces, but also responsible for the generation of wear particles which cause further cavitations and may lead to the failure of the mating components.

- Galling
- Fretting
- Seizure

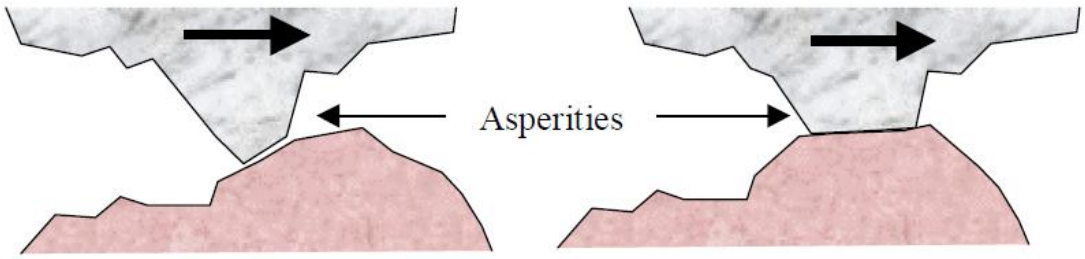

Fig. 1.2: Adhesive wear mechanism

1.2.3 Corrosive Wear - Corrosive wear is greatly influenced by the atmospheric conditions of a particular surface that is subjected to wear, the strong dynamic interaction

between the worn-out surface environment and surfaces play a very significant role, whereas other types of wear that is fatigue, adhesion and abrasion can be explained in terms of deformation properties and stress interactions mating surfaces.

1.2.4 Fatigue Wear – Fatigue wear is caused by the periodical repetitions of the particular level of stresses on the worn out component. All frequently repeating stresses in a sliding or rolling contact can be responsible for fatigue failure. These effects are mainly based on the stresses and their actions in or below the worn out surfaces, without the direct actual physical contact between surfaces under consideration.

- Brinelling
- Impact
- Pitting
- Spalling

1.2.5 Erosion Wear - it defined as the process of metal removal from a particular surface under consideration due to impingement of solid erodents on a surface. These erodents are generally in a fluid, such as in the form of flowing slurry. Erosive wearing action caused by sand particles and grit in high velocity flowing air streams would be one example, another would be the erosion wear caused in slurry handling pipelines slurries.

1.3 MECHANISM OF EROSION WEAR

In erosive wear problems, erodent particles that are generally entrained in a fast moving fluid can strong impact the worn-out surface. Due to the high kinetic energy of the flowing erodent particles they put heavy impact on the target surface during strike with it and cause damage of the target surface any cause removal of the small amount of material from target surface. There are several types of erosion wear mechanisms depending upon the nature of erodent material and target surface and nature of relative motion between then, main classification of erosion wear is given below:

- Extrusion and forging
- Ploughing

- Subsurface deformation and cracking

1.4 TYPES OF EROSION WEAR

Various types of erosion wear generally grouped into following categories based on the flowing medium:

- **Cavitation erosion:** it is the surface wear under consideration due to generation and implosive collapse of gas bubbles in the flowing slurry. For example, caviation erosion in slurry handling centrifugal pumps.
- **Jet erosion:** Due to the impact of high velocity flowing fluid, high kinetic energy and momentum is stored in the high velocity fluid jet, which when put heavy impact on a stationary solid body cause the erosion of solid body.
- **Liquid drop erosion:** it is surface wear caused by the impingement of liquid drops. For example, due to the presence of condensate droplets the wear of centrifugal gas compressor blades.
- **Particle erosion:** it is the surface wear carried out by the impingement of solid particles carried by a fluid or gas. For example, helicopter blade leading edges erosion in dusty environments.
- **Slurry erosion:** It is the erosion wear caused by flow of micro level erodent particles over the surface with high speed and generally with high concentration, which causes the loss of material from the surface of target material. For example erosion of pipelines or centrifugal pumps due to slurry flows.

1.5 PARAMETERS AFFECTING EROSION WEAR

The various individual factors that mainly influence erosion wear are discussed below. Erosion wear is generally influenced by the nature of eroding surface, nature of erodent materials and the various parameters of the flowing slurry, influence of different parameters is different on the erosion wear of the target materials.

I. Abrasive/Erodent Properties:

- Concentration of slurry
- Erodent fracture properties
- Hardness of erodent
- Particle size
- Particle shape
- Yield strength

II. Contact Conditions:

- Impact/Force level
- Impact/impingement angle
- pH
- Sliding/rolling
- Speed
- Temperature
- Wet/dry

III. Wear/Target Material Properties:

- Ductility
- Corrosion resistance
- Elastic modulus
- Fracture toughness
- Hardness
- Microstructure
- Toughness
- Work-hardening characteristics
- Yield strength

1.6 EROSION TEST RIGS

Large numbers of different erosion test gigs are used by different researchers, every erosion test rig have different features which affect the erosion of the target materials in the similar way. The material removal mechanisms vary due to field conditions and therefore various types of test rigs are developed by the different researchers, an attempt has been made to discuss different type of test rigs according to their features as given below:

- **Concentric cylindrical test rig:** This device can be used when the difference in density of liquid and solid particles is less as the particles may settle during the wear test. Two concentric cylinders are used to find out erosion.

- **Coriolis erosion tester:** This type of apparatus is used to evaluate erosion wear resistance on different target materials under low interaction intensity conditions that is at low normal velocity impact and low impingement angle.

- **Falling jet test apparatus:** Rotation of wear specimens is made in a vacuum chamber and due to gravity effect a jet of solid-liquid mixture falls on the target specimen. The vector additions of rotating speed of target specimen and jet fall velocity are used for the calculation of velocity and impact angle of jet. The spreading effect of jet is minimized by the presence of partial vacuum in the specimen chamber, which mostly occurs in jet impingement tester. However, use of the falling jet test rig is limited by the difficulty of maintaining the partial vacuum in the specimen chamber.

- **Jet impingement tester:** This apparatus consists of a jet submergence tank, adjustable head tank and a jet tube, a flat/circular target specimen is subjected to a high velocity jet of solid-liquid (slurry) mixture. The jet can be injected at the target specimen at different impact angles ranging from 0 to 90^0. Nozzle is used in this type of test rig to inject the jet on the target surface, along with pump arrangement.

- **Jet-in-slit apparatus:** For evaluating the slurry erosion properties of different type of coating and substrate materials jet-in-slit erosion tester is generally used. This test rig consists of transparent tank with two compartments; a upper one of bigger diameter/size to store liquid and a lower one which is smaller in diameter/size to store concentrated, pump is used for circulating the water into test section which is contained by the large diameter, test specimens are contained by test section which are subjected to uniform upward flow and in small diameter tank for the set up the fluidized bed remaining water is utilized. The slurry is injected into the target specimens by the nozzle and thereafter, the slurry is radially exhausted through the slit between the guide plate and target specimen.

The injecting slurry concentration can be easily regulated by changing the distributor for altering the liquid flow rate.

- **Pot tester:** slurry pot tester consists of a slurry carrying pot in which a already prepared slurry can be circulated. It is used for the testing of erosion resistance of target specimens with respect to different concentration and speed values. In the pot tester, the target specimens are fastened to a vertical rotating shaft, the rotating speed of vertical shaft can be easily altered and variations can be made in the slurry concentrations and hence thereby wear rates can be obtained at different operating conditions.

1.7 IMPACT OF SLURRY EROSION ON PIPELINE SYSTEMS

In India ash slurry is transporting at very low concentration and solid suspensions are heterogeneous, due to impact of solid particles striking on the wall of piping materials, life of piping system gets reduced. Erosion wear of slurry pipelines is recognised as a serious problem in thermal power plants in India.

The projections made by Planning Commission as well as Ministry of Power up to 2031-32 indicate that 2/3rd of power generation in the country would continue to depend on coal (FAU -2013) and Below are the facts of data received from 88 (Eighty eight) coal/ lignite based thermal power stations of various power utilities in the country during the year 2010-2012. (FAU - 2012)

- Total installed capacity: 80458 MW
- Coal consumed: 407.61 million-tonne

According to technical data obtained from M. P. Super thermal power plant, Adhinic power and natural resources limited, padampur, Jharkhand India. Estimated coal consumption per annum for 540MW unit production is 2.75 million tonne and bottom ash production is 0.25 million tonne. Which shows bottom ash content is 9.091%, on the bases of this total bottom ash produced in 88 plants is 37.056 million tonne.

This huge amount of bottom ash is generally conveyed by making slurry through piping system. Automatic ash handling systems developed as the size of coal-fired boilers increased beyond the sizes permitting manual handling of the quantity of ash. To remove ash from the

boiler vicinity to a remote disposal location, conveying systems utilizing pipe offered the greatest flexibility for routing.

Bottom ash particles are highly erodent causing the failure of pipes due to excessive erosion. Generally piping material used for slurry transportation is of ductile nature, and heterogeneous slurry flow inside the pipes exert great impact on the inner walls of the pipe, which leads to the erosion of pipe material continually until the failure of the piping system. The costs of repair of erosion wear damage caused by solid erodent particle impingement from ash slurry transportation and other solid particle-laden liquids in slurry pipelines can be extremely high. Therefore regular monitoring of the slurry pipeline wall thickness and other caring attempts are required to sustain the life of pipelines.

A proper understanding of the erosion wears mechanism in slurry pipelines is the demand of slurry transportation design system. Wear is the progressive mass loss of pipe material from a surface mainly due to erosion and/or corrosion. In slurry pipelines corrosion is one kind of chemical phenomenon which strongly depends on amount of oxygen dissolved in the slurry, on the other hand mainly two mechanisms are responsible for the erosion wear of pipelines namely deformation and cutting. Wear rate due to corrosion is generally less as compared to erosion and hence needs more careful attention for the pipeline designing system. Also the mass loss of pipe affects the life span of pipeline system and hence the initial capital cost.

In thermal power plant ash handling pipeline system for the transportation of ash slurry to the ash pond which is generally situated at a distance of 3000m to 8000m from thermal power plant centrifugal pumps. The coal used in thermal power plants of India contains large ash content (upto 50%), quartz which is very hard mineral is sometimes present upto 15% in this ash, which enhances the erosive wear property of ash. Erodent particle erosion is one kind of micromechanical process; this solid particle erosion mechanism is highly complicated due to large number of factors affecting the particle erosion, such as slurry flow rate, concentration of sand, slurry properties, flow regime, ash particle geometry, ash properties, wall material equipment etc.

For ductile pipeline materials, wear is generally caused by fatigue of material surface and localised plastic strain, whereas in case of brittle materials impacting erodent particles can cause chipping of microsize material pieces and pipeline surface cracks. In all cases it is

essential to predict the complex erosion phenomenon in pipelines to prevent pipeline equipment failure, whereas prediction of slurry erosion wear is a very complex situation due to various factors like erodent velocity, distribution of solid particles etc. So it is the very critical need of time to develop new substitutes of pipeline materials or to modify the existing materials so as to reduce the wear of pipes and on the other hand to save large amount of capital money and time, that goes either for the repair or for the replacement of damaged pipelines and pipeline systems because of failure of equipments due to excessive wear.

CHAPTER 2

LITERATURE REVIEW

Slurry erosion wear is serious problem in pipelines, since in India most of the thermal power plants use lignite coal that contains large amount of ash, and pipelines are generally in use to transport this large amount of ash in the form of slurry to the ash ponds that are located at distance of 3000m to 8000m from thermal power plants, so there is excessive wear of pipe lines due to such a huge level transportation of the slurry through pipelines. On the basis of this author is motivated for the study of the erosion wear problems in the pipelines.

Truscott [1975] have studied erosion wear in pipelines and demonstrated the main reasons contributing for the erosion wear in slurry pipelines, and had attempted to find out the range of variation of speed exponent in erosion wear that is contribution of speed factor of flowing slurry on the erosion wear of pipelines, he found velocity exponent may vary from the range of 1 to 3.5, that means lesser is the value of velocity exponent lesser is the influence of velocity on the erosion wear and vice-versa. Also generally for the ductile materials value of speed exponent is more and for brittle materials value of speed exponent is lesser.

Gupta et al. [1995] have studied the influence of particle size, concentration and particle velocity on the erosion wear, based on the experimental results obtained for equalized particulate ash slurries in the slurry pot tester they proposed two correlations, to predict the expected weight loss due to erosion wear of mild steel and brass pipe materials. The comparison between experimental erosion results and predicted erosion and experimental results shows agreement within $\pm 14\%$ for mild steel and $\pm 13.5\%$ for brass, pot tester results for erosion calculation are excellent and new correlations can be successfully developed using results obtained from slurry pot tester, they also concluded that better representative of diameter is the weighted mean diameter for the prediction of wear.

Schwetzke et al. [1999] have analysed phase composition and microstructure of WC-Co and WC-Co-Cr powders and coatings by using X-ray diffraction, optical and scanning electron microscopy. Different High-Velocity Oxygen Fuel (HVOF) spray systems (Top Gun, Jet Kote , DJ 2600 and 2700, JP-5000, Top Gun-K, Diamond Jet (DJ) Standard) were used for

coating and results were compared. Decarburization by the oxidation of WC elements leads to the formation of W2C and free tungsten in the coatings, while the reaction of cobalt or cobalt chromium matrix with the WC leads to a solution of carbide and tungsten in the coating matrix and can be responsible for the formation of mixed carbides The results shows that the these powders exhibit various degrees of phase transformation during the HVOF spray process depending on type of powder, spray parameters and spray system. There is only little effect these on coating properties. Therefore, coatings of high wear resistance and hardness can be produced with all above HVOF spray systems when the suitable spray powder and spray process parameters are chosen.

Stokes et al. [2004] have studied the residual stresses which will build up in thick deposits; these will be significant or can lead to a limiting problem. They examined residual stress-state that evolves in a coating deposit is largely directly dependent on the subjected thermal conditions, and is a combination of quenching medium/stresses, which arise during coating deposition, and cooling stresses, arising post-deposition. They conclude that precise control of these phenomena is very essential, if a thick and sound deposit is to be thermally sprayed. Also this research applies an analytical technique to find out residual stress in thermally sprayed (HVOF) deposits based on geometric properties. Residual stress results for WC–Co samples has been compared with experimental results (Hole –drilling method and X-ray diffraction) they have used a spraying distance of nearly 200 mm and powder feed rate of approximately 38 g/min. The results shows across each sample there is a negative stress change, the size of which reduces as the coating deposit thickness increases. The stress at the interface that is intersection of coating and substrate changes from a tensile at the substrate side to the compressive stress on the deposit interface side in each case. The results also show that for the 1-mm thick coating deposit surface is close to a stress-free state.

Kulu et al. [2005] have studied the erosive behaviour of nickel based self-fluxing alloy , tungsten carbide based hard metal, and composites on the basis of NiCrSiB alloy coatings which were deposited from these powders by the continuous detonation spraying, detonation gun, and spray fusion process. Silica abrasives of size varying between 0.1 and 0.3 mm were used for erosion testing. Differences in the wear behavior have been compared in terms of the coating structure and hardness. Also they have concluded that erosion mass loss of these coatings is strongly affected by particle angle of particles. But, material erosion behavior

depends on metal removal mechanisms while hardness number seems to be of less importance. Also in their turn, coating microstructure influence both material loss mechanism and hardness. For all the materials tested erosion rate was found 5 to 6 times higher at higher temperatures. However the impact angle influence has no great effect on erosion resistance of thermal deposited coatings in the case of higher test temperatures.

Desale et al. [2006] have studied the effect of erodent properties on slurry erosion using a pot tester by evaluating wear of two materials of ductile nature namely AISI 304L and AA6063 steel. Three different erodent's alumina, quartz and silicon carbide have been used to prepare slurry to find out the mass loss of the both target materials at different angle orientations. Shape factor for erodent is also determine, it is found that with decrease in shape factor, wear increases. They concluded that the erodent properties other than erodent hardness play a considerable role in erosion of ductile materials. Also for erosion wear maximum angle is function of material properties of target independent of erodent, mechanism of material removal is a function of erodent density and shape.

Picas et al. [2006] have analysed characteristics Cr3C2 75% + NiCr20 25% weight coating deposited on a steel substrate having 150μm coating thickness, Three CrC–NiCr powders was deposited by HVOF spraying process. The fine agglomerates of CrC–NiCr shows a higher decomposition during HVOF spraying, produce lower hardness coatings, the wear behaviour of this almost 50% better than the standard CrC–NiCr coatings. Kerosene was used as liquid fuel, the pullout of fine carbide particles will cause less damage to the fine coating of nearly 1μm particle size and as result the wear rate decreases with decrease in the carbide size. They also proposed HVOF coatings can be used as alternative to hard chromium, as it leads to the optimize many factors like friction coefficient, wear resistance, environmental issues and cost. This will also reduce the effort for grinding and blasting operations.

Sidhu et al. [2006] have studied the behaviour and the phase composition of (HVOF) high velocity oxy fuel sprayed Cr3C2–NiCr and WC–Co coatings applied on steel; They used SEM/EDX, XRD and metallography techniques for examining coating characteristics. A comparison between the microstructure, surface roughness, porosity and microhardness of these coating has been made. Coating thickness is in the range of 250-300 micro meters, Microhardness across the cross-section of Coated specimens showed that the Cr3C2–NiCr has slightly lower hardness than the WC–Co, although both of these coatings have

considerably high hardness as compared to the substrate material, WC–Co coatings have lower porosity as compared to other coating of Cr3C2–NiCr, carbides with high volume that was well-dispersed in the coating matrix has been found. This is the Probable factor responsible for lower porosity and higher microhardness values.

Sidhu et al. [2007] have studied the erosion behaviour of coated and uncoated boiler steel materials with jet erosion testing machine. Ni-Cr(80%-20%) and Stellite-6 was used as coating materials, HVOF was used as coating process. Abrasive sand slurry of angular silica sand of size approximately 150-200μm was injected at target coated and uncoated materials at 30^0 and 90^0 angles. Coating thickness was found to be nearly 300μm for both of the coatings and hardness in the range of 300-400 Hv and 500-600Hv was observed for NiCr and Stellite-6 coatings respectively. And they concluded that substrate materials show less erosion as compared to coatings due to sand particle penetration, NiCr showed ductile manner of erosion which was found to be more suitable as compared to brittle manner erosion in satellite-6.

Wang et al. [2007] have analysed the hardness, microstructure and erosion phenomenon of HVOF coated and heat treated materials, NiAl coatings with three different criteria of 2%, 5% and 8% CeO_2 addition were examined through blast nozzle erosion tests. Final results showed that after heat treatment at elevated temperatures, Al2O3, $NiAl2O_3$ and CeAlO3 were formed in the intermettalic structure of NiAl coatings. Hardness observed in three CeO_2 2%, 5% and 8% variations was found to be 108-220, 220-250 and 200-250 respectively. They also concluded that 2% addition of CeO_2 showed less erosion as compared 8% addition also work hardening was observed during erosion testing process and in 5% CeO_2 work hardening was observed maximum, ductile erosion phenomenon was found dominated over brittle erosion in these coatings.

Cho et al. [2008] have studied the microstructure of High velocity oxy-fuel sprayed nano (n) and micron (m) coating WC–Co (88 wt.% - 12 wt.%) powders, it was found that coating hardness is strongly dependent on spray parameters and powder size Hardness of nano (0.1–1μm) WC–Co was lower than that of micro (1–40μm) WC–Co because of hard WC decomposition as compared to less hard W_2C, W and graphite. Porosity of micro WC–Co coating was smaller than that of Nano WC–Co because of less evolution of unwanted carbon

oxide gasses through micro WC–Co coating, also friction coefficient of micro coating is larger compared to nano coatings of WC-Co, because of the considerably lower decomposition of W, friction coefficient was found to be increased with increase in surface temperature as adhesion increases at elevated temperatures.

Bolelli et al. [2009] have studied the e\wear behaviour, impact resistance, micromechanical properties and microstructure of HVOF sprayed WC–10%Co-4%Cr coatings of powder size -45+15μm which were deposited on aluminium substrate The coating thickness was varied in the range of 50–150μm by different number of coating torch scans in front of the Al substrate. This variation was found to be responsible for have considerable influence on the coatings characteristics. it was also found that thinner HVOF coatings are more defective, as compared to thicker ones because the penetration of coating particles impacting onto the soft Al substrate surface was restrained to much extent by the deformation of the substrate surface itself, and The sprayed coatings became more denser and significantly more harder with increase in number of torch scans ,the cyclic impact resistance was also enhanced in same manner, three torch scans was seen enough to produce a sound coating having desirable characteristics.

Cho et al. [2009] have studied HVOF coating characteristics of WC-12%Co powder, which was coated onto an 420J2 steel substrate (72% Fe, 14% Cr, 12% Ni, 1%Si, 1% Mn) and the bond coats of Nickel, NiCr, and Ni/NiCr. Small portions of WC was decomposed during spraying to the less-hard W_2C, W and free carbon because of 1250°C decomposition temperature of WC, which is mainly responsible for increasing porosity (4.3±1.0%) and decreasing hardness. The surface hardness of coating 1120±100 Hv (10,980±980 MPa) was strongly dependent on the spray parameters, The friction coefficient was found increased by nearly 17% when surface temperatures was increased from 25°C to 500°C because of the enhanced local cold-welding characteristics of asperities at the elevated temperature of 500°C. Also adhesion between the WC pieces and Co matrix inside the WC-Co coating was much stronger than the adhesion (forces in different particles) of sub/WC-Co (9600±300 psi).

Fang et al. [2009] have investigated the porosity, hardness, microstructure and crystalline phase characteristics of high velocity oxy-fuel thermal sprayed WC–CrC–Ni (68% W, 21% Cr, 6% Ni) powder on Inconel 718 substrate, Oxygen flow rate have considerable affects on coating hardness. The phase of coating has been a portion of carbides, such as Cr_7C_3, Ni_3C

and WC decomposed to Cr, Ni and W_2C and free carbon. Also porosity (1.2±0.2%) and Hardness (1150±50 Hv) of coating had improved by optimization. The optimal parameters for HVOF coating process was selected as (53 FMR hydrogen flow rate, 38 FMR oxygen flow rate, 25 g/min coating powder feed rate and 7 inch gun spray distance). They also concluded that important sequence of parameters is spray distance <feedrate <hydrogen flow rate <oxygen flow rate, also the excess lubrication due to free carbon formed from the decomposition of metal oxides and carbides debris as formed during the coating results in considerable decrease of friction coefficients at the surface of the HVOF WC–CrC–Ni coating as compared to IN 718 substrate.

Mishra et al. [2009] have investigated the influence of different parameters on the erosion wear using taguchi analysis approach. As fly ash erosion of materials is influenced by large number of parameters which are significantly very important and makes the erosion process very complex. For the erosion wear of quartz coating impact angle had found most influencing parameter and they made efforts to investigate the influence of three different impact angles and found that at 90^0 impact angle maximum erosion was noticed as compared to 30^0 and 60^0 impact angle. Extruded lips and indentations was noticed due to erosion at 90^0 impact angle and work hardening was noticed of lips due to further impact of erodent particles, whereas plowing and micro cutting was noticed mainly responsible for erosion wear at acute impact angles.

Shivamurthy et al. [2009] have studied the erosion wear mechanisms and slurry erosion properties of nickel based colmonoy 88 and cobalt based satellite 6 coatings, and also finds out the circumstances under which minimum and maximum erosion occurred. Substrate material selected was 13Cr-4Ni steel on which laser surface alloying was done. Erosion tests was done for coated materials at 12m/s constant slurry velocity and for $10kg/m^3$ constant slurry concentration of sharp edged and irregular shaped SiO_2 particles, the particle size was of average 375μm and 100μm and also at 30, 45, 60, and 90^o impingement angles. In results they concluded that substrate 13Cr-4Ni steel > Stellite 6 LSA steel > Colmonoy 88 LSA steel is the decreasing order of erosion rate, for Colmonoy 88 coatings erosion rates showed more influence with the decrease in angle of impingement when it was eroded with 375μm particles, but when eroded with particles of 100μm showed a considerably strong angle of impingement dependence.

Wang et al. [2009] have studied the abrasive wear behaviour tested on wet sand rubber wheel tester of conventional and multimodal WC-12Co powder coatings deposited on mild steel substrate with HVOF thermal spraying process. By using XRD the phase composition of available feedstock powders and the powder coatings were analyzed. Multimodal coating showed better abrasive wear resistance, denser coating and higher micro-hardness than the conventional counterpart. Both these coatings exhibit more excellent abrasive wear resistance behaviour in comparison with substrate material mild steel and hard chrome plating. The multimodal powder was prepared by mixing coarse grain (2–3mm particles of WC-12Co) with nano phase WC-12Co particles, with WC grain size of nearly 30nm.

Zhang et al. [2009] have investigated the microhardness, wear performance and microstructure of high velocity oxygen fuel sprayed WC–CrC–Ni (68%W, 21%Cr and 6%Ni) coatings with and without laser heating treatment. The microstructure of the coatings was found to be changed considerably after the LH treatment. X-ray diffraction patterns showed that Cr_3C_2 and WC, as major phases, were found present in both these HVOF and HVOF laser heat treated coatings, and only a limited amount of Ni phase present in the LH-treated coatings Cr_3C_2 and WC phases was increased after LH treatment, the thickness and porosity of the LH coatings had a increase with increasing the scanning velocity. The wear resistance and friction of the coating were improved significantly by optimal laser heating process due to improvement of cohesion strength of the coatings by nickel and Cr_3C_2 matrix.

Babu et al. [2010] have studied the abrasive wear mechanisms of detonation gun thermally sprayed WC-12Co coating material with dry erosion tests by using Al_2O_3, SiC and SiO_2 erodent's. Dry erodent rubber wheel tests were carried out to calculate abrasion and decarburization influence (4.4 – 45%) of WC-12Co was evaluated. Abrasion rate observed in decreasing order with different erodent's SiC > Al_2O_3> SiO_2, The abrasive wear of coating was controlled by cracking of WC and was fractured in the case of bulk WC–12Co and with cuboids' pull out in case of WC coatings deposited at OF ratios of 1.50 and 1.16, also abraded surfaces showed consistent surface roughness with proposed mechanisms of abrasive wear.

Ramesh et al. [2010] have analysed the solid erosion behaviour of HVOF sprayed WC-Co/ NiCrFeSiB coatings at boiler tube substrate steel GrA1 material with angular silica sand as erodent material of size approximately 125-180μm, which was impacted at a velocity of

approximately 40m/s, the high retention of tungsten – carbide in coating matrix had confirmed lower porosity of order 0.5% with a hardness of 1223Hv. Petroleum gag was used as fuel gas for coating purposes, brittle and ductile failure mechanism was observed with dominating brittle mechanism of failure, craters and groove formation was observed at major level, the low hardness ratio between substrate steel and silica erodent particles was responsible for lower erosion loss due to penetration of impacting particles inside ductile substrate.

Kasem [2011] have studied the major effects on erosion mechamisms and erosion rates of 5117 steels with respect to particle shape and particle size using slurry whirlingarm ring, erodent particles are characterized in terms of their circularity factor, aspect ratio and diameter values also the variations in the erodent particle diameters is taken as in six different diameters which varies from 516.4 μm to 112.7μm. Erosion results show at 200μm particle size diameters erodent particles posses' threshold energy and cause suddenly change in erosion rate was noticed. The erosion wear tests were carried out at 90 degree and 30 degree impact angles with 15m/s impact velocity using a slurry concentration of 1 percent by weight Erosion mechanism noticed was ploughing above 200μm erodent particle size while material extrusion and indentations mechanism was noticed below 200μm erodent particle size.

Shrinivasulu et al. [2011] have studied the improvement in surface finish of a metal forming process using taguchi approach, uses a flow forming machine with single roller for the manufacturing of AA6082 alloy steel thin walled tubes with a target to get minimum surface finish in their process, taguchi approach method was used for the design of experiments so as to study the surface roughness improvement process. Also the influence of various parameters effecting the roughness of tubes was investigated, the various factors affecting the roughness values was recognised as roller radius, speed of mandrel and axial feed of the roller and in the final results they found that for the manufacturing of flow formed tube with a minimum roughness of 2.30μm value, speed of the mandrel, roller radius and roller feed are the most influencing factors.

Goyal et al. [2012] have investigated the erosion mechanism in the high velocity oxy-fuel sprayed Al_2O_3+13TiO_2 and WC-10Co-4Cr powders on the CF8m turbine steel material, wear was carried out in high velocity erosion test rig, the effect of three variables namely slurry concentration, speed and erodent particle diameter was also evaluated in their study which

was found to be in good agreement with previous researches and ductile type of erosion mechanism was noticed in WC-10Co-4Cr coating which showed excellent improvement in the erosion resistance of the coated turbine steel material as compared to Al_2O_3+13TiO_2 coated turbine steel material which showed brittle as well as ductile mechanisms of erosion wear.

Thakur et al. [2013] have investigated the dry erosion and slurry erosion behaviour of conventional cermet materials and high velocity oxy-fuel sprayed WC-CoCr cermet materials, dry erosion was carried out in erosion test rig (dry jet) and pot type erosion tester was used for slurry erosion testing, impact angle of 90 degree and impact velocity of 60m/s was selected in dry erosion testing. Carbide pullout, chipping and carbide fracture was observed in carbide phase of coating while lip formation, groove formation and crater formation was mainly observed in binder phase of coating. Considerable improvement in fracture toughness and micro hardness was noticed in WC grain coated cermet coatings as compared to conventional cermet coatings that come out to be mainly responsible for increase in erosion resistance.

Venter et al. [2013] have studied the integral performance parameters of high-velocity oxygen-fuel (HVOF) WC-Co coatings, mainly the interactions between the substrate and coatings that is thermal expansion coefficients difference between substrate and coating, associated thermo-mechanical interaction. Investigation carried out had given reports results on the wear resistance, substrate-coating misfit, chemical phase content and microstructures. For the depth resolved studies of the substrate and coatings, the neutron diffraction technique in their study in conjunction with sub-mm sized gauge volumes was enabled, it was concluded in final results that on increasing macro hardness and compressive stress there was improvement in wear and after heat treatment due to enhancement in compressive stress there was more improvement in wear characteristics.

Enayati et al. [2014] have investigated the influence of wear on the high velocity oxy-fuel sprayed Ni-Al coatings; Ni-Al powders were initially prepared by mechanical alloying of these two different powders and then sprayed on the substrate material by HVOF process with optimally determined parameters. Slightly oxidation of Al (50μm-70μm) and Ni (30μm-110μm) was also noticed after spraying process which was responsible for minute decrease in hardness of coating as well as small increase in the porosity of coating and the coatings were

also investigated with (XRD) x-ray diffractometry and (HRTEM) high resolution transmission electron microscopy.

Goyal et al. [2014] have studied the effect of slurry concentration, speed and erodent size on the erosion wear of high velocity oxy-fuel sprayed Cr_3C_2-NiCr coating on the CA6NM turbine steel material. In the final result they found excellent improvement in the erosion wear resistance in the Cr_3C_2-NiCr coated turbine steel material as compared to uncoated CA6NM uncoated turbine steel material. Main mechanism of erosion wear on the uncoated CA6NM observed was lip formation and crater formation, whereas in case of Cr_3C_2-NiCr coated materials plowing, cutting and plastic deformation was mainly observed as erosion wear mechanism. Also erodent velocity was found most influencing factor on the erosion wear and was followed by erodent size and slurry concentration by weight.

Murugan et al. [2014] have studied the different parameters of high velocity oxy-fuel process so as to optimize the coating characteristics so as to minimize the porosity and oxide content of the HVOF coatings, coating powder used in their study was WC-10Co-4Cr that was sprayed on naval brass substrate with liquefied petroleum gas as fuel, different parameters like spray distance, powder feed rate and flow rate were used with different variations so as to improve the coating hardness and porosity values which are very important factors in high velocity oxy-fuel spray processes. Statistical tools such as response surface methodology, analysis of variance and design of experiments were also used so as to attain the required optimal objectives, in the final results it was observed that spray distance had least influence on the coating hardness and porosity values and followed by powder feed rate, LPG flow rate and oxygen flow rate.

Oksa et al. [2014] have studied improvement in corrosion resistance in the high velocity oxy fuel sprayed Ni-24Cr-16.5Mo and Ni-22Cr coatings on carbon steel boiler material as compared to uncoated carbon steel material and found considerable improvements in the corrosion resistance of the coated materials. It was noticed that chlorine induced corrosion caused extremely severe corrosion together with lead, copper, potassium and zinc deposits in the carbon steel material. Also C_3H_8 was used as fuel for librating energy in the high velocity oxy fuel process with stand-off distance of nearly 250mm.

As most of the thermal power plants use mild steel as pipeline material for the transportation of ash slurry, and there is large wear of mild steel pipeline material during ash slurry transportation. This motivated the author to do research on different type materials so as to reduce the piping material loses and to suggest new type of coatings, that may enhance the life of existing pipe materials. Table 2.1 gives the pipe material used in various thermal power plants in India for transporting ash slurry.

Thermal power plant	Pipe material
Gandhinagar Thermal Power Station (2 x 210 MW), Gujarat	Mild Steel
Guru Hargobind Thermal Plant, Bathinda, (2 x 210 MW), Punjab	Mild Steel
Guru Gobind Singh Super Thermal Plant, Ropar (6 x 210 MW), Punjab	Mild Steel
Kota Thermal Power Station Stage-3, (1 x 210 MW), Rajasthan	Cast Iron
National Fertilizers Limited captive Power plant, Bathinda, Punjab	Mild Steel
National Fertilizers Limited captive Power plant, Panipat, Hariyana	Mild Steel
Shriram Fertilizers and Chemical Captive Power Plant (1 x 35 MW) Kota, Rajasthan	Mild Steel

Table 2.1: Pipeline material used in thermal power plants in India

CHAPTER 3

TESTING MATERIALS AND COATINGS

Most coal-fired utility plants produce bottom ash and fly ash with a typical production ratio of 20% bottom ash and 80% fly ash, and most of them are usually disposed of together as a waste in utility disposal sites by means of trucks and pipes. In pipe transportation generally water is mixed with bottom ash to make slurry and this slurry is transported, due to erosive effect of slurry pipe material gets wear out, so different kind of hardness enhancing methods are used to increase the pipe hardness.

3.1 BOTTOM ASH

Bottom ash is the solid particle residues from coal combustion process in thermal power plants. Bottom ash refers to part of the non-combustible residues of combustion that settles down at the bottom during combustion process. It comprises of coarse particles and it does not rise during of coal and stays at bottom. Major constituents of bottom ash are SiO_2, Al_2O_3 and Fe_2O_3. Bottom ash properties greatly influence of the slurry behaviour during transportation through pipelines, major bottom ash properties which affect the slurry flow are discussed below.

Properties	Bottom ash
Particle size (d_{50}) μm	230
Specific gravity	2.25
pH of slurry (upto C_w =50%)	7.72-7.75
Final settling of suspension (initial concentration C_w = 20%)	57%

Table 3.1: Physical properties of bottom ash, kumar et al., [2014]

Flow behaviour of bottom ash slurry shows newtonian behaviour upto concentration of 50% by weight and relative viscosity values are also below 6 upto 50% concentration by weight. Relative viscosity is dynamic viscosity of the slurry to the dymanic viscosity of water under same conditions.

3.2 TESTING MATERIALS

These are the materials which are generally used for pipe manufacturing. Three type of pipe materials are selected in present study which are as follows.

3.2.1 Mild Steel:

Mild steel, also known as plain-carbon steel because it contains less than 0.4% carbon which makes it ductile and malleable, it is the most common form of steel because its price is relatively low while it provides material properties that are acceptable for many applications, more so than iron. Mild steel has a relatively low tensile strength, but it is cheap and malleable.

3.2.2 Stainless Steel 202:

200 series stainless steels have an austenitic crystalline structure, which is a face-centered cubic crystal structure. These are austenitic chromium-nickel-manganese alloys to retain an austenitic structure at all temperatures from the cryogenic region to the melting point of the alloy.

3.2.3 Stainless Steel 304:

300 series stainless steel having approximately (not exactly) 18% chromium and 8% nickel. It is also known as 18/8 steel, is the most common stainless steel. Metals as the main non-iron constituents. It is an austenite steel. It is not very electrically or thermally conductive, and is non-magnetic.

3.3 CHEMICAL COMPOSITION OF MATERIALS

The chemical composition of Mild Steel, SS 202 and SS 304 is determined by the spectrometer analysis. A spectrometer is a device used to measure chemical composition of ferrous materials. The chemical composition is measured by the light intensity produced by arc. A spectrometer is used in spectroscopy for producing spectral lines and measuring their wavelengths and intensities.

Fig. 3.1: WAS foundry master spectrometer

Components	Percentage Composition (by Weight)		
	Mild Steel	SS 202	SS 304
Fe	98.9	74.5	69.5
Cr	0.0356	13.4	18.5
Ni	0.0311	0.182	8.90
Mn	0.420	9.64	1.34
C	0.131	0.0959	0.114
Si	0.161	0.403	0.494
Co	0.0055	0.037	0.135
P	0.0705	0.0600	0.0594
Al	0.0174	0.0402	0.0079
Cu	0.0649	1.45	0.281
S	0.0529	0.0422	0.0260

Table 3.2: Material composition of Mild Steel, SS 202 and SS 304

The average percentage of important components is given in above Table 3.2 as measured from spectrometer analyses, two readings of component percentage is taken for each of the material namely Mild steel, SS 202 and SS 304, and average values are calculated.

3.4 SAMPLE PREPARATION

Mild steel, SS 202 and SS 304 samples were cut from long bars using power hacksaw. Then the specimens were grinded with the help of surface grinder to get the dimensions required for the testing. A hole was drilled in the centre of the specimen so that it can be held in the fixture. Sample specifications are measured by digital micrometer and are given in Table 3.3.

Material	Length(mm)	Width(mm)	Height(mm)
Mild steel	74.9	25.2	5.1
SS 202	74.8	25.1	5.2
SS 304	74.9	25.2	5.1

Table 3.3: Dimensions of testing specimens

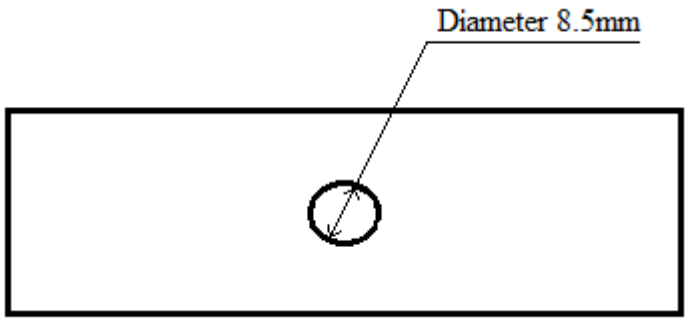

Fig. 3.2: Drawing of specimen

3.5 MICROHARDNESS

Vickers diamond pyramid test is used to find out the microhardness of these materials. Materials are polished with emery papers ranging from 150 grit up to 2000 grit so as to get scale free and super finished surface. The variation in surface hardness may be due to anisotropic properties of these materials and localised impurities in the microstructure of these materials. Diamond cone indentations are taken at 50μm separation and no crack formation is noticed around the indentations after measuring the hardness in all the testing specimens.

Fig. 3.3: METATECH MVH-1 microhardness tester

Two or three readings are taken for each of the material and average value is taken as the hardness of that particular material. Hardness values which are recorded by Vickers microhardness tester are given below in Table 3.4.

Material / Microhardness (H_V)	Mild Steel		SS 202		SS 304	
1	102	106	181	184	158	155
2	098	103	178	172	155	151
3	104	101	184	186	157	159

Table 3.4: Vickers microhardness of testing materials

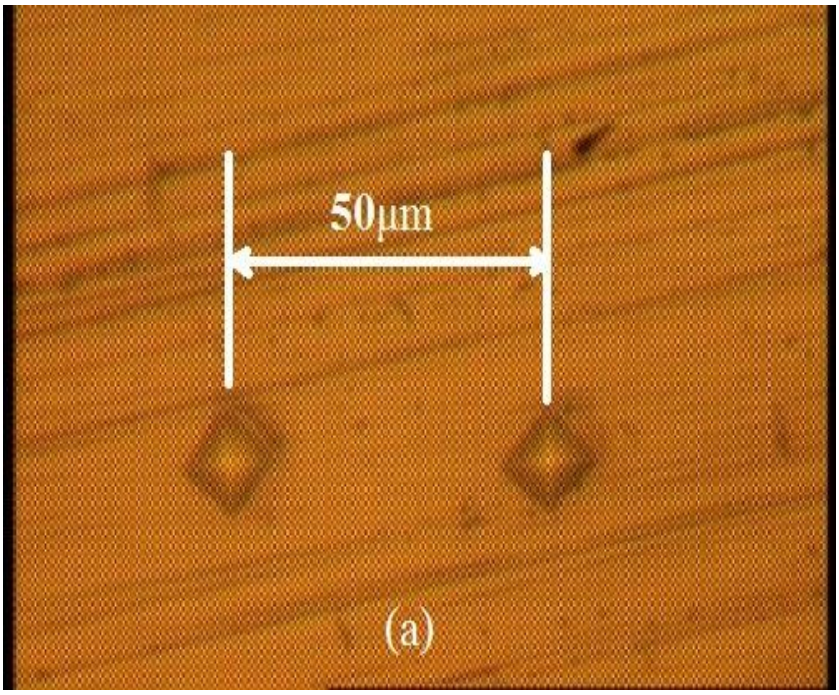

Fig. 3.4: Diamond indentations marks on specimen

Vickers microhardness is determined for above mentioned three materials at 50gm load, above figures show the indentation marks at regular separation distances so as to avoid any type of cracking of material due to weight put by indenter during the indent formation.

3.6 SURFACE ROUGHNESS

It is a measure of the surface texture. Surface roughness represents the vertical deviations of a real practical surface from its ideal known form. If these deviations are small, the surface under observation is smooth and if they are large the surface under observation is rough. For determining the how a particular surface interact with its environment, measurement of roughness plays an considerable, smooth surfaces generally wear/erode less as compared to rough surfaces and have lower coefficient of friction than rough.

Two readings are taken for each for each of two samples of all three materials on arithmetic mean roughness scale (R_a). MITUTOYO SJ.400 model is used to find out the roughness values. Table 3.5 gives the values of surface roughness recorded Mild steel, SS 202 and SS 304 materials before erosion wear experimentation process. It is found that Mild steel have

maximum surface roughness values as compared to other two materials and SS 304 is found to have minimum surface roughness values.

Fig. 3.5: MITUTOYO SJ-400 surface roughness tester

SS 202 material have intermediate roughness values as compared to other materials for approximately all the observations. Higher roughness values of mild steel material may be due to rapid oxidation of this material in the presence of oxygen, as surface of mild steel if highly reactive due to more amount of oxygen presence. All the specimens which are used for roughness testing are corrosion free, no scale is seen to be deposit on the surface.

Material / Roughness (R_a) µm	Mild Steel		SS 202		SS 304	
1	2.23	2.16	1.24	1.45	0.95	1.11
2	2.08	2.11	1.16	1.08	0.86	0.98

3	1.98	2.09	1.22	1.18	1.02	1.22

Table 3.5: Surface roughness values (R_a) of testing materials

All the important properties of pipeline materials are discussed above which have major influence on the erosion wear. Also bottom ash properties which are important from erosion behaviour point of view are discussed above. And it is found that these testing materials possess high erosion characteristics. If they remain in erosive environment for long duration, surface of materials may get easily eroded.

3.7 OVERVIEW OF SURFACE HARDENING TECHNIQUES

In the engineering applications there are some cases in which conventional surface hardness is not sufficient for the application of particular material in the design process, so some other means are used to increase the surface hardness of the materials, most of the times these methods helps to improve the surface hardness and hence make the suitability of the materials for the engineering applications. Different surface hardening techniques are given below:

- Electrochemical and Chemical Methods
- Thermo-Chemical Coatings
    - Carburizing
    - Nitriding
    - Combined techniques:
- CVD and PVD Techniques
- Spray Coatings
    - Cold spraying
    - Detonation spraying
    - Flame spraying
    - High velocity oxy-fuel coating spraying (HVOF)
    - Plasma spraying
    - Warm spraying
    - Wire arc spraying

3.8 HVOF THERMAL SPRAY PROCESS

In HVOF process a mixture of oxygen and liquid or gaseous fuel is fed into a combustion chamber, after their ignition high energy is liberated and at high pressure powder mixed spray is fed onto the coating specimen, a very high velocity generally in the range of 1000km/s is used for the spraying process dye to the high pressure hot gases. Generally acetylene, methane, liquefied petroleum gas is used as fuel gases. Impact of high velocity gases on the coating specimen produces high level sound, and high velocity is mainly responsible for the less porosity and high strength of process.

3.8.1 Advantages of HVOF Coating

- Fine surface finish
- High density
- Excellent bond strength
- Excellent Wear Resistance
- Optimum Hardness.
- Improved Toughness
- Higher Coating Thickness.
- Beneficial Residual Stress.
- Superb Corrosion Resistance

3.8.2 Disadvantages of HVOF Coating

- Complex installation
- Not suitable for all kind of coatings.
- The use of pure oxygen requires special protection measures.

3.9 HVOF THERMAL SPRAYING SYSTEM

The HVOF thermal spraying system is complex as compared to other thermal spraying systems, it consists of large number of components but few of them are discussed following, components here discussed are not in deep details instead are just introduced so as to highlight their independent importance in coating process.

i. Gas supply and flow meter unit
ii. Powder feed unit

iii. Diamond Jet (DJ) gun

iv. Support system

- Cooling system
- Exhaust system
- Facility isolation
- Furnace
- Grit blasting unit
- Safety equipment
- Traverse Unit

Fig. 3.6: HVOF machine

3.10 HVOF SPRAYING PROCEDURE

High velocity oxy-fuel process is used here for coating of WC-12Co and Ni-20Cr_2O_3 powders on three substrate materials as discussed below.

3.10.1 Surface Preparation

In most coating processes the integrity of the deposit is critically dependent on the substrate surface condition. The HVOF thermal spraying is no exception, but unlike other methods, it

is often applied on site in ambient atmosphere. Thus surface cleanliness in the true scientific sense is never achieved.

- **Polishing:** Substrate materials after cutting are surface finished by using emery papers from 150 grit up to 2000 grit so as to remove the surface scales.

- **Grit blasting:** It is generally carried out by eroding the substrate surface by a harder material It can remove surface scale as well as providing a course texture to support the thick coating. Al_2O_3 shots are used to clean the surface.

3.10.2 Spraying Process

A freshly prepared surface is very reactive (with the oxygen in air) and therefore the thermal spraying operation must be carried out as soon as possible after blasting.

- **Holding fixture:** A fixture which is already manufactured to hold the job in place with firm grip is used, the purpose of using this specially manufactured fixture is to hold the pieces in close position so as to minimize the coating powder loss.

Fig. 3.7: Fixture used to hold the specimens

- **Coating deposition:** After firmly holding the pieces with the help of using nut and bolts, pieces are coated with above mentioned powders with HVOF spraying process gun as shown Fig. 3.8 and coating parameters are given in Table 3.6 below.

Fig. 3.8: Gun used for HVOF coating

Coating Parameters	WC-12Co	Ni-20Cr_2O_3
Spray distance (mm)	100-140	100-140
Particle size (μm)	-45+15	-45+15
Air flow rate (L/cm^2)	6400	6900
Oxygen flow rate (LPM)	260	245
Fuel (LPG) flow rate (LPM)	75	70
Powder feed rate (g/min)	30	25

Table 3.6: WC-12Co and Ni-20Cr_2O_3 coating parameters

3.11 XRD (X-RAY DIFFRACTION)

X-ray diffractometer is used to carry out the surface studies of WC-12Co and Ni-20Cr_2O_3 coated surfaces. From the impingement of an electromagnetic wave on the atoms with in crystal X-ray diffraction are produced. Because wavelength of X-rays is of same order of magnitude as the spacing between crystals plane and these are used to produce the diffraction pattern (1–100 angstroms). PANALYTICAL ('X' pert pro) model of diffractometer is used mineralogical composition study of coated materials. Fig. 3.9 shows the WC-12Co coated minerological composition of three different substrate materials and shows the presence of tungsten monocarbide (WC), Tungsten hemicarbide (W_2C) and cobalt in all the cases. W_2C is less hard material than WC.

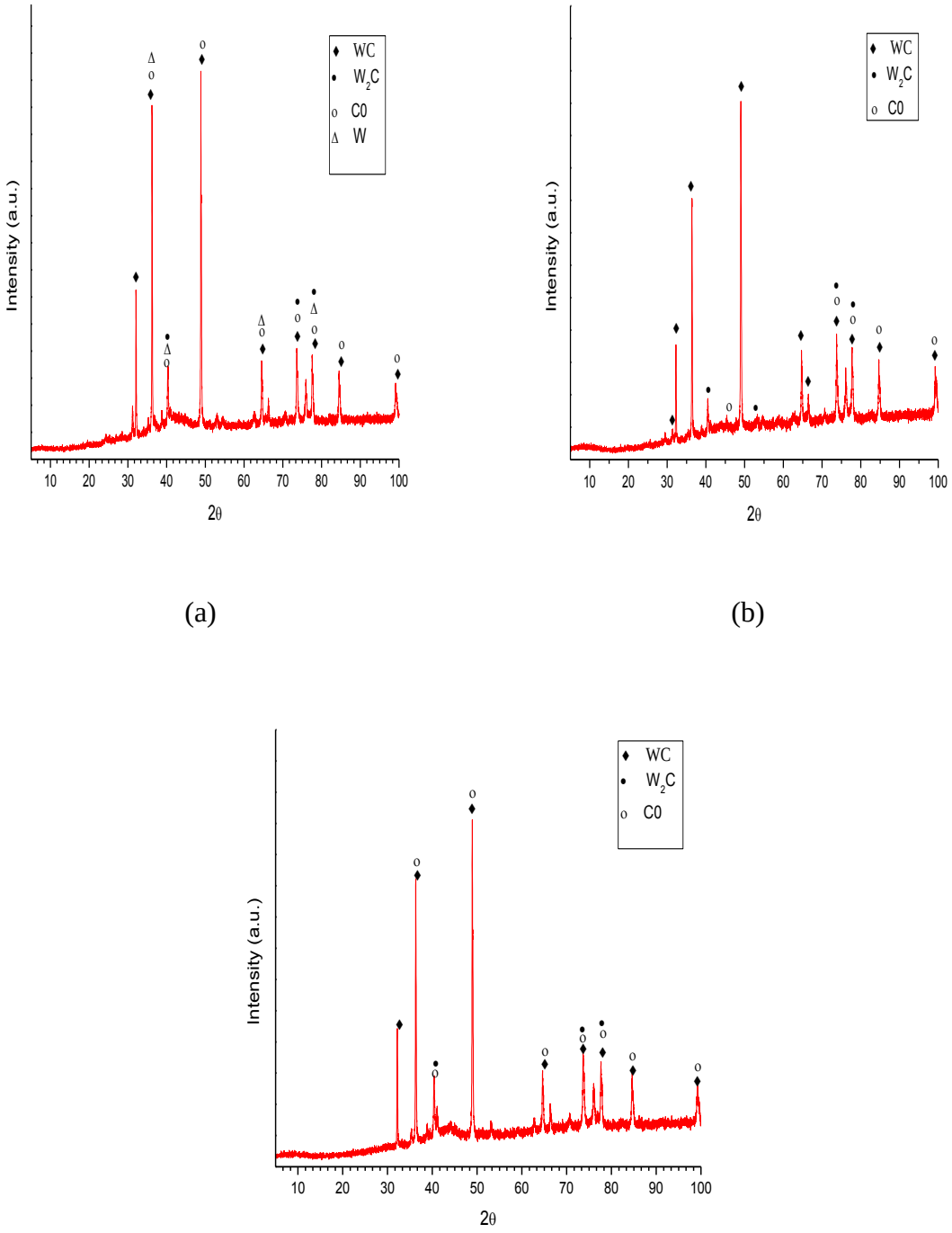

(a) (b)

(c)

Fig. 3.9: XRD graphs for mineralogical composition of WC-12Co coated (a) SS 202, (b) SS 304 and (c) Mild steel materials

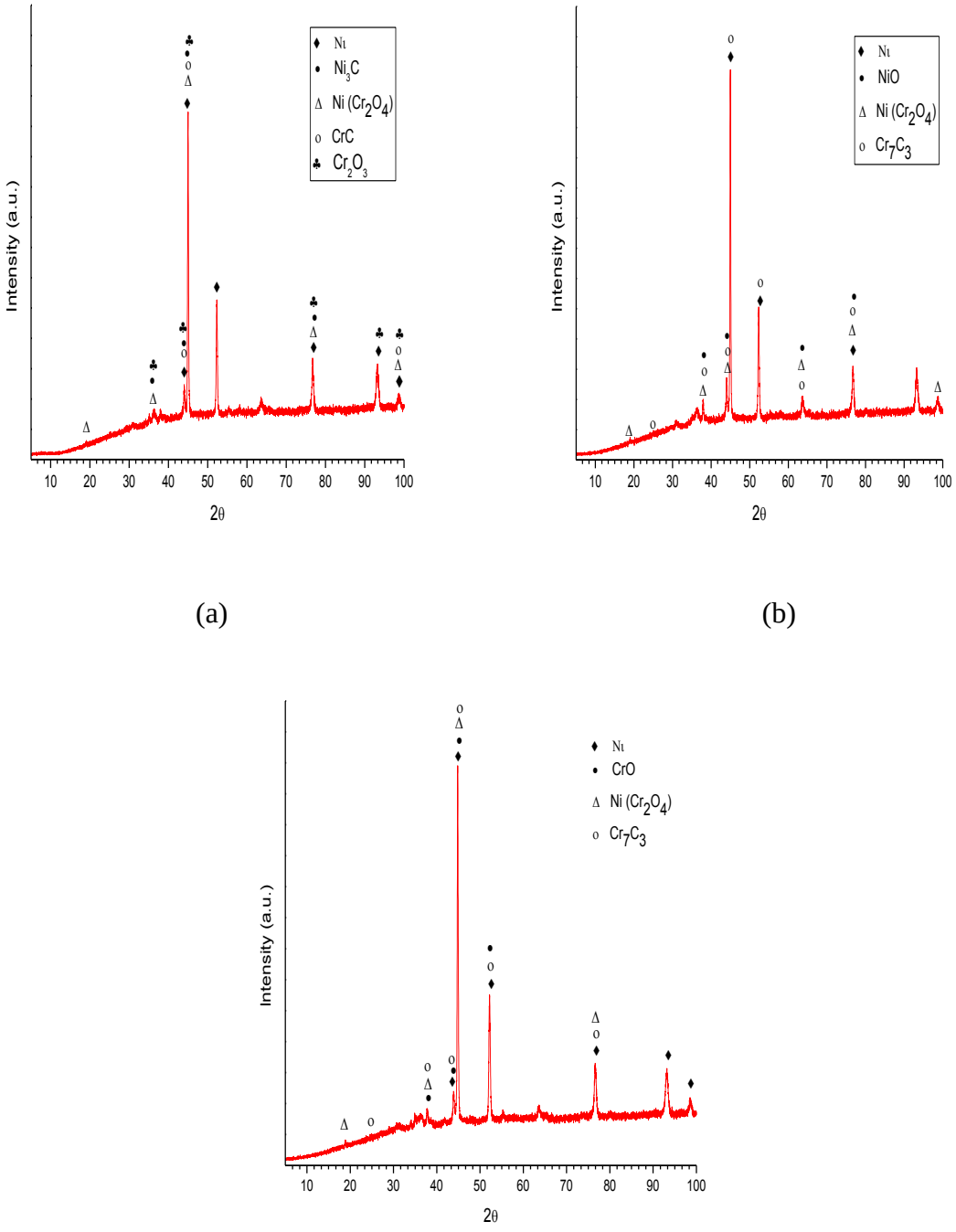

(a) (b)

(c)

Fig. 3.10: XRD graphs for mineralogical composition of Ni-20Cr_2O_3 coated (a) SS 202, (b) SS 304 and (c) Mild steel materials

Nickel is seen present in large quantity in all the three coatings with different substrate materials and small amount of chromium carbide is also observed in the mineralogical study of the coatings Fig. 3.10. In case of SS 202 nickel carbide and chromium carbide is present as

compared to other coated materials, this may be responsible for slightly increase in the hardness of coating.

3.12 SEM (SCANNING ELECTRON MICROSCOPY)

A scanning electron microscope (SEM) use focused beam of electrons to produce images of sample and is a type of electron microscope. The interaction of electrons with the atoms in the sample, produces various type signals and these signals can be detected and information can be collected about the sample composition and topography that is contained in it.

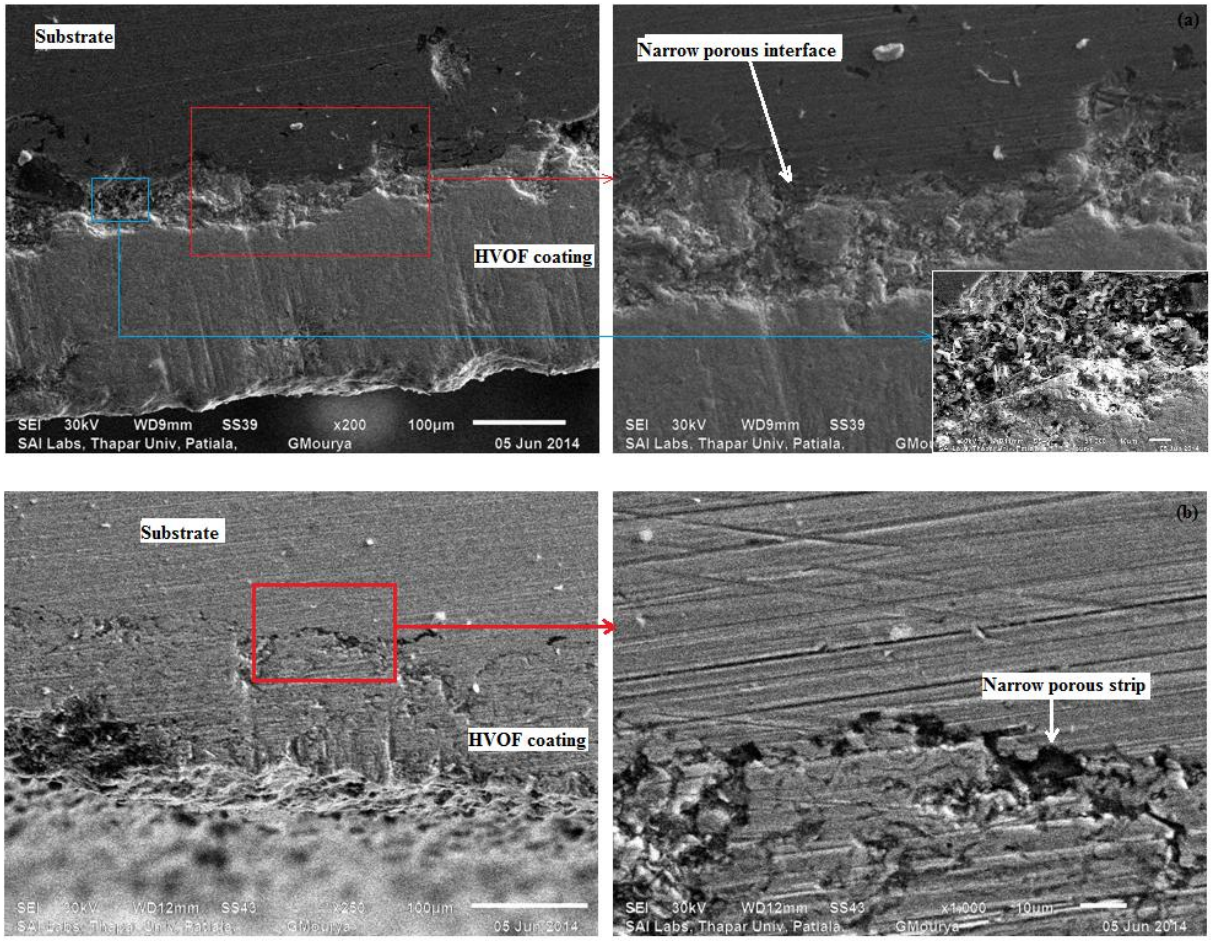

Fig. 3.11: Cross-section SEM images of (a) WC-12Co coated Mild steel and (b) Ni-20Cr_2O_3 coated SS 202

In the present study JEOL, 6510LV model of scanning electron microscope is used for taking secondary electron images and Cross-sectional SEM images of coated WC-12Co and Ni-20Cr_2O_3 materials is shown in Fig. 3.11, thickness of tungsten based coating is in the range of 230-250µm and nickel based coating is in the range of 130-150µm. EDS results of coating

along with substrate material is also taken, this shows the presence of required constutuents in the coating.

Coating	Substrate material	Thickness (μm)	Average microhardness (H_v)	Roughness (R_a)
WC-12Co	SS 202	230-250	972 ± 11	5.26
	SS 304	230-250	1015 ± 08	5.89
	Mild steel	230-250	983 ± 07	5.41
Ni-20Cr_2O_3	SS 202	130-160	745 ± 16	4.55
	SS 304	130-160	723 ± 09	4.86
	Mild steel	130-160	734 ± 13	4.21

Table 3.7: Properties of coatings

Coating thickness is more in case of tungsten based coatings that is in the range of 230μm to 250μm as shown in Table 3.7 and in case of nickel based coatings thickness is small which is 130μm to 160μm. Maximum hardness observed in tungsten based coating is 1015 H_v and maximum hardness in case of nickel based coating is 745 H_v. Variations in the microhardness in the coatings is due to anisotropic properties of thermal spray coatings and coatings may contain voids, pores, splats, splat boundaries, melted and unmelted coating particles.

Surface roughness of nickel based coating is found more as compared to tungsten based coatings, but before erosion of coated specimens these are polished with emery paper of 150 grit size so as to ensure uniform wear of all the specimens, because otherwise erosion results may show different weight loss.

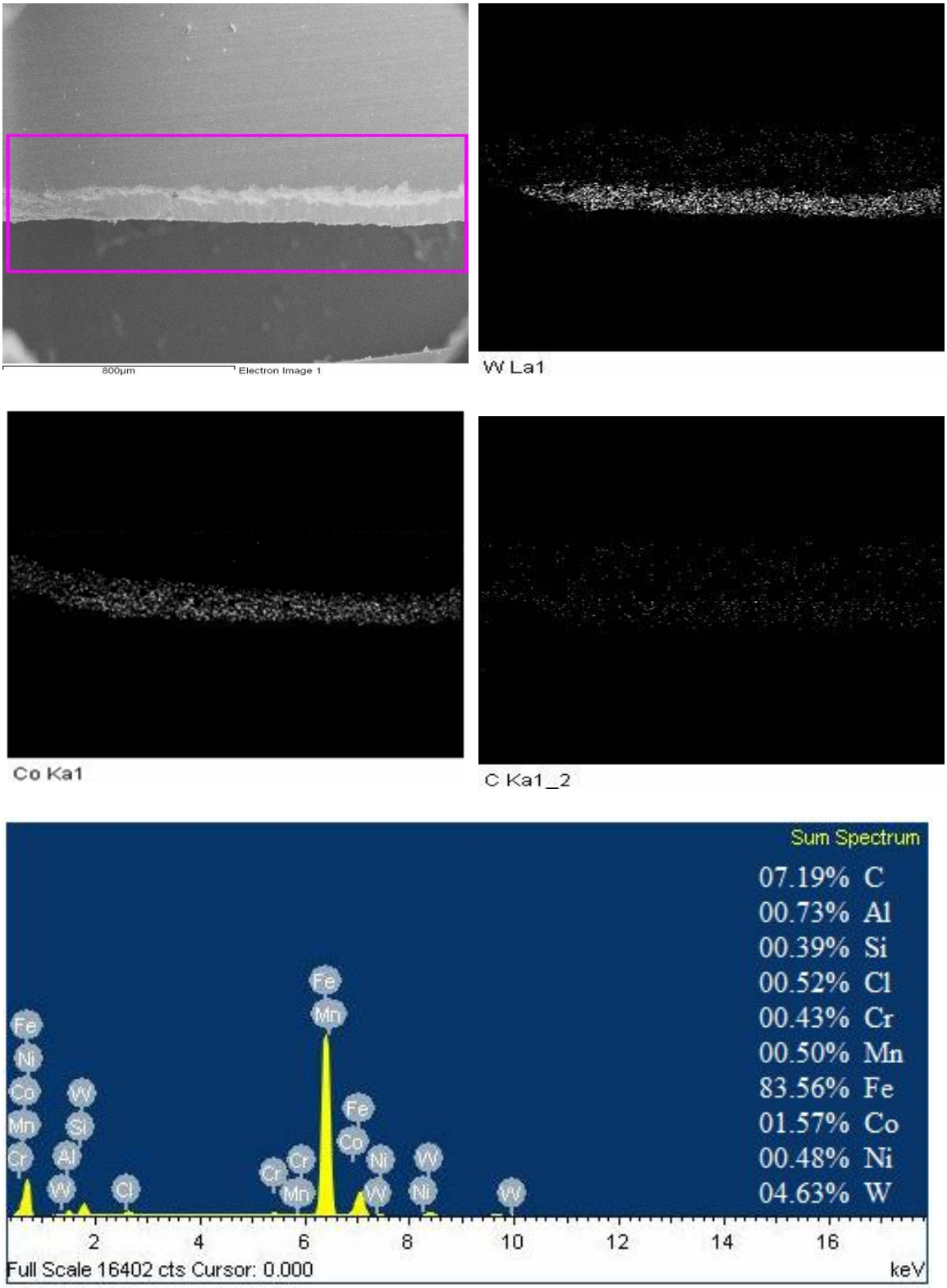

Fig. 3.12: Cross-sectional EDS anlysis of WC-12Co coated Mild steel

Cross-sectional Electro dispersive x-ray spectroscopy (EDS) analysys of WC-12Co coated Mild steel substrate shows the presence of carbide and cobalt in huge amount as compared to other constituents, this shows the presence of coating on the substrate material and also small

amount of carbon is found present as shown in Fig. 3.12, OXFORD INSTRUMENT, INCA x-act model is used for EDS analysis. Before analysing these coated specimens all these specimens are polished with upto 1500 grit emery papers so as to get good surface finish and hence to get best images, but due to more hardness of coatings surface finish is relatively less

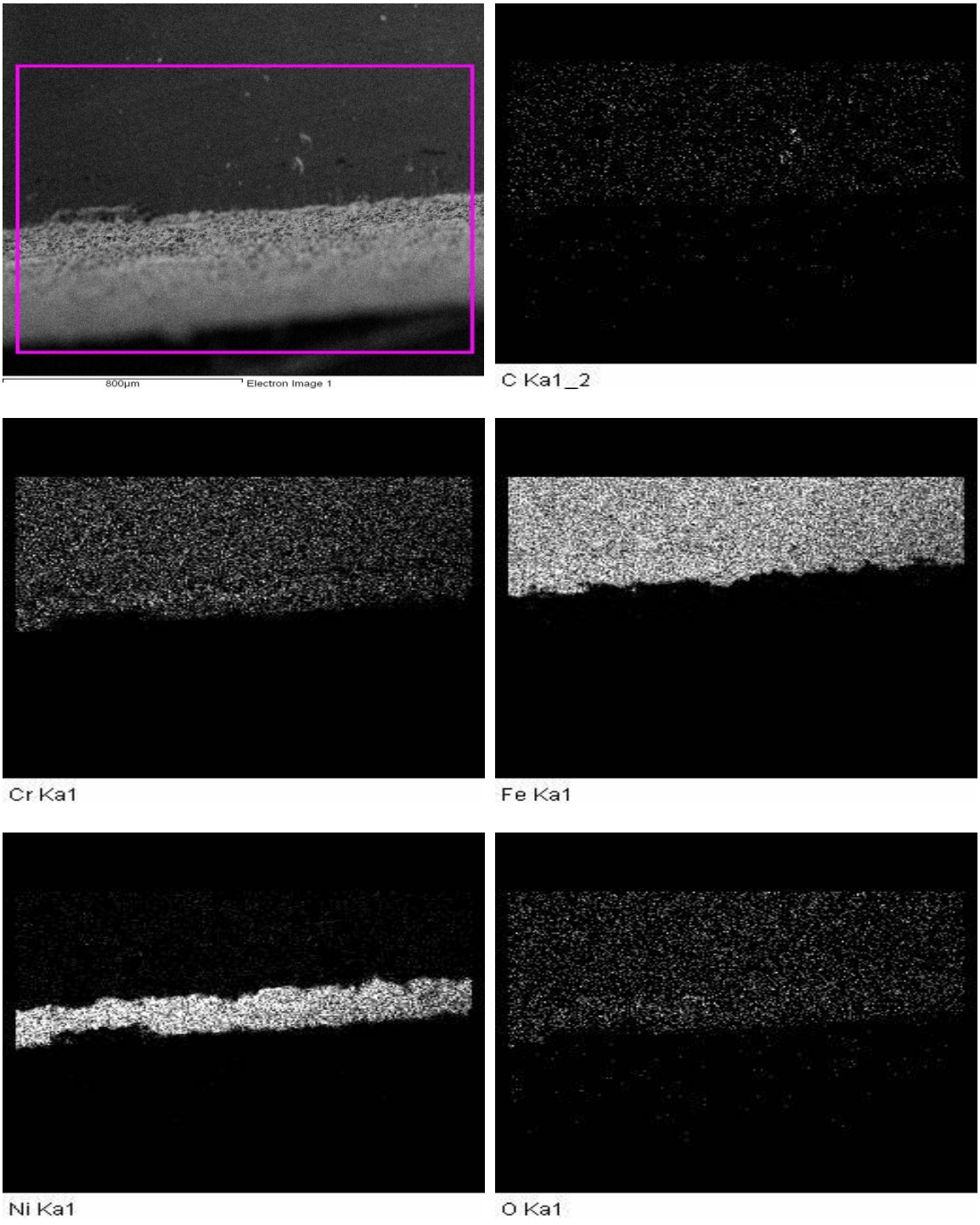

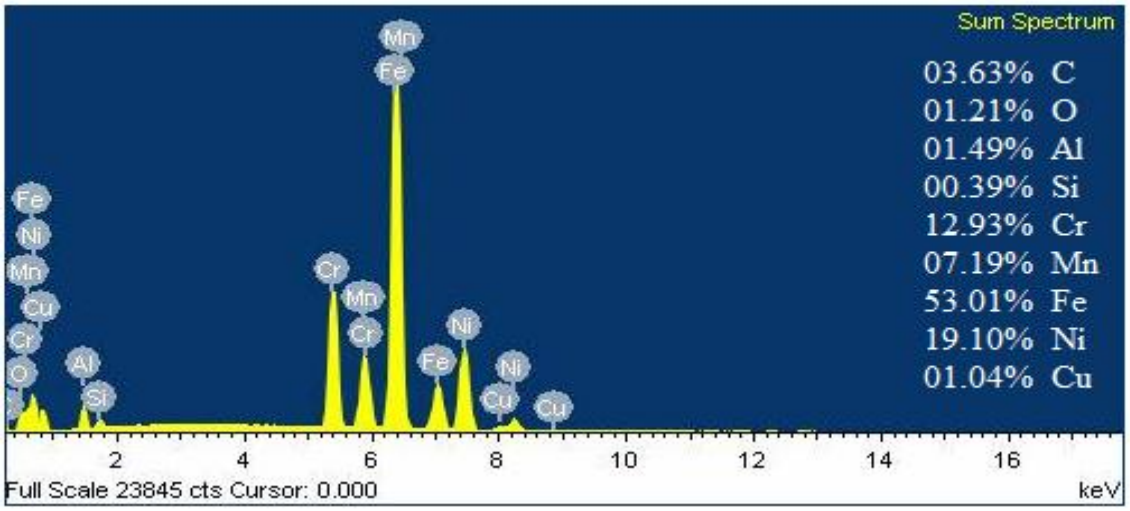

Fig. 3.13: Cross-sectional EDS analysis of Ni-20Cr_2O_3 coated SS 202

Ni-Cr_2O_3 coating on SS 202 substrate materials is also analysed using EDS as shown in the above Fig. 3.13, it is clear that nickel is present in large amount in the coating, chromium and oxygen is also present in the coating, which signifies the presence of chromium oxide, very few amount of oxygen is also present in the coating. Small amount of irregularity is found in the coating analysis due to micro breakage of the coating during the cutting process.

CHAPTER 4

EROSION AND RESULTS

Slurry erosion tests are performed on Mild steel, SS 304 and SS 202 materials with and without coating by using slurry pot tester under different test conditions so as to evaluate the different erosion phenomenon, amount of wear of each coated and uncoated material.

4.1 SLURRY POT TESTER

As slurry pot tester is already introduced in first chapter, slurry pot tester consistes of a cylindrical pot in which already prepared slurry is poured and this pot is adjustable can move in up and down motion with the help of a fixture and testing specimen is fastened to rotating shaft, rotating speed of vertical shaft can be altered with different values and at different speeds and different concentrations, weight loss of materials can be calculated.

Fig. 4.1: DUCOM slurry pot tester

4.2 PARTS OF SLURRY POT TESTER

Slurry pot tester consists of simple mechanism as discussed following.

- **Rotating shaft:** This is rotated with the help of electric motor which located at the top of machine and is covered from all sides. Maximum speed of rotating shaft is 1500 RPM.
- **Stirrer:** Function of stirrer is to make uniform distribution if prepared slurry during the operation of slurry pot tester. Generally it is of rectangular shape.
- **Workpiece:** It is the material which is under experimentation, and this is mounted on the rotating shaft with the help of bolt arrangement together with stirrer
- **Slurry pot:** All the slurry which is prepared is poured into slurry pot, maximum capacity of slurry pot is 1.8L, and pot can be separated from the tester for cleaning purposes.
- **Fixture:** fixture is consisted of a moveable jack, which is responsible for up and down motion of the slurry pot. Slurry pot casing is hinged with the fixture, after filling the pot with slurry; fixture is rotated with the help of rod so as to move the pot in upward direction up to the top of rotating shaft.

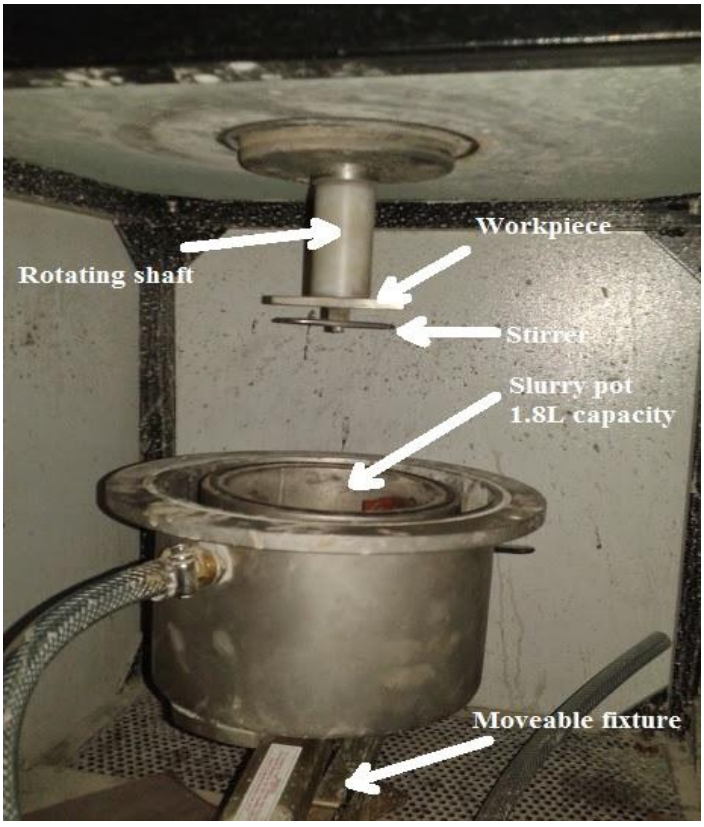

Fig. 4.2: Parts of slurry pot tester

4.3 EXPERIMENTAL PARAMETERS

Erosion of all the three materials Mild steel, SS 202 and SS 304 without and with coating is tested on slurry pot tester by using bottom ash as erodent material at different test conditions as given in Table 4.1. all the specimens are polished with 150 grit emery paper before experimental work.

Parameters:	Specifications:
Material	Mild steel, SS 202 and SS 304
Erodent material	Bottom ash
Particle size (μm)	230 (d_{50})
Slurry concentration (C_w)	25 and 45
Speed (RPM)	500, 800, 1100 and 1400
Time (min)	90 and 180

Table 4.1: Experimental parameters and specifications

4.4 EXPERIMENTAL RESULTS

Erodent particles are responsible for the considerable erosion of the piping materials as found out from the erosion tests, as testing materials face strong impact due to rotation of erodent particles inside the pot tester, testing materials looses weight due to various type of wear mechanisms, and the various results which are obtained are presented in the table form as follows.

Kasem [2011] used the following relation to calculate the number of erodent particles striking per unit time with testing specimen, it is shows that number of erodent particles striking per unit time are inversely proportional to the diameter of erodent particles that is number of striking particles per unit time increase with decrease in erodent particle diameter.

$$N_{ep} = \frac{\dot{m}_e}{\frac{\pi}{6}(d_e^3)\rho_e} \quad (4.1)$$

Following Fig. 4.3 illustrate the general idea of difference between number of erodent particles striking per unit time when their area is small and large.

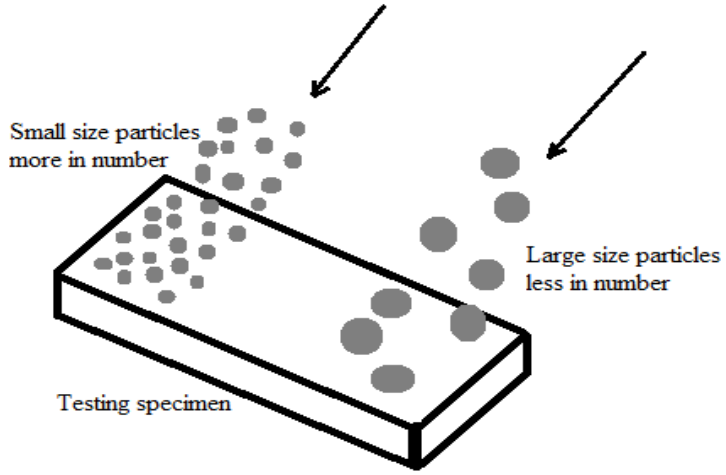

Fig. 4.3: Erodent particles with different size impacting on testing specimen

Gupta et al. [1995] derived and **Goyal et al. [2014]** also used the following correlation to predict the erosion wear using experimental data.

$$E_w = kV^a d_e^b C_w^c \quad (4.2)$$

In this equation there are four variables and four constants k, a, b and c. Values of constants depend upon nature of testing materials and erodent particles. An attempt has been made in present study to find out the values of exponent 'a' and 'c' from the experimental data.

4.4.1 Effect of Rotational Speed of Rotor on Erosion Wear

Effect of shaft rotation speed on the erosion wear of testing materials is discussed below, it is clear that more is the speed of erodent particles more is the momentum stored in them and when these particles strike with testing materials, they exert more force on them according to the conservation of momentum theory.

Value of exponent 'a' / Material	Actual	Expected range
Uncoated Mild steel	1.96	
Uncoated SS 202	1.53	

Uncoated SS 304	1.69	1-3.5
WC-12Co coated Mild steel	1.07	
WC-12Co coated SS 202	1.02	
WC-10Co coated SS 304	1.03	
Ni-20Cr_2O_3 coated Mild steel	1.13	
Ni-20Cr_2O_3 coated SS 202	1.10	
Ni-20Cr_2O_3 coated SS 304	1.12	

Table 4.2: Values of exponent 'a' for Mild steel, SS 202 and SS 304

Value of exponent 'a' for Mild steel, SS 202 and SS 304 based upon experimental results conducted for 3hr erosion testing is found to be 1.96, 1.53 and 1.69 respectively, and in good agreement with **Gupta et al. [1995]** and **Goyal et al. [2012]** it is concluded that impact of velocity on Mild steel is more as comparison to other two materials SS 202 and SS 304. These values are found to be lying in limit as concluded by researchers which is 1 to 3.5, **Truscott [1975], Goyal et al. [2012]** and **Goyal et al. [2014].** Similar trend has been observed for tungsten and nickel based coatings. SS 202 material found to have least impact of rotational speed. At higher speed more number of erodent particles is supposed to be strike with testing target material and also erosion rate is expected to be proportional to the kinetic energy of striking erodent particles, there for expected value of exponential is to be greater than 2, but slightly lower value in this case is expected to be due to inelastic collision and rebounding of the erodent particles after striking with testing specimen, also since erodent particles ate in continuous motion and are not able to transmit whole of the kinetic energy to the testing target specimen during impact .

As the number of revolutions of workpiece increases consequently relative motion between the workpiece and slurry increases as a result of which impact forces on the testing material increases, hence which is responsible for the wear of the testing material. Fig. 4.4 represents the mass loss of all the three uncoated and WC-12Co coated materials at 45% slurry concentration, slurry pot tester run for 180 min.

It is seen that rate of mass loss is more for starting speeds, as speed increases from 500 rpm to 1400 rpm; fall in the rate of mass loss is noticed. Wear of mild steel is found more than other two materials, it is certainly due to the less microhardness of mild steel as compared to other two materials. After mild steel, SS 304 losses mass at more rate as compared to SS 202, because hardness of SS 202 is more as compared to other two materials.

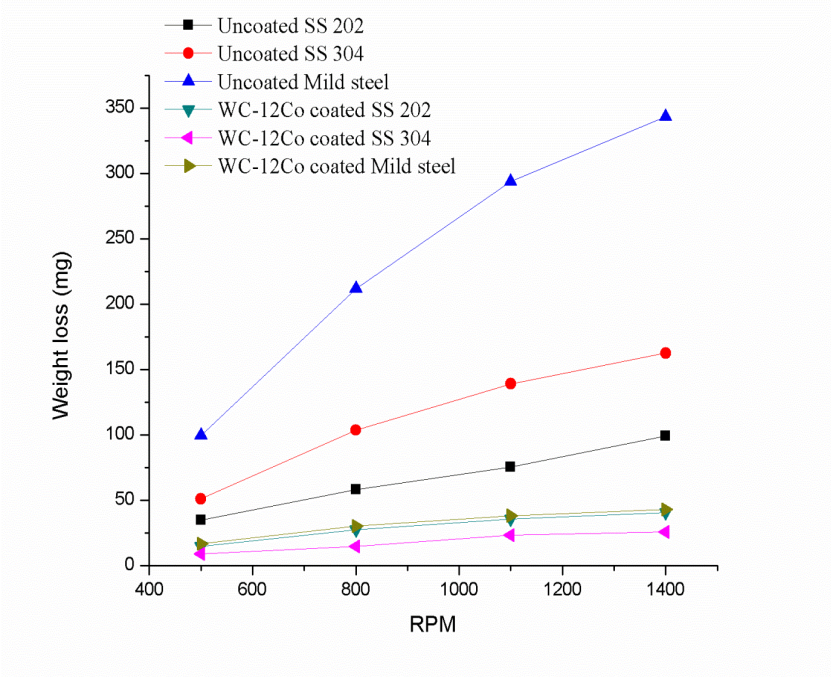

Fig. 4.4: Erosion of WC-12Co coated materials at 45% concentration and for 180 min

As speed increases from 500 rpm towards 1400 rpm, initially from 500 rpm to 800 rpm rate of erosion wear of all the three materials is large, and then from 800 rpm to 1100 rpm rate of mass loss is decreased for both 90 min and 180 min slurry pot run, as shown in Fig. 4.4 and

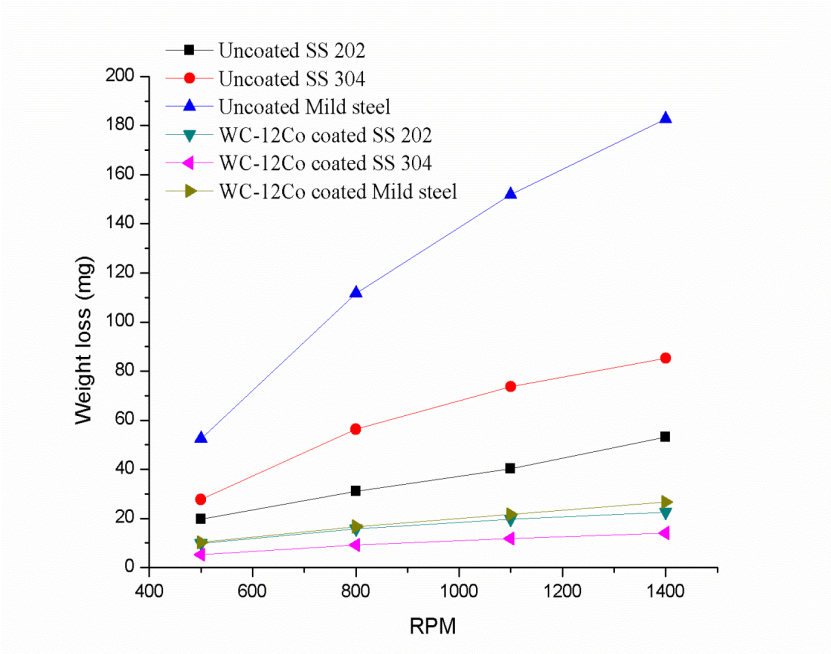

Fig. 4.5: Erosion of WC-12Co coated materials at 45% concentration and for 90 min

Fig. 4.5, then for the 1100 rpm to 1400 rpm run rate of mass loss is drops to much extent. Similar trend has been observed in WC-12Co coated materials also, and it is also found that erosion results of WC-12Co coating with SS 304 are best as compared to other materials with similar coating. While almost similar erosion is observed in SS 304 and Mild steel with similar coating with 45% concentration.

Uncoated Mild steel shows largest erosion as compared to other materials and it if found that its performance has increased best with tungsten based coating that is up to 4 to 6 times, and these values are least for other two types of materials.

At 25 % slurry concentration a similar trend has been observed as for 45% concentration, for both of 90 min and 180 min experiment run. For the coated materials along with uncoated materials weight loss is found to be dropped as rpm proceeds from lower to higher values.

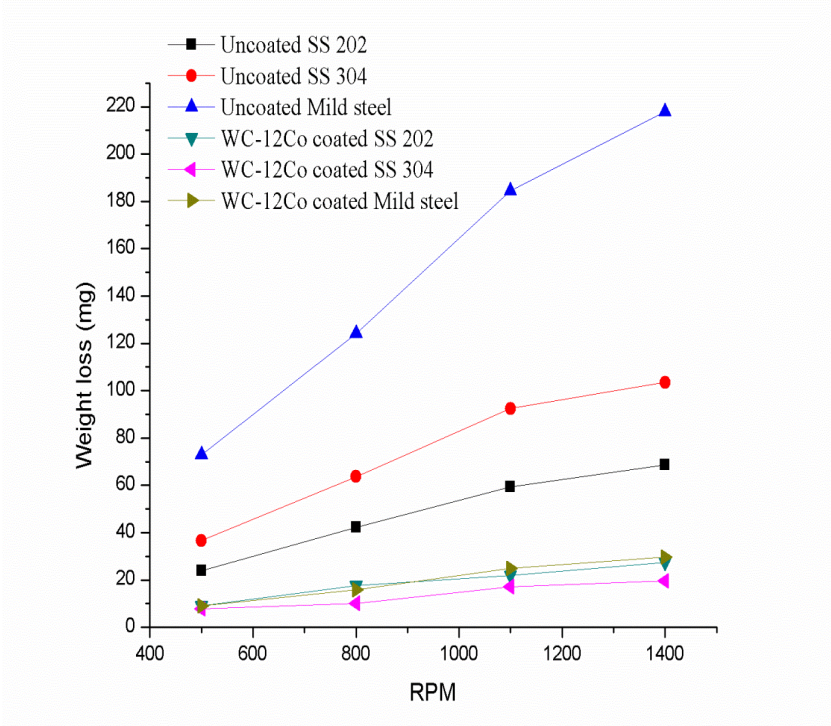

Fig. 4.6: Erosion of WC-12Co coated materials at 25% concentration and for 180 min

Fig. 4.6 and Fig. 4.7 shows the erosion wear of uncoated and WC-12Co coated materials at slurry 25% concentration, similar trend has been also seen at 45% slurry concentration, SS 304 coated material shows less erosion wear as compared to others.

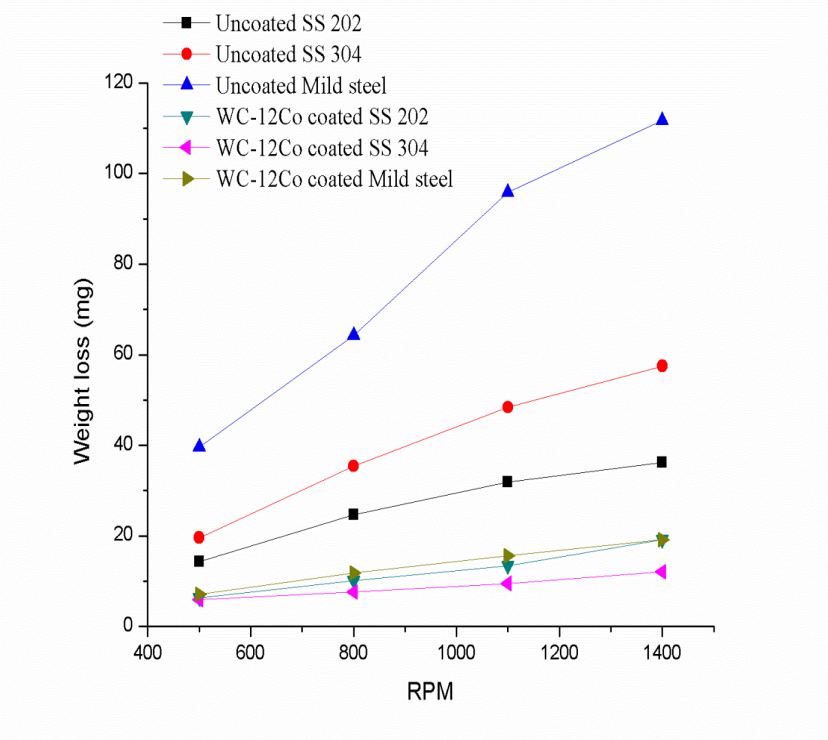

Fig. 4.7: Erosion of WC-12Co coated materials at 25% concentration and for 90 min

Erodent particle speed have a great influence on the wear of piping materials, as it is clear from Fig. 4.4 and Fig. 4.6 for the same 180 min tester run, mass loss is more for 45% concentration as compared to 25% concentration. But at greater speeds wear is found to be decreased and that may be due to because at higher speeds erodent particle motion is so random that inter particle collisions are more and these collisions are causing decrease in the momentum of erodent particles, which may lead to decrease in mass loss at higher speeds.

Ni-20Cr_2O_3 coating shows more erosion wear as compared to WC-12Co coatings as clear from the Fig. 4.8, mainly it is because of less surface hardness nickel based coatings as compared to tungsten based coatings, small addition of chrome oxide helps to improve the hardness of coatings but still these are not comparable with tungsten based coatings because of small chrome oxide addition. It is also found that nickel based coating increased the erosion resistance of Mild steel and SS 304 materials. But in case SS 204 it is not able to increase the erosion resistance up to considerable mark, it may be due to slightly ductile nature of nickel based coating.

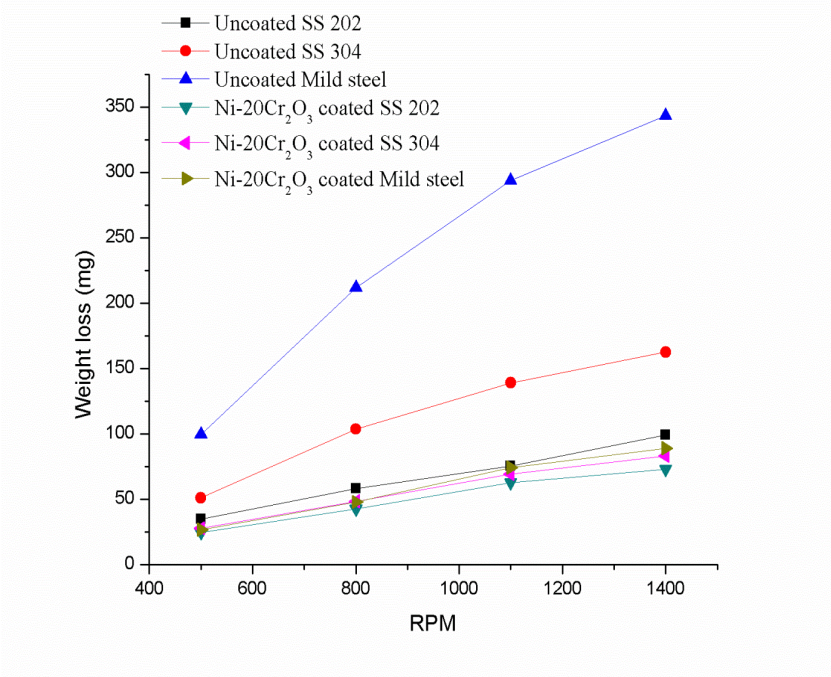

Fig. 4.8: Erosion of Ni-Cr_2O_3 coated materials at 45% concentration and for 180 min

It is also observed that erosion rate for 800 rpm to 1100 rpm is less as compared to 500 rpm to 800 rpm and 1100 rpm to 1400 rpm observations in some cases, because at higher speeds erodent particles gets blunt shape in earlier collisions and after that erodent particles are

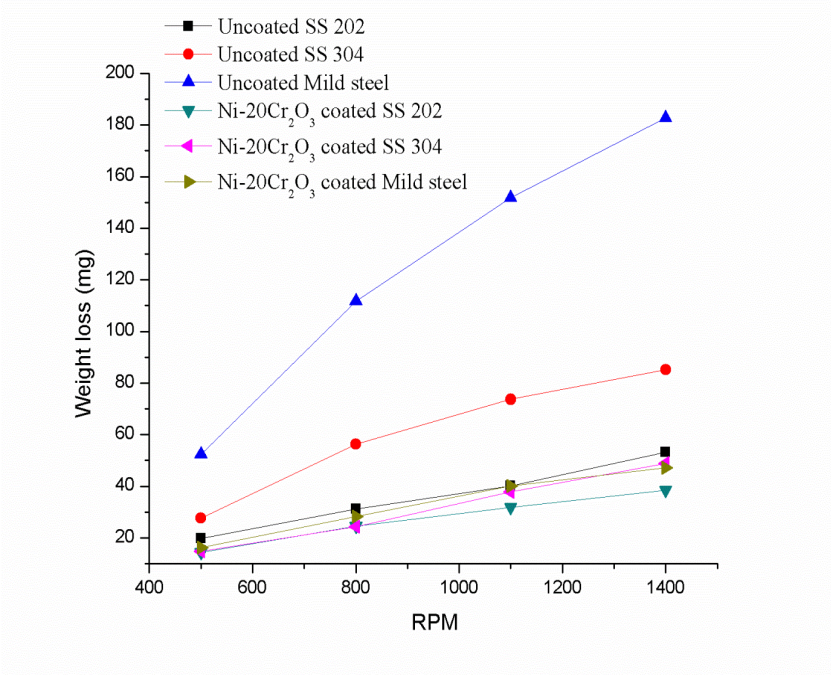

Fig. 4.9: Erosion of Ni-Cr_2O_3 coated materials at 45% concentration and for 90 min

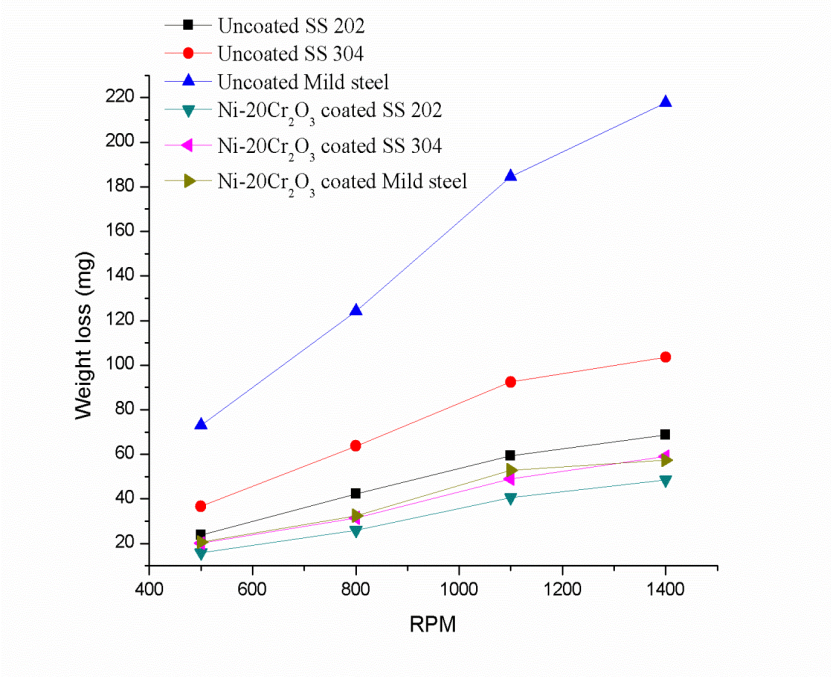

Fig. 4.10: Erosion of Ni-Cr_2O_3 coated materials at 25% concentration and for 180 min

unable to erode the testing materials as at earlier rates, and at further higher speeds due to greater impact erosion rate increases again. SS 202 material shows least erosion with nickel based coatings as compared to other two substrate materials.

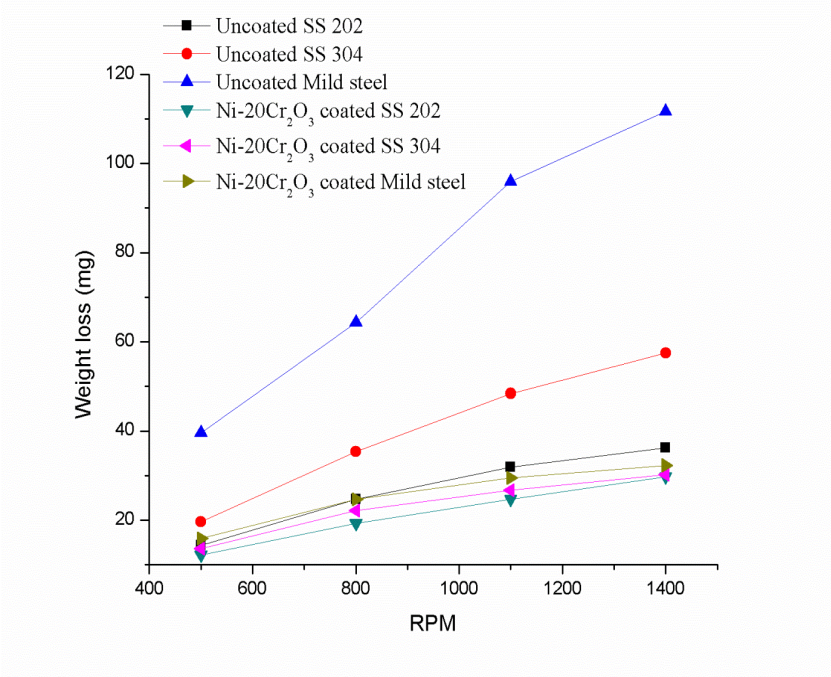

Fig. 4.11: Erosion of Ni-Cr_2O_3 coated materials at 25% concentration and for 90 min

But there is not sufficient improvement of erosion resistance of SS 202 with nickel based coating, that is limited up to only 1.5 times improvement of erosion resistance and in case of mild steel increase in erosion resistance is up to 3 times as it is clear from Fig. 4.10 and Fig. 4.11, and in case of SS 304 substrate material improvement of erosion resistance is up to 2 times and this is the intermediate value as compared to other two materials.

4.4.2 Effect of Bottom Ash Concentration on Erosion Wear

As discussed earlier concentration plays important role on the wear of piping systems, concentration represents the number of erodent particles per unit mass of slurry, more is the concentration more is the number of particles in unit slurry, consequently in running slurry pot tester more are the number of impacts on the testing materials.

Value of exponent 'c' / Material	Actual	Expected range
Uncoated Mild steel	0.49	< 1
Uncoated SS 202	0.36	
Uncoated SS 304	0.47	
WC-12Co coated Mild steel	0.92	
WC-12Co coated SS 202	0.77	
WC-10Co coated SS 304	0.46	
Ni-20Cr_2O_3 coated Mild steel	0.61	
Ni-20Cr_2O_3 coated SS 202	0.75	
Ni-20Cr_2O_3 coated SS 304	0.61	

Table 4.3: Values of exponent 'c' for Mild steel, SS 202 and SS 304

Value of exponent 'c' for the Mild steel, SS 202 and SS 304 on the basis of experimental study carried out for 3hr duration is found to be 0.49, 0.36 and 0.47. These limits are showing same as found by **Gupta et al. [1995], Goyal et al. [2012]** and **Goyal et al. [2014]**, expected value of exponent 'c' is expected to be below 1 as proposed by researchers.

Fig. 4.12 shows the erosion wear of uncoated, WC-12Co and Ni-20Cr_2O_3 coated SS 202 material at 25% and 45% concentration for 180 min test run, tungsten based coating at 25% concentration shows minimum erosion rate as compared to other all the combinations.

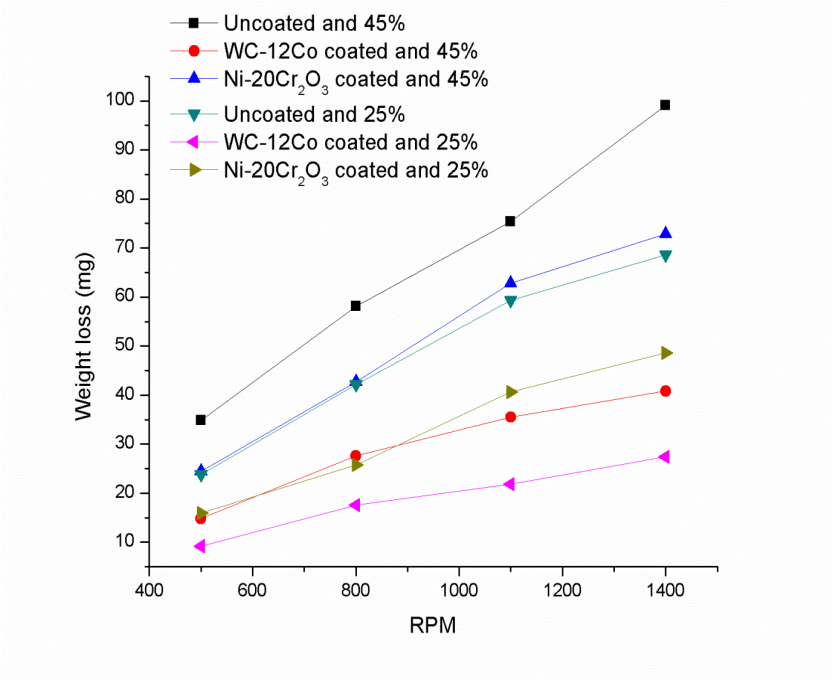

Fig. 4.12: Relative erosion of SS 202 for 180 min

It is clear from above fig. that more is the concentration more is the wear of testing material, again at large concentrations inter particle motion gets so disturbed that average momentum of erodent particles gets decreased and number of particles striking per unit time with testing material gets decreased, which may lead to decrease in the mass loss at together at higher concentration and higher speeds.

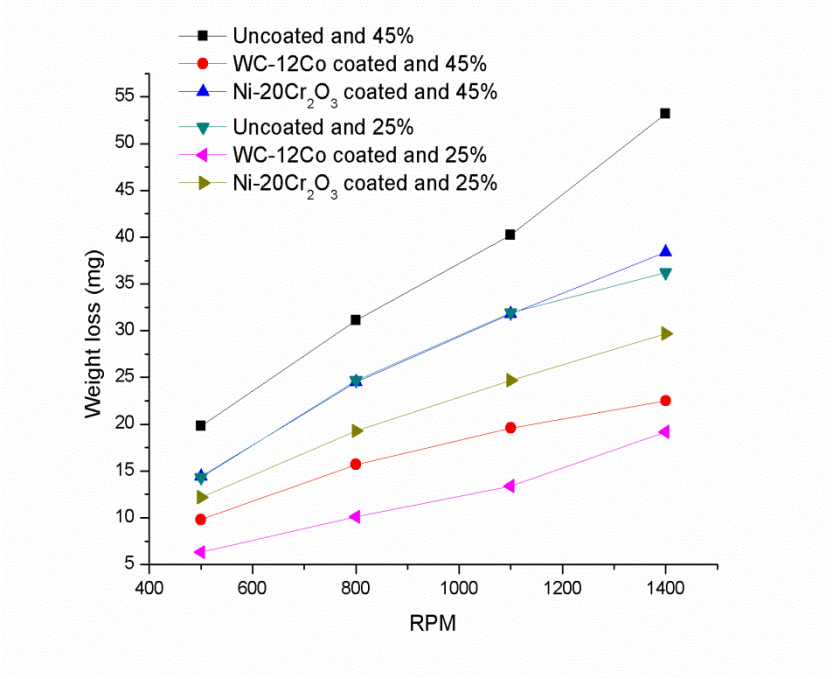

Fig. 4.13: Relative erosion of SS 202 for 90 min

Mass loss for SS 202 is found to be less at 25% and 45% concentrations, also from Fig. 4.13 it is found that for a particular concentration mass loss for 180 min test run is not double as

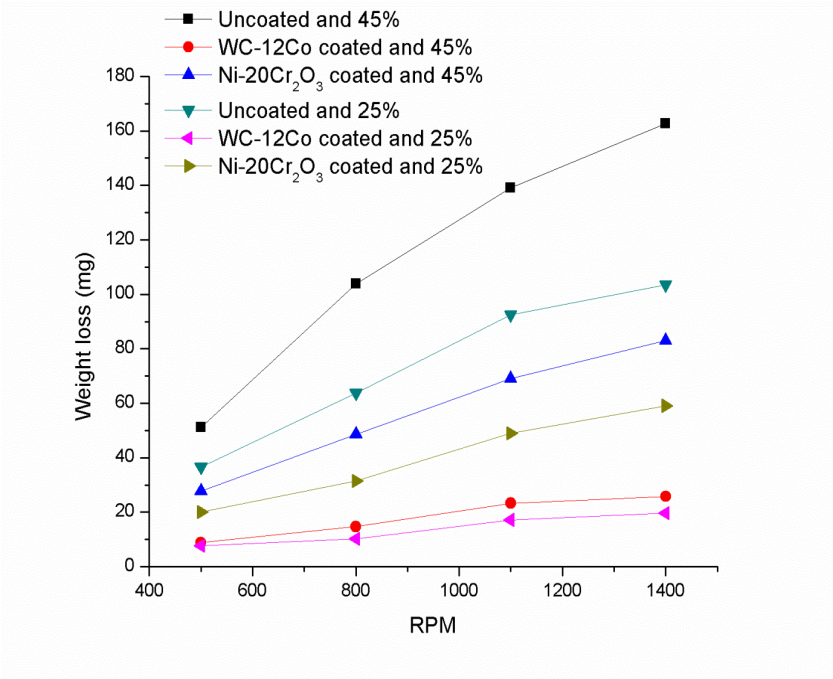

Fig. 4.14: Relative erosion of SS 304 for 180 min

compared to 90 min test run, or there is non-linear relation between these, it may be due to blunt out of new erodent particles at earlier stages of test run and also may be due to metallurgical changes in the properties of testing materials because as long as test proceeds, temperature of the slurry gets increases, consequently there are effects on the erosion phenomenon.

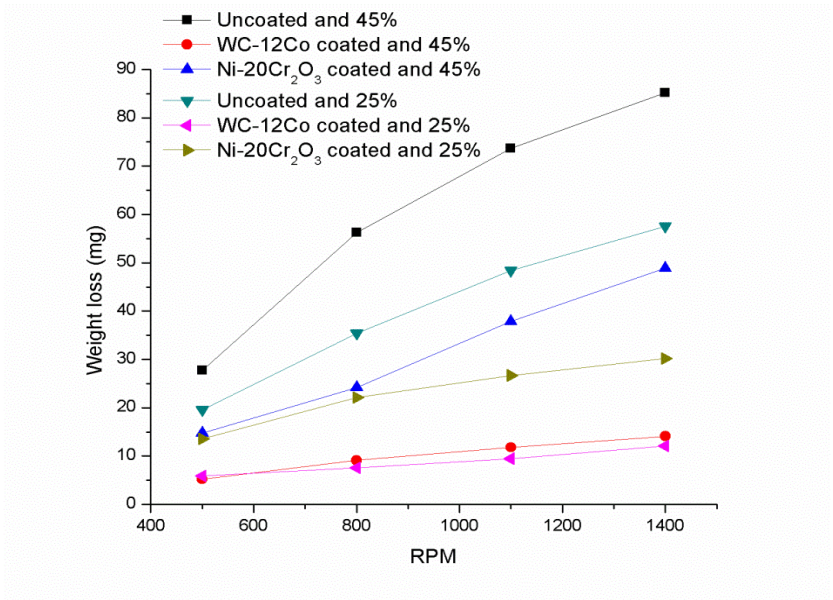

Fig. 4.15: Relative erosion of SS 304 for 90 min

It is found that at higher concentrations wear of testing materials is more and for 25% concentration with 180 min test run and for 45% concentration 90 min test run mass loss is almost same and shows similar trend for SS 304 and mild steel.

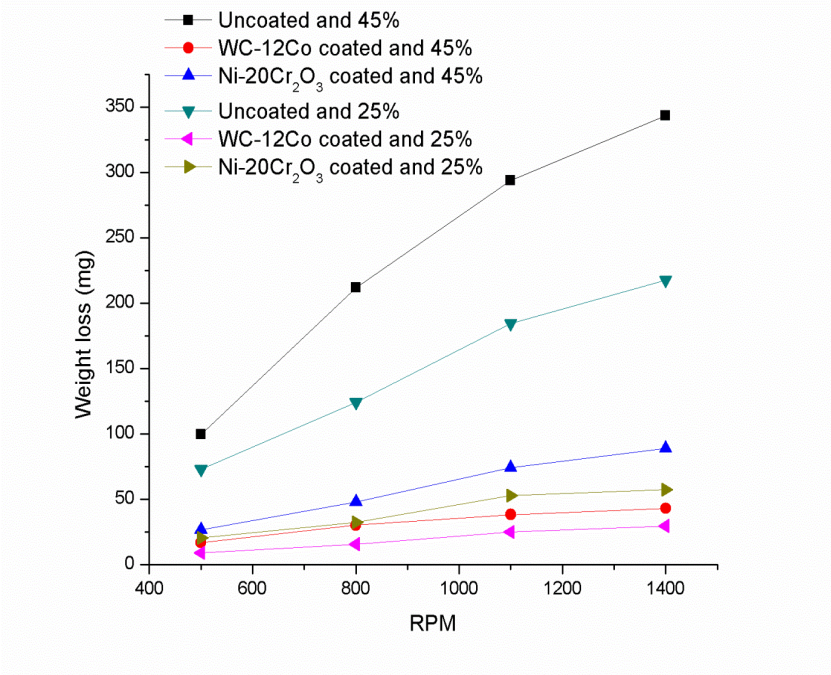

Fig. 4.16: Relative erosion of Mild steel for 180 min

It is also important that difference in the mass loss of all these three materials is also due to different erosion mechanisms. Since hardness of all these materials is different consequently

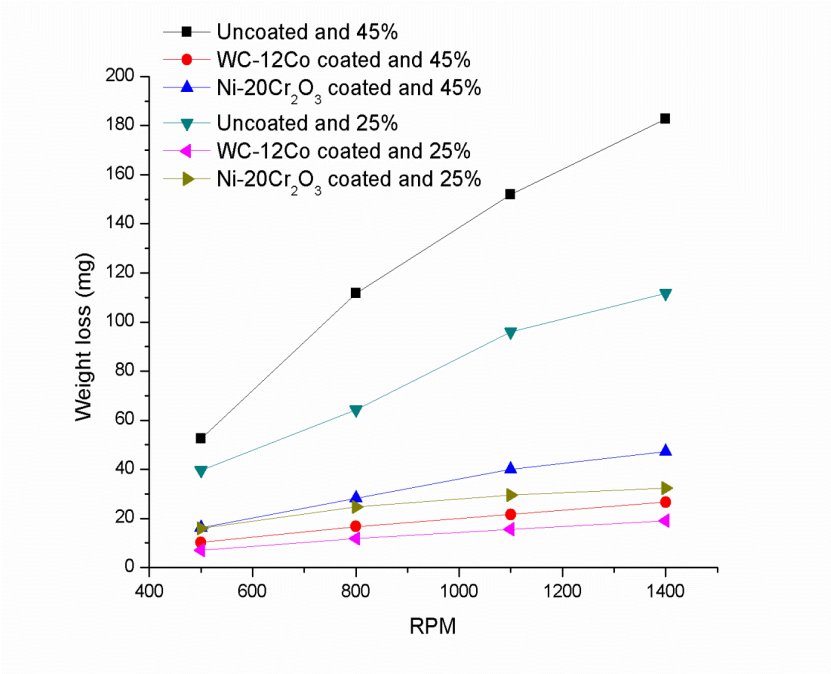

Fig. 4.17: Relative erosion of Mild steel for 90 min

micro-structure of these materials posses different phases, which may lead to different erosion wear mechanisms such as cutting, ploughing etc.

From Fig. 4.16 and Fig. 4.17 it is clear that erosion resistance of mild steel increased much with both type of coatings, but with tungsten based coating wear resistance improved in excellent way as compared to nickel based coating.

Also major constituents of bottom ash are much hard than these three testing materials which cause erosion of these materials at mass level mainly in ductile manner of erosion and hardness of these materials is relatively low and these posses ductile nature of failure. Mass loss at mass level is responsible for the failure of the piping system. Coating improved the erosion resistance of these three materials, but tungsten based coating improved the erosion resistance on all the materials considerably as compared to nickel based coating.

4.5 EXAMINATION OF MATERIAL REMOVAL MECHANISM

Scanning electron microscopes images are taken of all the coated materials for the examination of erosion or material removal mechanism after 180 min experimental run at 45% concentration and at 1400 rpm, all these factors are chosen because at these extreme conditions maximum erosion is noticed in earlier experiments. Backscattered electron topographic images of worn out top surface are also taken to visualize the micro structure of the surfaces.

Fig. 4.18 (a), (b) and (c) shows the backscattered electron topographic images of worn out WC-12Co coated SS 20, SS 304 and Mild steel materials respectively, black colour in the images shows the presence of tungsten carbide and cobalt matrix, as shown by the electron dispersive x-ray spectroscopic images, from these figures it seems that tungsten carbide phase is more in area in case of SS 202 substrate, as compared to other two substrate materials, and it seems in less quantity in case of mild steel substrate. This may be the cause due to which mild steel shows more erosion as compared to other two materials because tungsten carbide is the hardest material present in the cobalt matrix and always present in the large quantity as compared to cobalt, cobalt acts as binder material in this case.

More erosion of mild steel as noticed in tungsten based coating may also be due to less affinity of Mild steel towards coating material as compared SS 202 and SS 304 materials, since less tungsten carbide phase is detected on the surface of coated Mild steel substrate. 54.40% tungsten weight is detected in black colour phase. Also small amount of erodent are

also found to be present in the images on the surface of materials that may be due to embedment of hard erodent particles in the relative soft matrix to cobalt.

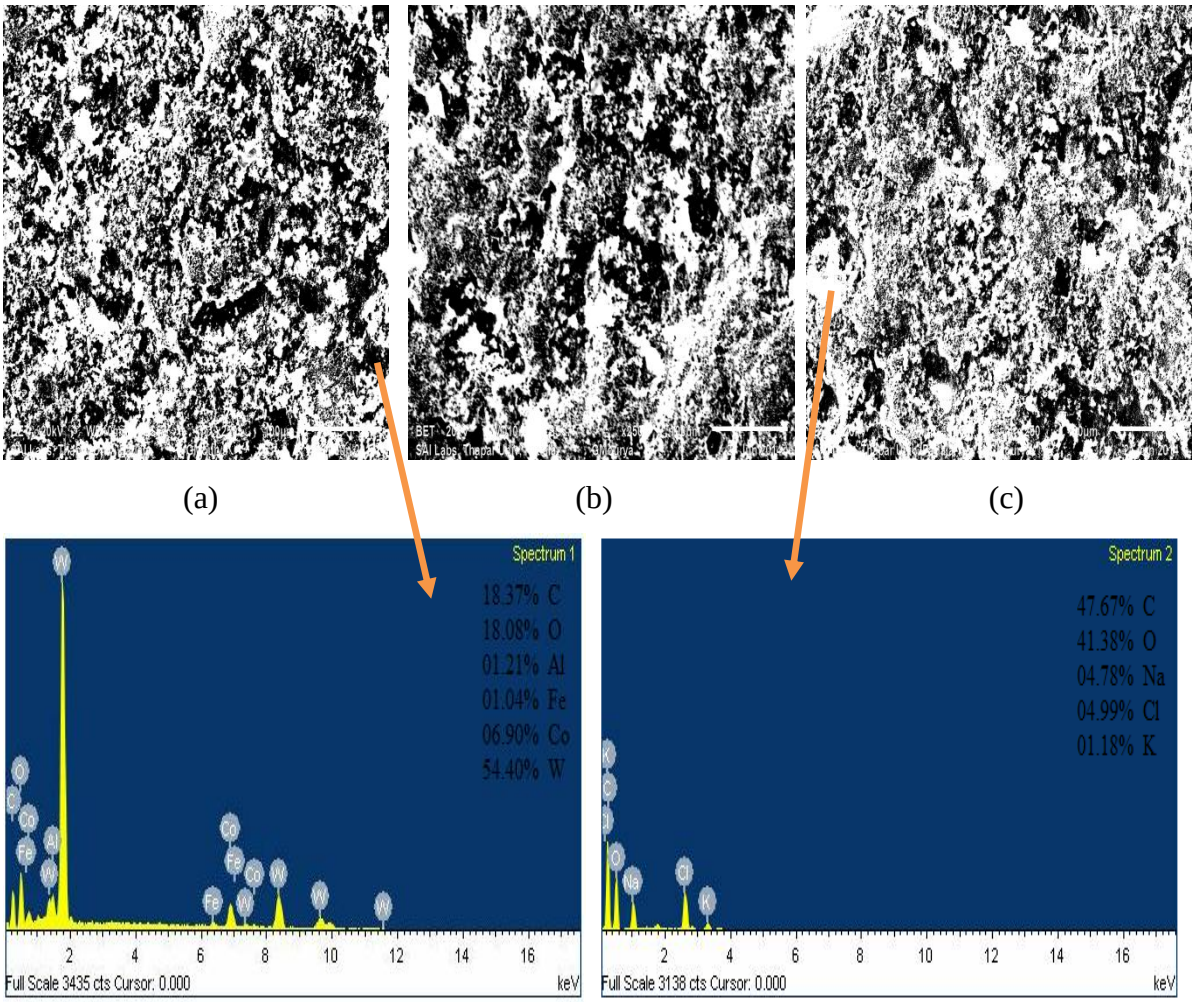

Fig. 4.18: BET and EDS images of WC-12Co coated SS 202 (a), SS 304 (b) and Mild steel (c)

A long peak of tungsten and other small peaks of tungsten confirm its presence in the dark phase of topography. Fig.4.19, Fig. 4.20 and Fig. 4.21 shows the scanning dispersive x-ray spectroscopy images of eroded WC-12Co coated SS 202, SS 304 and Mild steel substrates respectively, all the coating surfaces are eroded for 180 min in slurry pot tester at 1400 rpm using 45% slurry concentration. It is observed from these images the erosion of tungsten based coating is mainly because of brittle wear mechanisms and slightly ductile erosion wear is detected on the coating of mild steel substrate, mainly crater lip, carbide fracture and carbide pullout wear mechanisms are observed from the SEM images, while micro cutting is found dominated in case of coated mild steel materials. It may be due to more splats, splat

boundaries and melted particles of coatings, also conversion of tungsten monocarbide (WC) into tungsten hemicarbide (W_2C) which is less hard material.

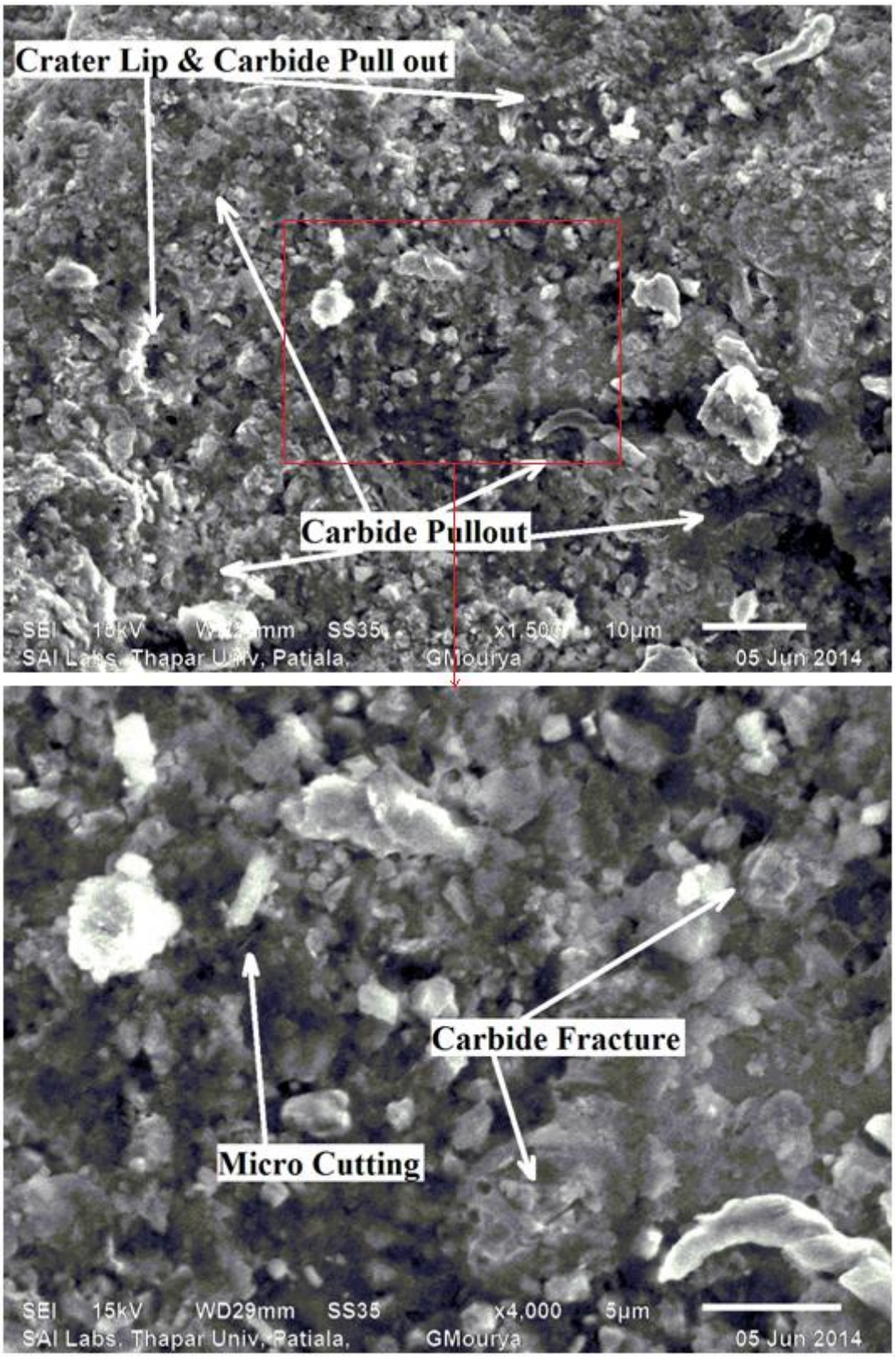

Fig. 4.19: SEM images of eroded WC-12Co coated SS 202 material, for 180 min at 1400 rpm using 45% slurry concentration

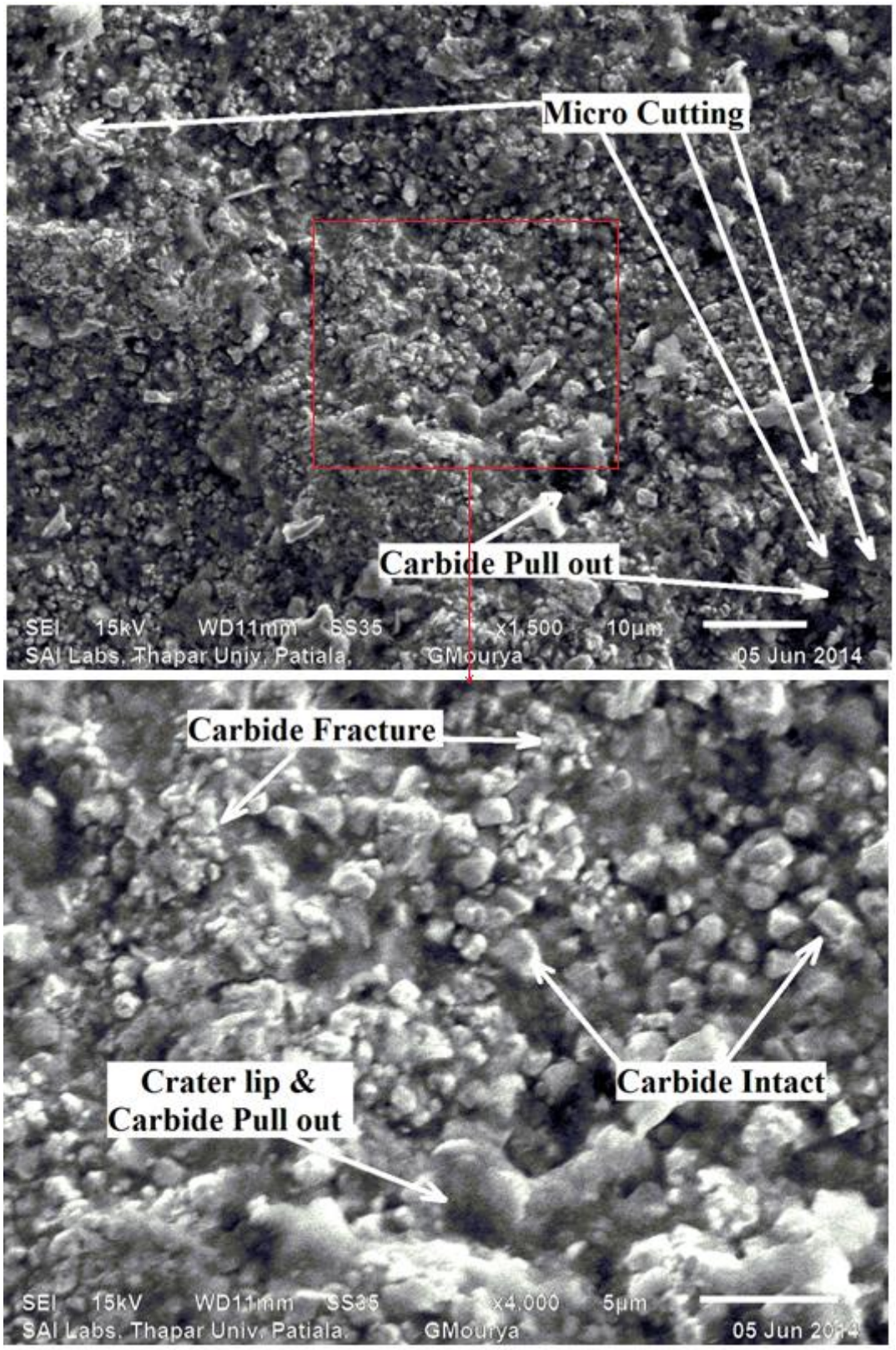

Fig. 4.20: SEM images of eroded WC-12Co coated SS 304 material, for 180 min at 1400 rpm using 45% slurry concentration

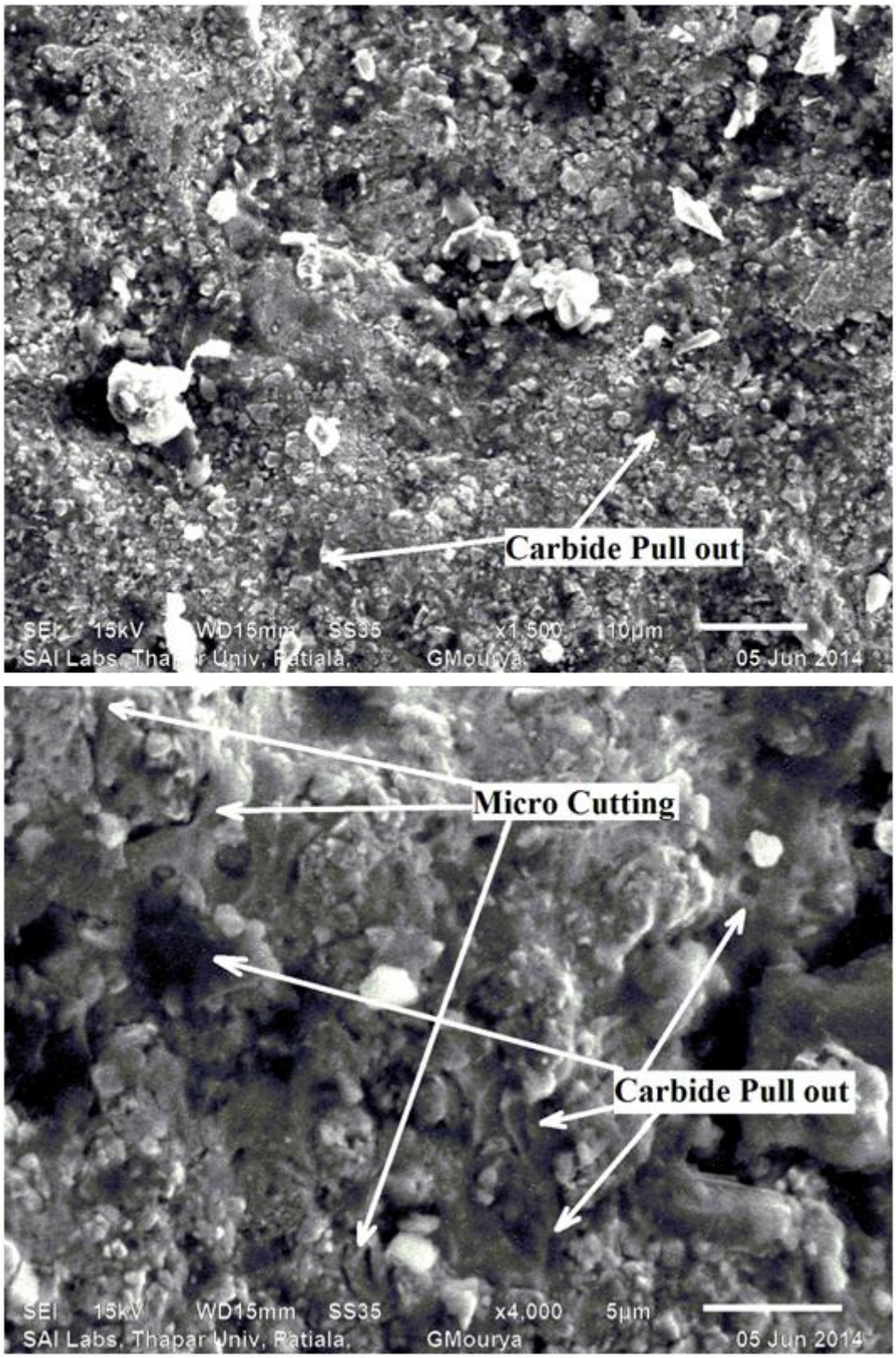

Fig. 4.21: SEM images of eroded WC-12Co coated Mild steel material, for 180 min at 1400 rpm using 45% slurry concentration

From the analysis of above micrographs mainly the following erosion mechanisms are observed in tungsten based coating, because hardness observed in these coating in high that's why mainly brittle mechanisms are found dominated as shown in Fig. 4.22.

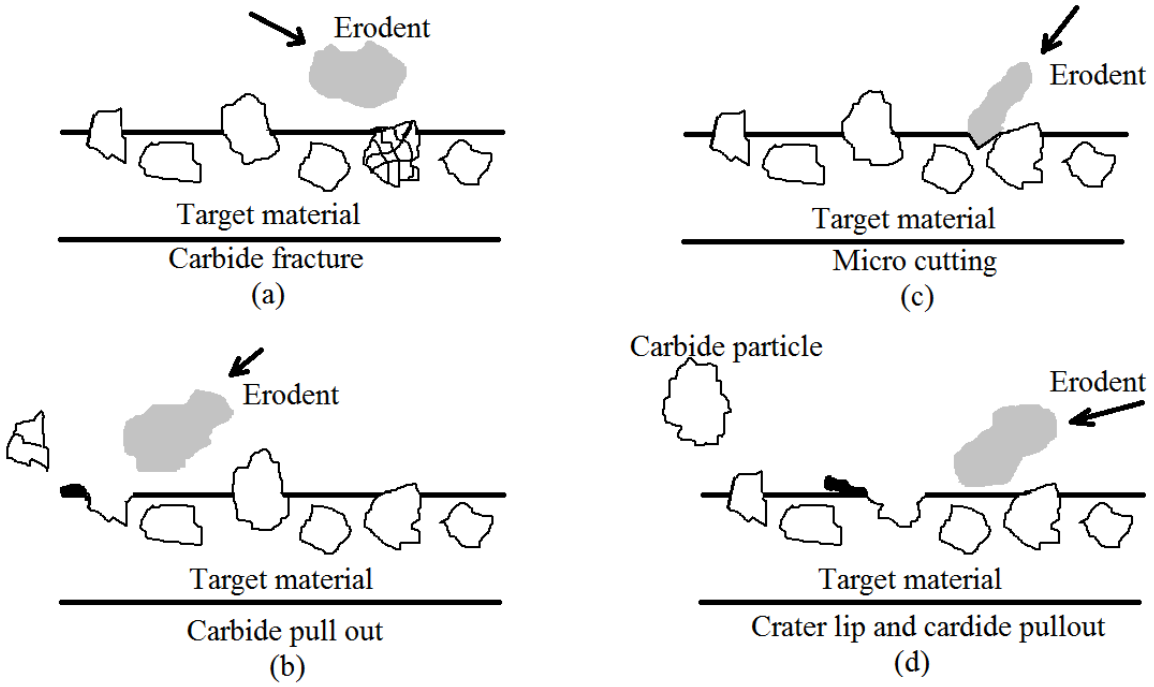

Fig. 4.22: Mechanisms of progressive wear/fracturing of tungsten carbide phases in WC-12Co coating

Concentration of tungsten carbide particles is high in cobalt matrix, due to which erodent particle mainly strikes with tungsten carbide particles and either fracturing of carbide occurs or pull out of carbide is noticed with or without fracturing. In above fig. (a) Shows the carbide fracture, in (c) case micro cutting is shown, it is observed in cases when there is some inter-particle difference between carbide particles and erodent particles gets embedded into cobalt matrix, but these micro cuts are not so deep in this case, in case (b) pull out of carbide particle from the cobalt matrix which is due to weak adhesive bond between the carbide particle and cobalt matrix, and a small lip is formed during the carbide pull out process, in case (d) crater formation is there during the carbide pullout process due to less angle between the target surface and path of erodent movement. Fig. 4.23 below shows the backscattered electron topographic images of Ni-20Cr_2O_3 coated SS 202, SS 304 and Mild steel materials. That shows the presence of nickel and chromium phases as shown in electro dispersive x-ray spectroscopy results.

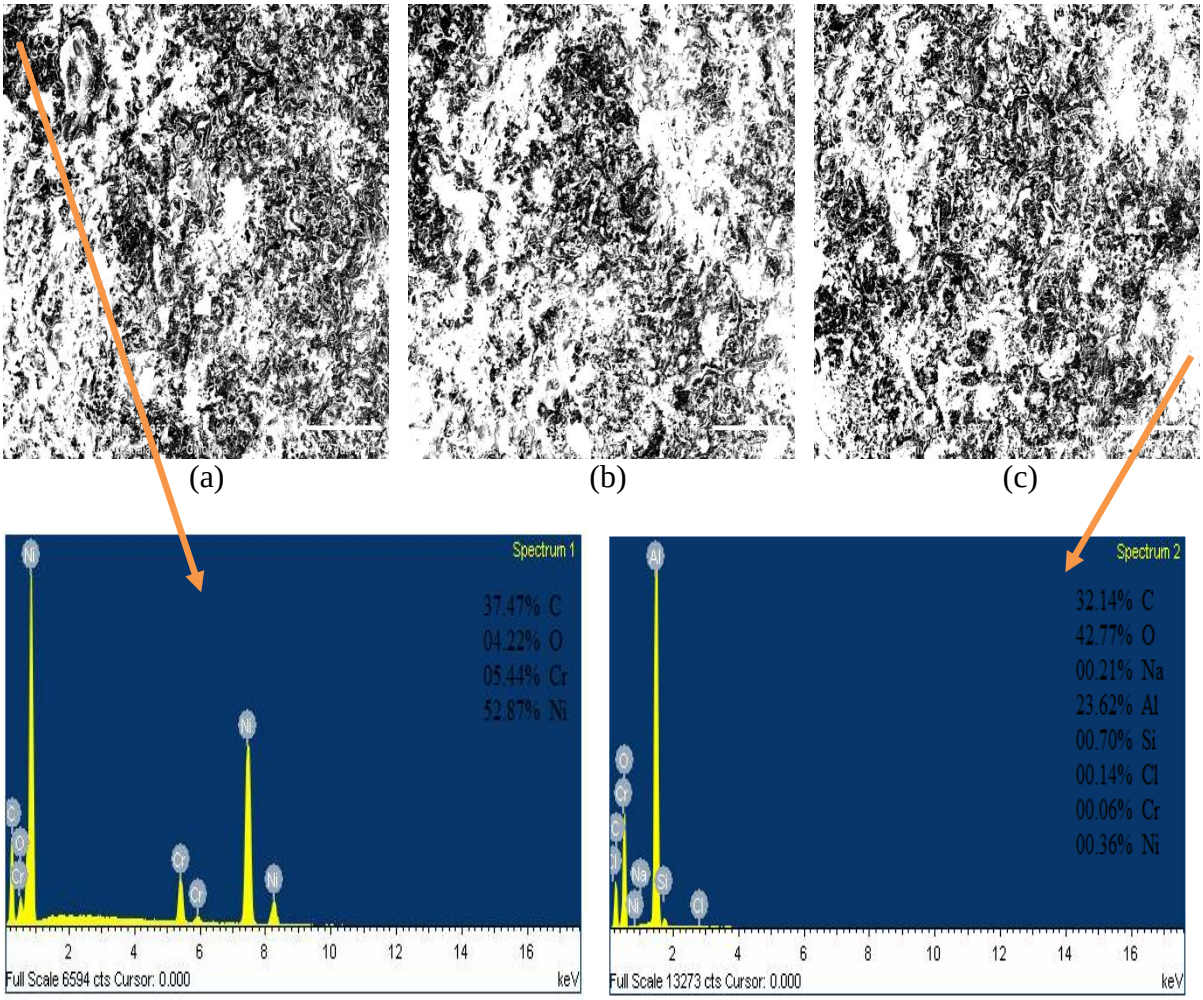

Fig. 4.23: BET and EDS images of Ni-20Cr_2O_3 coated SS 202 (a), SS 304 (b) and Mild steel (c)

Dark phase shows the presence of large amount of nickel and small amount of chromium present in the coating topography.

Mainly ductile erosive mechanisms are observed in the wear analysis. Fig. 4.24, Fig. 4.25 and 4.26 shows the SEM images of eroded SS 202, SS 304 and Mild steel respectively, these target materials are eroded in slurry pot tester for 180 min at 1400 rpm at 45% bottom ash slurry concentration. lip formation, crater formation, chip breakage and micro cutting is mainly observed in the progressive erosion wear mechanisms.

Large frequency of micro cutting is found dominated in the nickel based coatings, it may be due to ductile nature of nickel based coating and less carbide formation in the nickel matrix due to small presence of chromium oxide and chromium carbide particles, it is also observed that there are very few number of micro pores are present in the nickel based coatings and these pores are slightly large in number as compared to tungsten based coatings, this may be

due to relatively less velocity during the high velocity oxy-fuel spray process in nickel based coatings as compared to tungsten based coatings.

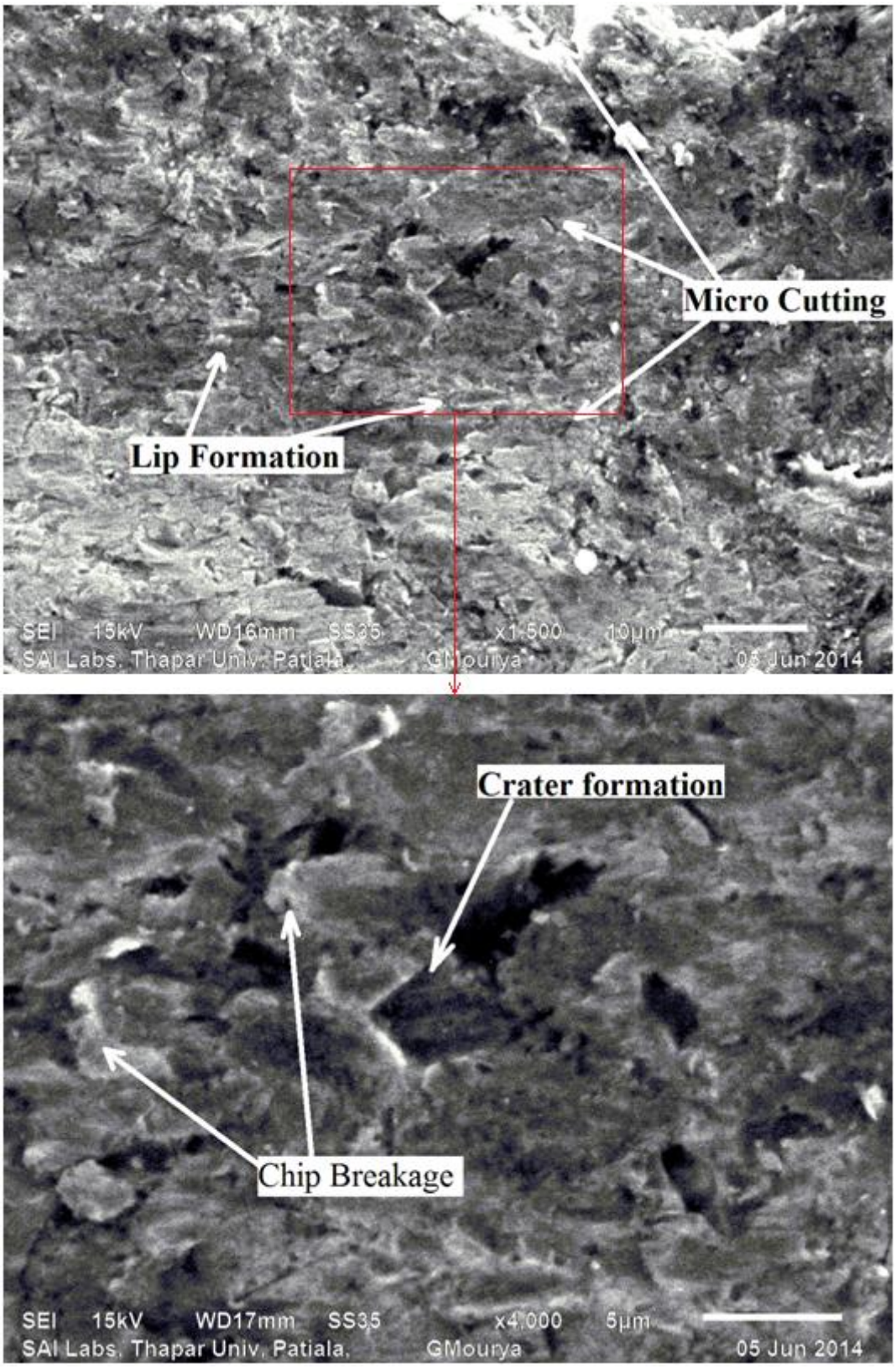

Fig. 4.24: SEM images of eroded Ni-20Cr_2O_3 coated SS 202, for 180 min at 1400 rpm using 45% slurry concentration

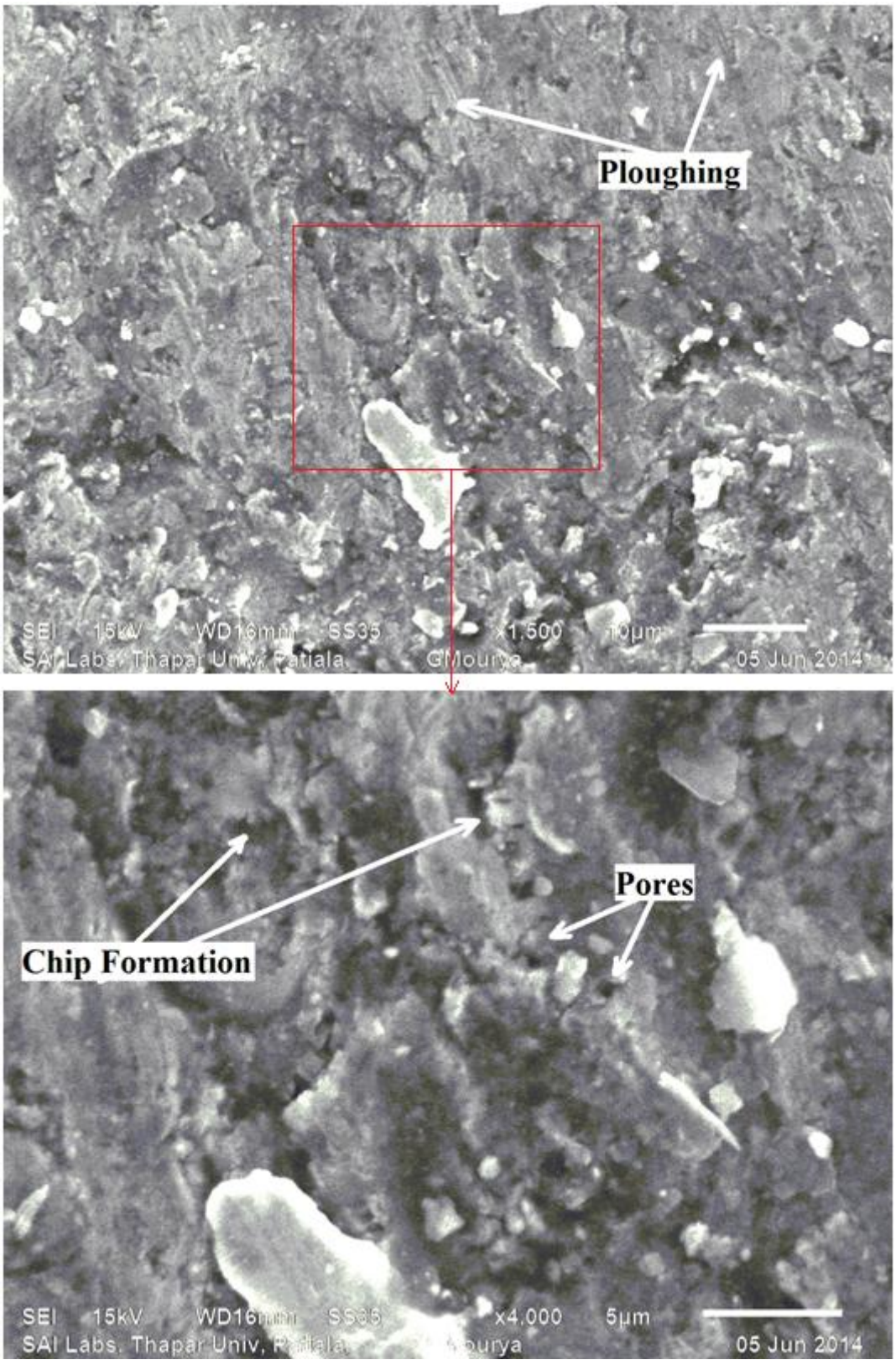

Fig. 4.25: SEM images of eroded Ni-20Cr_2O_3 coated SS 304, for 180 min at 1400 rpm using 45% slurry concentration

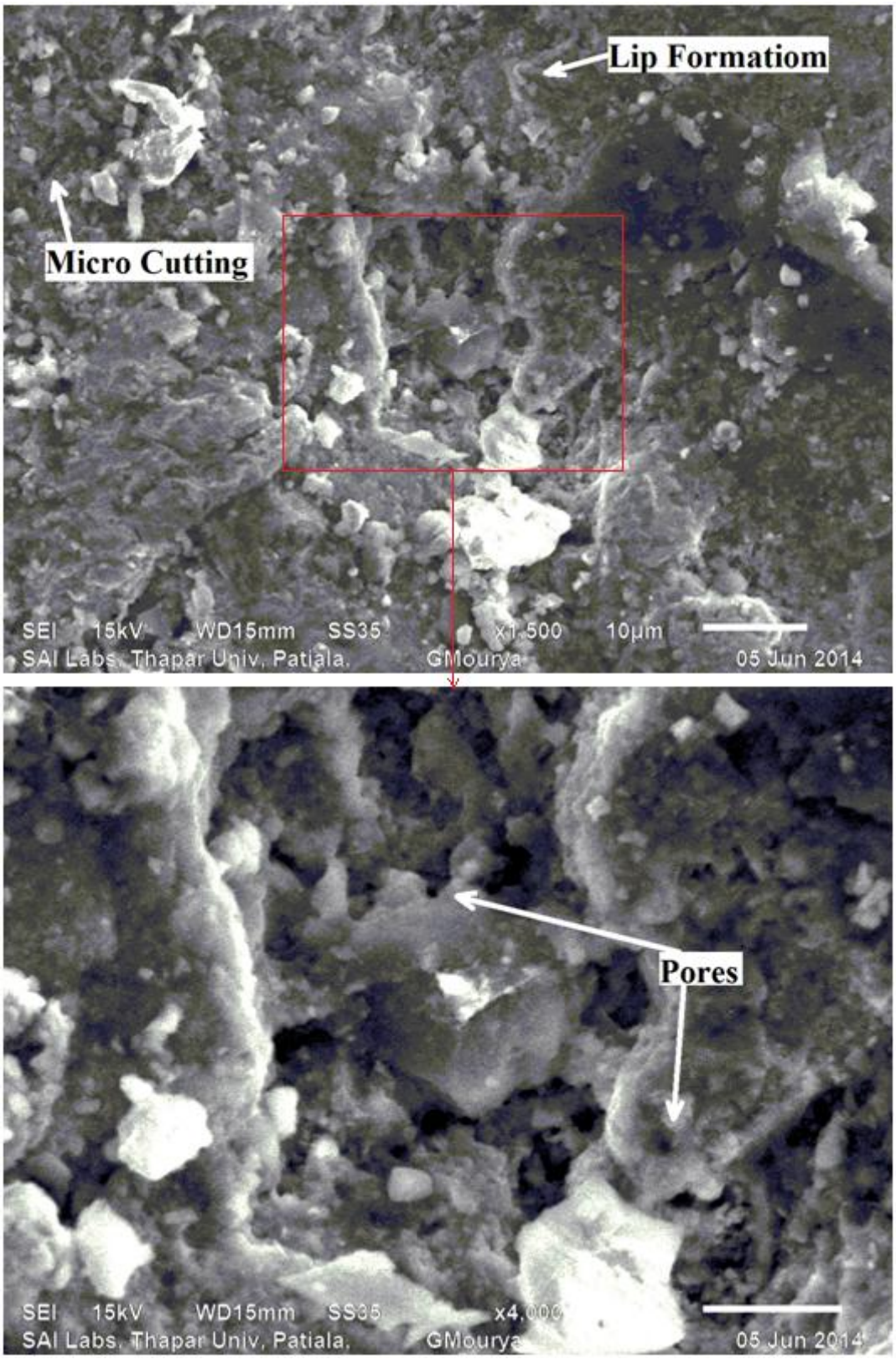

Fig. 4.26: SEM images of eroded Ni-20Cr_2O_3 coated Mild steel, for 180 min at 1400 rpm using 45% slurry concentration

In coated mild steel surface presence of carbide is seen in the coating, but these carbides are small in number that is why nickel based coatings mainly erode with ductile nature. As ceramic chrome oxide powder add is only limited up to 20% in nickel, large amount of chrome oxide addition may help to improve the carbide formation and hence further improve the erosion resistance of nickel based coatings. Fig. 4.27 shows the erosive wear mechanisms observed in nickel based coatings.

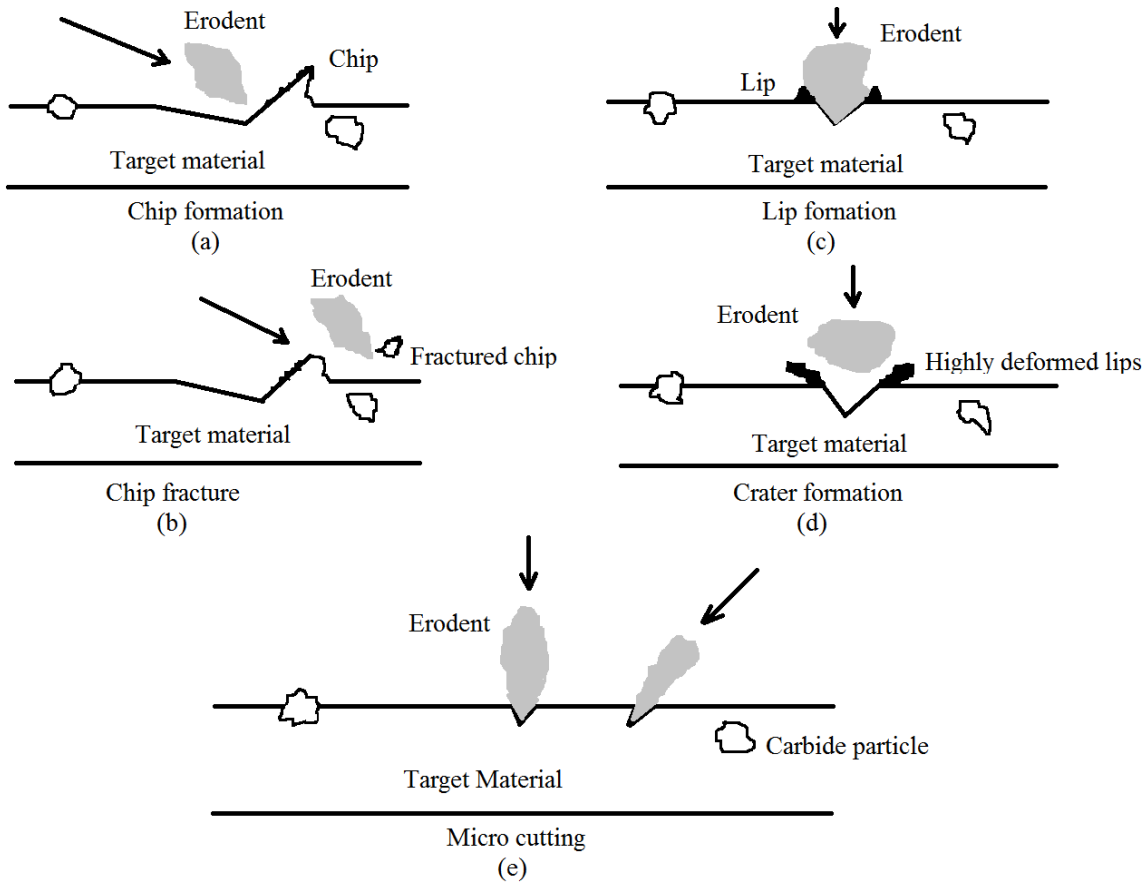

Fig. 4.27: Mechanisms of progressive wear/fracturing in Ni-Cr_2O_3 coating

In case of (a) chip formation is shown in the coating surface, a fast moving erodent particle when strikes with the target surface at obtuse angle between the target surface and direction of erodent motion. In (b) after chip formation due to further strike of same or different erodent with formed chip, chip breakage occurs and this broken chip if taken away by the slurry. In case of (c) mainly due to the strike perpendicularly flowing erodent particle with the target surface lips formation may occurs, when erodent particle gets embedded into the target surface and due to further striking of erodent particles with these formed lips, lips gets distorted and crater formation occurs (d). Micro cutting formation occurs when sharp edged

erodent particle gets slightly embedded into the target coated surface (e), this cutting action is dominated in nickel based coatings from which further cutting or erosion of coated surface gets started and rate of erosive wear increases.

CHAPTER 5

EXPERIMENTAL INVESTIGATIONS USING TAGUCHI APPROACH

Taguchi approach is used in present study for optimizing process parameters and also to find out the optimal combination of experimental factors. The input parameters/variables used in present study are also discussed earlier in this chapter, on the basis of that an orthogonal array is made as given below.

Symbol	Parameters	Level 1 (L1)	Level 2 (L2)	Level 3 (L3)	Level 4 (L4)
S	Speed (rpm)	500	800	1100	1400
C	Concentration (C_w)	25	45		
T	Time (min)	90	180		

Table 5.1: Parameters and their levels

ANOVA (Statistical analysis of variance) is performed in present study to find out the influence of experimental parameters for the erosion process. Motive of the study is to find out optimal combinations of parameters to minimize erosion for all the three materials.

5.1 ANALYSIS OF RESULTS

In Taguchi's approach results are analyzed on the basis of three basic quality characteristics.

1. The bigger the better
2. The nominal the better
3. The smaller the better

The bigger the better is used where our prime motive is to maximize the output, the nominal the better is used when output should be nominal and the smaller the better is used when to minimize the output is primary concern. The output of nine experiments given by orthogonal array is recorded and results are obtained according to the quality characteristic the smaller the better because here minimum erosion of specimens is requirement. Mean standard deviation and signal to noise ratio is calculated by using the following equations.

$$\text{MSD} = \frac{1}{\text{n}}\sum_{\text{i}}^{\text{n}}(\text{E}_{\text{w}})^2 \qquad (5.1)$$

Where n represents the repetition of experiment and E_w represents the erosion of specimens. Then S/N ratio of performed experiments was calculated by using the following equation.

$$\frac{S}{N}ratio = -10\log(MSD) \qquad (5.2)$$

S/N ratio is a generalized term which denotes the output to error ratio. So to have the minimum erosion output, an experiment must produce the highest S/N ratio.

Experiment no.	Parameter level			Experimental results for erosion (uncoated)					
				Mild steel		SS 304		SS 202	
	S	C	T	Mass loss (mg)	S/N ratio	Mass loss (mg)	S/N ratio	Mass ratio (mg)	S/N ratio
1	1	1	1	39.6	-31.95	19.6	-25.85	14.3	-23.11
2	1	1	2	72.9	-37.25	36.6	-31.27	23.8	-27.53
3	1	2	1	52.4	-34.39	27.7	-28.85	19.8	-25.93
4	1	2	2	99.8	-39.98	51.1	-34.17	34.8	-30.83
5	2	1	1	64.3	-36.16	35.4	-30.98	24.7	-27.85
6	2	1	2	124.1	-41.88	63.7	-36.08	42.2	-32.51
7	2	2	1	111.8	-40.97	56.3	-35.01	31.1	-29.86
8	2	2	2	211.9	-46.52	103.8	-40.32	58.1	-35.28
9	3	1	1	95.9	-39.64	48.4	-33.70	31.9	-30.08
10	3	1	2	184.5	-45.32	92.4	-39.31	59.3	-35.46
11	3	2	1	151.8	-43.63	73.7	-37.35	40.2	-32.08
12	3	2	2	193.8	-49.36	139.1	-42.87	75.4	-37.55
13	4	1	1	111.7	-40.96	57.5	-35.19	36.2	-31.17
14	4	1	2	217.8	-46.76	103.5	-40.30	68.6	-36.73
15	4	2	1	182.7	-45.23	85.2	-38.61	53.2	-34.52

16	4	2	2	343.5	-50.72	162.6	-44.22	99.1	-39.92

Table 5.2: Experimental layout using L16 array for uncoated materials

Experiment no.	Parameter level			Experimental results for erosion (WC-12Co coated)					
				Mild steel		SS 304		SS 202	
	S	C	T	Mass loss (mg)	S/N ratio	Mass loss (mg)	S/N ratio	Mass ratio (mg)	S/N ratio
1	1	1	1	8.6	-18.69	5.9	-15.41	6.3	-15.99
2	1	1	2	9.1	-19.18	7.7	-17.73	9.2	-19.28
3	1	2	1	11.2	-20.98	5.2	-14.32	9.8	-19.82
4	1	2	2	16.9	-24.56	8.9	-18.99	14.8	-23.40
5	2	1	1	11.8	-21.44	7.6	-17.62	10.1	-20.09
6	2	1	2	15.8	-23.97	10.2	-20.17	17.6	-24.91
7	2	2	1	16.7	-24.45	9.1	-19.18	15.7	-23.92
8	2	2	2	30.2	-29.60	14.7	-23.35	27.6	-28.82
9	3	1	1	15.6	-23.86	9.5	-19.55	13.4	-22.54
10	3	1	2	24.9	-27.92	17.2	-24.71	21.8	-26.77
11	3	2	1	21.6	-26.69	11.8	-21.44	19.6	-25.85
12	3	2	2	38.3	-31.66	23.3	-27.35	35.5	-31.01
13	4	1	1	19.1	-25.62	12.1	-21.66	19.2	-25.67
14	4	1	2	29.7	-29.45	19.6	-25.84	27.4	-28.75
15	4	2	1	26.6	-28.49	14.1	-22.98	22.5	-27.04
16	4	2	2	43.1	-32.69	25.8	-28.23	40.8	-32.21

Table 5.3: Experimental layout using L16 array for WC-12Co coated materials

Signal to noise ratio (S/N) of weight loss after experiment run for uncoated, WC-12Co and Ni-20Cr_2O_3 coated materials (Mild steel, SS 304 and SS 202) is given in Table 5.2, 5.3 and 5.4 respectively, general behaviour of obtained S/N ratio for a particular experiment is proportional to the weight loss obtained in that particular experiment, that is more is the weight loss more is the S/N ratio and less is the weight loss lesser is the S/N ratio.

Experiment no.	Parameter level			Experimental results for erosion (Ni-20Cr_2O_3 coated)					
				Mild steel		SS 304		SS 202	
	S	C	T	Mass loss (mg)	S/N ratio	Mass loss (mg)	S/N ratio	Mass ratio (mg)	S/N ratio
1	1	1	1	15.9	-24.03	13.6	-22.67	12.2	-21.73
2	1	1	2	20.5	-26.24	20.1	-26.06	15.9	-24.03
3	1	2	1	16.2	-24.19	14.8	-23.41	14.4	-23.17
4	1	2	2	26.8	-28.56	27.8	-28.88	24.5	-27.78
5	2	1	1	24.7	-27.85	22.1	-26.89	19.3	-25.71
6	2	1	2	32.5	-30.24	31.5	-29.97	25.8	-28.23
7	2	2	1	28.3	-29.04	24.4	-27.75	24.5	-27.78
8	2	2	2	47.9	-33.61	48.6	-33.73	42.7	-32.61
9	3	1	1	29.5	-29.40	26.7	-28.53	24.7	-27.85
10	3	1	2	52.9	-34.47	48.9	-33.79	40.6	-32.17
11	3	2	1	40.1	-32.06	37.9	-31.57	31.8	-30.05
12	3	2	2	74.4	-37.43	69.1	-36.79	62.8	-35.96
13	4	1	1	32.3	-30.18	30.2	-29.60	29.7	-29.46
14	4	1	2	57.4	-35.18	59.1	-35.43	48.6	-33.73
15	4	2	1	47.2	-33.48	48.9	-33.79	38.4	-31.69
16	4	2	2	89.1	-38.99	83.1	-38.39	72.9	-37.25

Table 5.4: Experimental layout using L16 array for Ni-20Cr_2O_3 coated materials

For uncoated all the three materials Mild steel, SS 304 and SS 202 S/N ratio for independent factor (speed, concentration and time) is given in Table 5.5, 5.6 and 5.7 respectively. In all these cases effect of speed on the erosion is obtained maximum followed by time and concentration parameters. For speed that is number of revolutions of specimen, value of delta is maximum (10.03) for Mild steel uncoated material this signifies effect of speed is more for this material and value of delta is minimum (8.73) for SS 202 this signifies effect of speed is less for this uncoated materials as compared to other two uncoated materials. Similar trend is also seen in case of concentration and time parameters, and accordingly ranks are also given in tables for different dominating parameters on the erosion of all these three uncoated materials.

Factors	Mild steel					
	L1	L2	L3	L4	Delta	Rank
S	-35.89	-41.38	-44.49	-45.92	10.3	1
C	-39.99	-43.85			3.86	3
T	-39.12	-44.72			5.6	2

Table 5.5: S/N response table for uncoated Mild steel

Factors	SS 304					
	L1	L2	L3	L4	Delta	Rank
S	-30.04	-35.60	-38.31	-39.58	9.18	1
C	-34.08	-37.68			3.60	3
T	-33.19	-38.57			5.38	2

Table 5.6: S/N response table for uncoated SS 304

Factors	SS 202					
	L1	L2	L3	L4	Delta	Rank
S	-26.85	-31.38	-33.79	-35.58	8.73	1
C	-30.56	-33.25			2.69	3
T	-29.32	-34.48			5.16	2

Table 5.7: S/N response table for uncoated SS 202

Contour plots on erosion wear for uncoated Mild steel, SS 304 and SS 202 are shown in Fig. 5.1, 5.2 and 5.3 respectively. Erosion vs S/N ratio, speed plot shows that for higher signal to noise ration erosion that is weight loss is minimum at lower speeds, but as we proceed towards the higher speed for the same signal to noise ratio erosion wear increases as clearly noticed from figure and in S/N ratio vs speed, concentration plot shows the maximum signal to noise ratio for the least values of speed and slurry concentration, as we proceed towards the higher speed and concentration values in that particular area value of signal to noise ratio is comparatively less with respect to initial situation. Similar trend is noticed in all the three uncoated materials but main variations in plots is due to difference in the erosion wear and signal to noise ratio in all the three different cases.

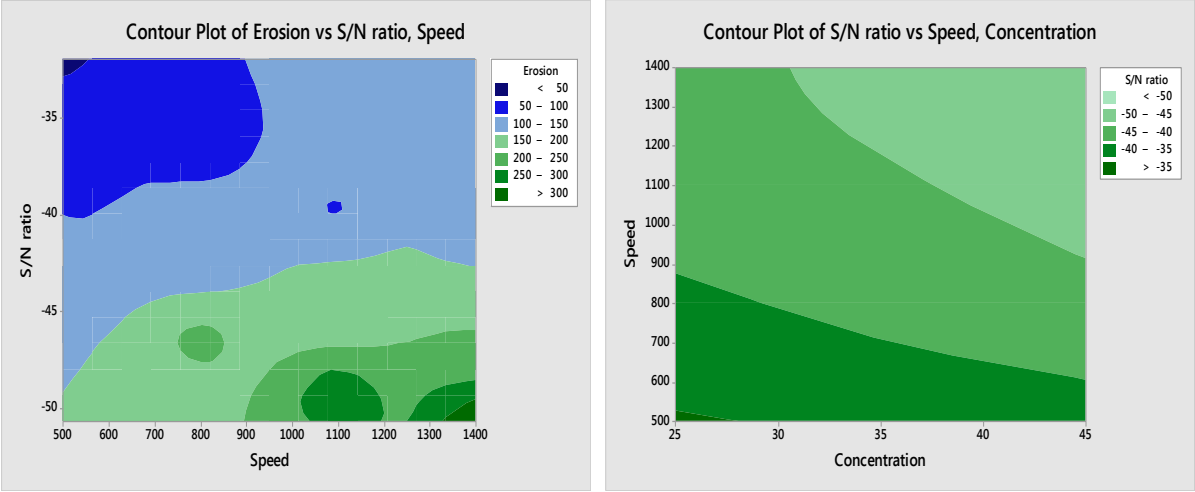

Fig. 5.1: Contour plots on erosion wear for uncoated Mild steel

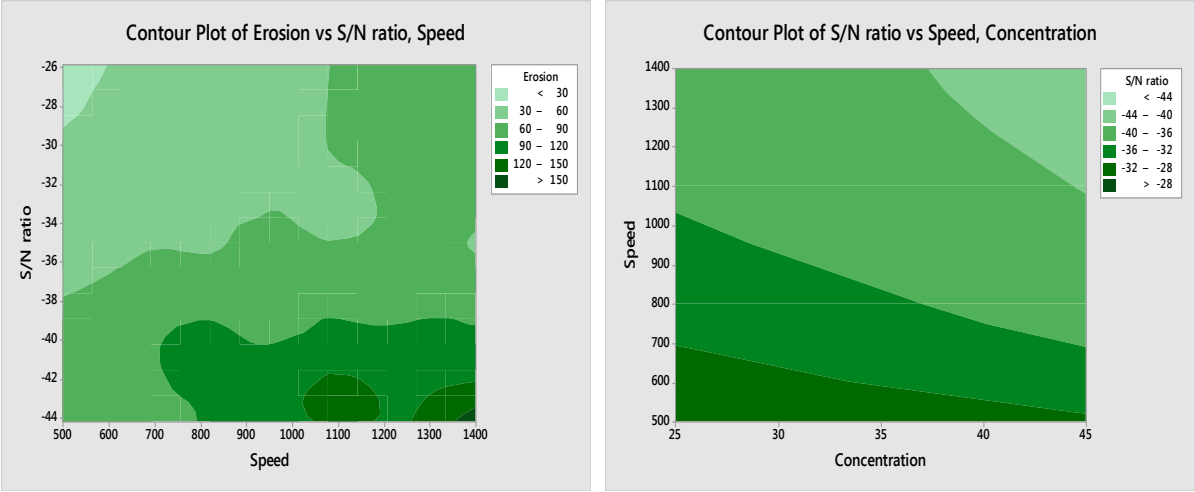

Fig. 5.2: Contour plots on erosion for uncoated SS 304

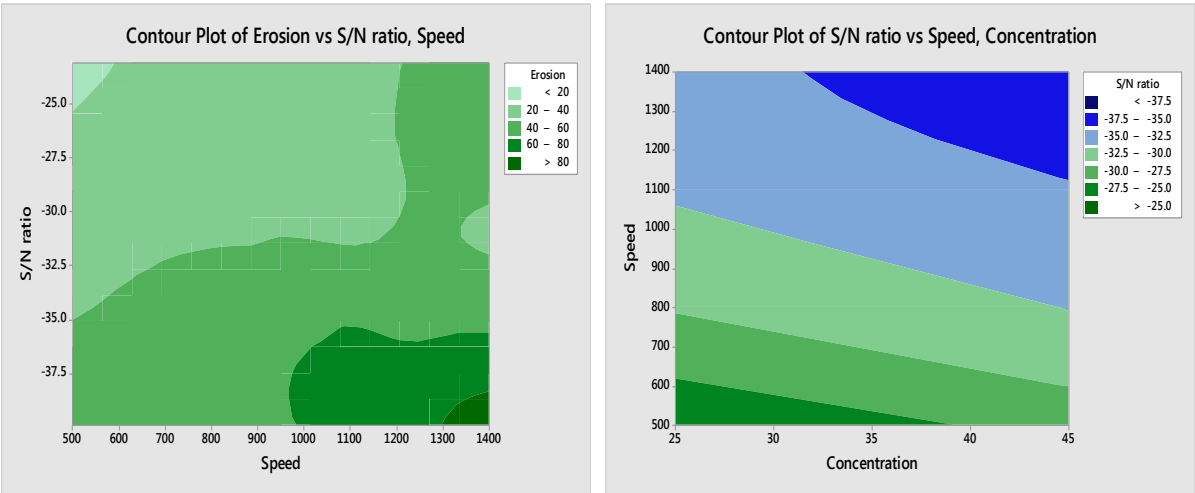

Fig. 5.3: Contour plots on erosion wear for uncoated SS 202

WC-12Co coated materials also found behaving in similar way as discussed above, Table 5.8, 5.9 and 5.10 gives the S/N response table for tungsten based coated Mild steel, SS 304 and SS 202 substrate materials respectively. Effect of speed is found dominated followed by time and concentration parameters, value of delta for speed parameter is maximum (8.83) for Mild steel and minimum (8.07) for SS 304. That is in case of tungsten based coating instead of SS 202 substrate material, SS 304 substrate material have less effect of number of revolutions of the specimen in the erosion tester. Effect of concentration is also minimum (1.64) for SS 304 tungsten based coated material and maximum (3.73) for Mild steel substrate material that is more than double as compared tungsten based coated 304 substrate material.

Factors	WC-12Co coated Mild steel					
	L1	L2	L3	L4	Delta	Rank
S	-20.23	-24.87	-27.53	-29.07	8.83	1
C	-23.56	-27.29			3.73	3
T	-23.47	-27.38			3.91	2

Table 5.8: S/N response table for WC-12Co coated Mild steel

Factors	WC-12Co coated SS 304					
	L1	L2	L3	L4	Delta	Rank
S	-16.61	-20.08	-23.26	-24.68	8.07	1
C	-20.34	-21.98			1.64	3
T	-19.02	-23.30			4.28	2

Table 5.9: S/N response table for WC-12Co coated SS 304

Factors	WC-12Co coated SS 202					
	L1	L2	L3	L4	Delta	Rank
S	-19.62	-24.43	-26.54	-28.42	8.80	1
C	-23.00	-26.51			3.51	3
T	-22.61	-26.89			4.28	2

Table 5.10: S/N response table for WC-12Co coated SS 202

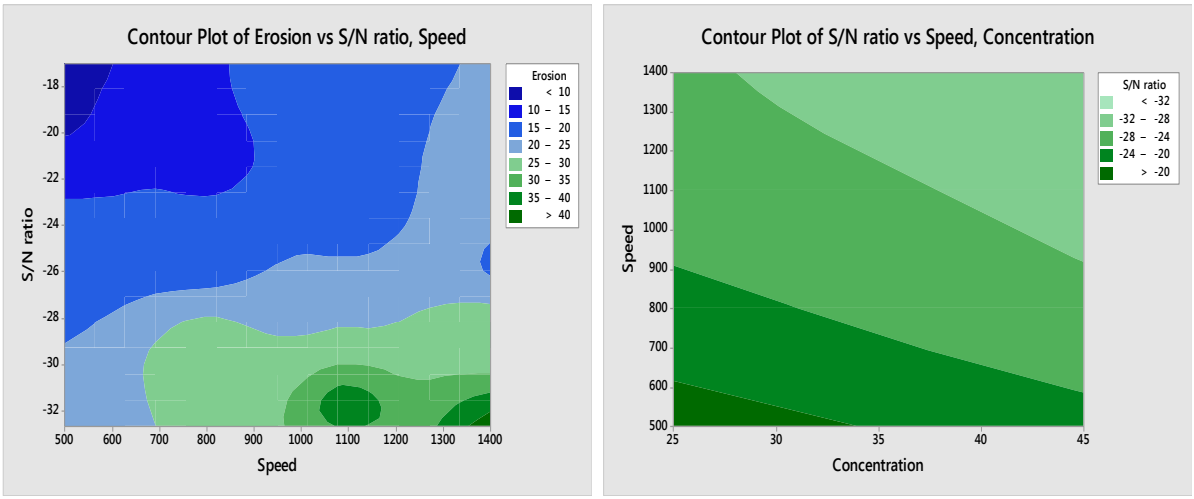

Fig. 5.4: Contour plots on erosion wear for WC-12Co coated Mild steel

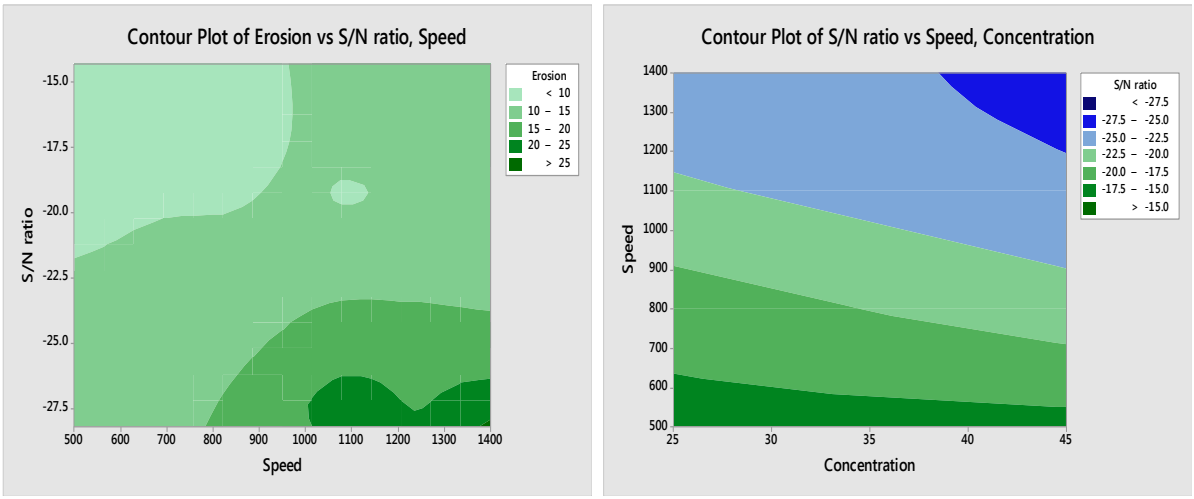

Fig. 5.5: Contour plots on erosion wear for WC-12Co coated SS 304

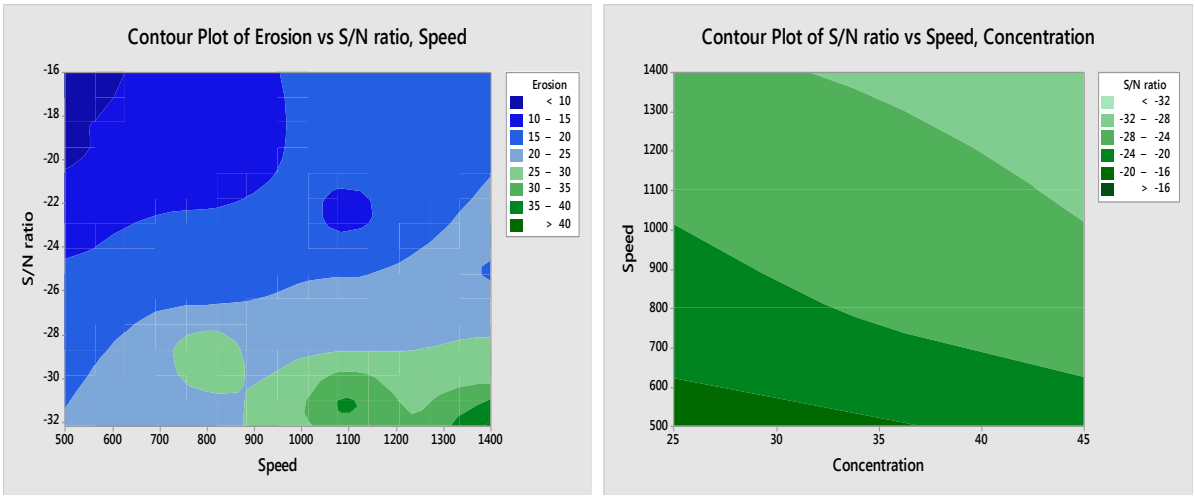

Fig. 5.6: Contour plots on erosion wear for WC-12Co coated SS 202

Contour plots WC-12Co coated Mild steel, SS 304 and SS 202 material are shown in Fig. 5.4, 5.5 and 5.6 respectively. The entire trends obtained in this case are similar to the uncoated materials, as for large signal to noise ratio values; speed and concentration values are minimum on the plot. Mainly for SS 304 plot behaviour is slightly different from other two coated materials because of less erosion measured in this case.

Factors	Ni-20Cr_2O_3 coated Mild steel					
	L1	L2	L3	L4	Delta	Rank
S	-25.75	-30.18	-33.34	-34.46	8.71	1
C	-29.70	-32.17			2.47	3
T	-28.78	-33.09			4.31	2

Table 5.11: S/N response table for Ni-20Cr_2O_3 coated Mild steel

Factors	Ni-20Cr_2O_3 coated SS 304					
	L1	L2	L3	L4	Delta	Rank
S	-25.26	-29.58	-32.67	-34.30	9.05	1
C	-29.12	-31.79			2.67	3
T	-28.03	-32.88			4.86	2

Table 5.12: S/N response table for Ni-20Cr_2O_3 coated SS 304

Factors	Ni-20Cr_2O_3 coated SS 202					
	L1	L2	L3	L4	Delta	Rank
S	-24.18	-28.58	-31.51	-33.03	8.86	1
C	-27.86	-30.79			2.92	3
T	-27.18	-31.47			4.29	2

Table 5.13: S/N response table for Ni-20Cr_2O_3 coated SS 202

Signal to noise response tables for Ni-20Cr_2O_3 coated Mild steel, SS 304 and SS 202 are shown in Table 5.11, 5.12 and 5.13 respectively. Again in this case also trend noticed is same as in previous coated and WC-12Co coated materials, as effect is found to be dominated over the concentration and time parameters and is followed by time and concentration.

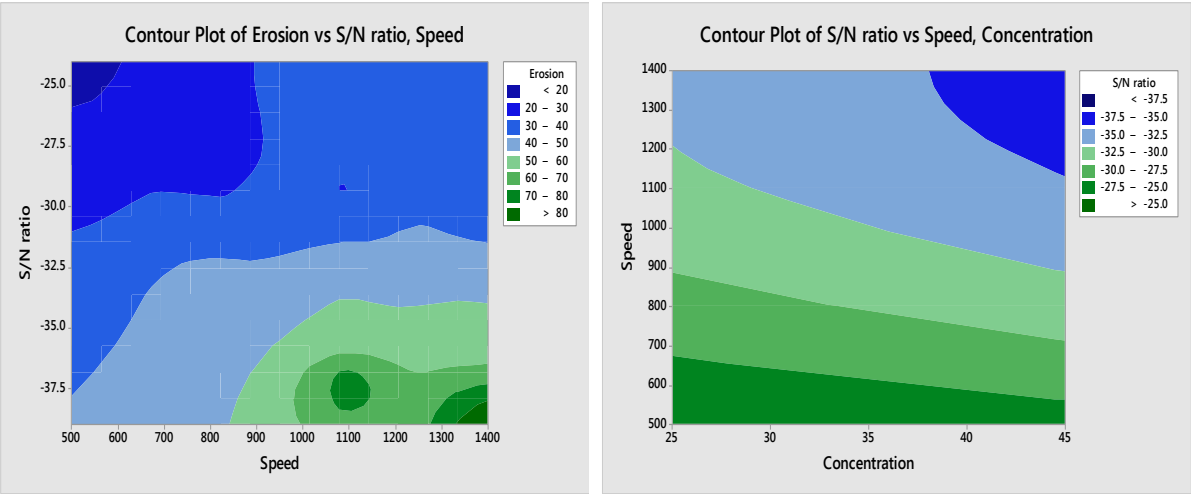

Fig. 5.7: Contour plots on erosion wear for Ni-20Cr_2O_3 coated Mild steel

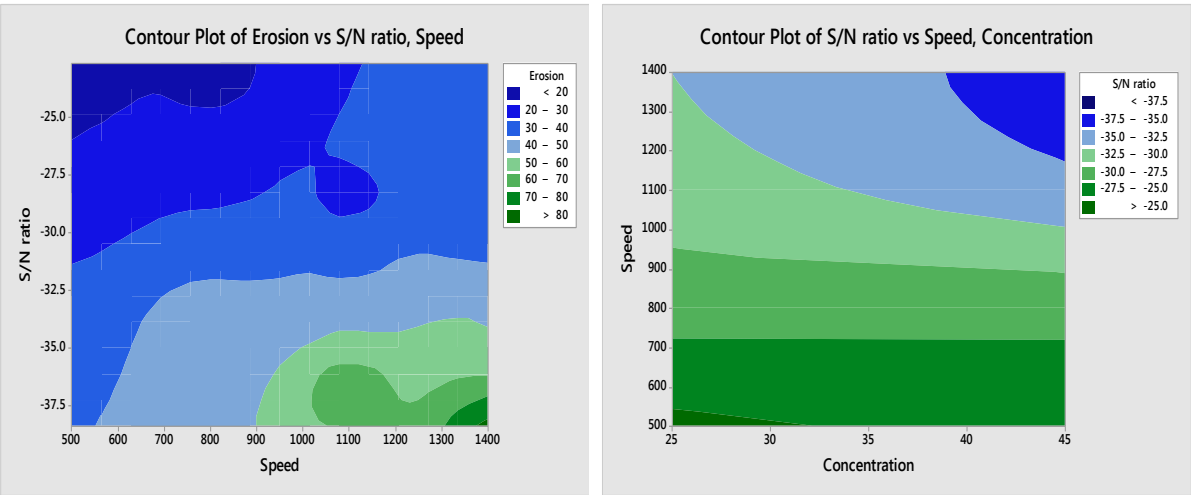

Fig. 5.8: Contour plots on erosion wear for Ni-20Cr_2O_3 coated SS 304

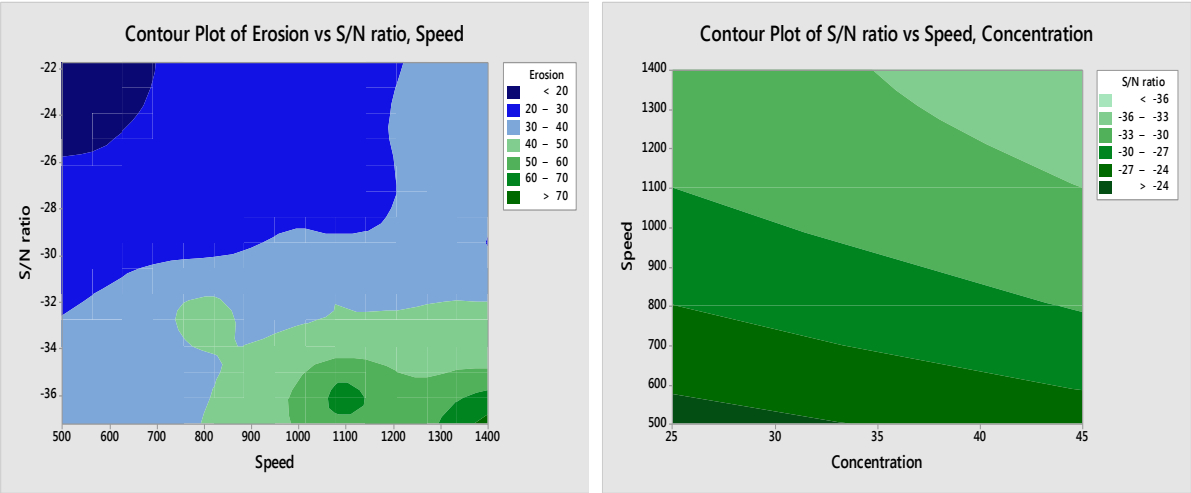

Fig. 5.9: Contour plots on erosion wear for Ni-20Cr_2O_3 coated SS 202

Ni-20Cr_2O_3 coated Mild steel, SS 304 and SS 202 shows the slight variations from the previously discussed uncoated and WC-12Co coated materials in the contour plots as shown in Fig. 5.7, 5.8 and 5.9 respectively, since nickel coated SS 202 has minimum value of signal to noise ratio consequently there are variations in the plots.

5.2 VALIDATION STUDIES BY ANOVA (ANALYSIS OF VARIANCE)

The results obtained from Taguchi method for optimization of linseed oil methyl ester production were statistically verified by ANOVA (analysis of variance). The term variance ratio, which is ratio of variance of factor to error variance, distinguishes the more significant factors from less significant. More than 9 variance ratio for a factor represents that the factor is having an erosion of specimens and tables below shows the analysis of variance using S/N ratios of performed experiments for all parameters.

The various terms of ANOVA that are used for the calculation are given below in the series of small equations:

$$C.F. = \frac{T^2}{n} \tag{5.3}$$

$$S_T = \sum_i^n y_i^2 - C.F. \tag{5.4}$$

$$S = \frac{A_1^2}{N_1} + \frac{A_2^2}{N_2} + \frac{A_3^2}{N_3} - C.F. \tag{5.5}$$

$$V = \frac{S}{f} \tag{5.6}$$

$$F = \frac{V}{V_e} \tag{5.7}$$

$$S_P = S - f \times V_e \tag{5.8}$$

Where T is total of all the weight loss obtained, n is total number of experiments, A_1 is sum of all the S/N ratios under level 1 of any parameter, N_1 is number of experiments having level 1 of any parameter, A_2 is sum of all the S/N ratios under level 2 of any parameter, N_2 is number of experiments having level 2 of any parameter, A_3 is sum of all the S/N ratios under level 3 of any parameter, N_3 is number of experiments having level 3 of any parameter, f is the degree of freedom of parameter and V_e is the error variance.

Factor	D.o.f	Sum of squares (S)	Variance (V)	F-ratio (F)	Pure-sum (S_p)	Percent (%)
S	3	236.68	78.89	307.24	235.91	55.56
C	1	59.58	59.58	232.01	59.32	13.97
T	1	125.80	125.80	489.92	125.54	29.57
Error	10	2.57	0.257			00.90
Total	15	424.625				100

Table 5.14: ANOVA table for uncoated Mild steel

Factor	D.o.f	Sum of squares (S)	Variance (V)	F-ratio (F)	Pure-sum (S_p)	Percent (%)
S	3	215.39	71.80	837.27	215.14	56.11
C	1	51.55	51.55	601.14	51.46	13.42
T	1	115.63	115.63	1348.43	115.54	30.13
Error	10	0.858	0.086			00.34
Total	15	383.431				100

Table 5.15: ANOVA table for uncoated SS 304

Factor	D.o.f	Sum of squares (S)	Variance (V)	F-ratio (F)	Pure-sum (S_p)	Percent (%)
S	3	171.72	57.24	352.2	171.23	55.51
C	1	29.00	29.00	178.41	28.83	9.35
T	1	106.13	106.13	653.00	105.96	34.34
Error	10	1.63	0.163			0.8
Total	15	308.47				100

Table 5.16: ANOVA table for uncoated SS 202

Analysis of variance evaluates the percentage contribution of all the speed, slurry concentration and time parameters on the erosion wear the materials. After the taguchi analysis results are further validated with analysis of variance. Results shows uniformity of trend found in both of the analysis, effect of speed over erosion is dominating and is followed by time and concentration in all the uncoated cases as given in Table 5.14, 5.15 and 5.16.

Factor	D.o.f	Sum of squares (S)	Variance (V)	F-ratio (F)	Pure-sum (S_p)	Percent (%)
S	3	179.86	59.95	113.79	178.27	59.03
C	1	55.67	55.67	105.66	55.14	18.26
T	1	61.17	61.17	116.11	60.64	20.08
Error	10	5.27	0.53			02.63
Total	15	301.98				100.00

Table 5.17: ANOVA table for WC-12Co coated Mild steel

Factor	D.o.f	Sum of squares (S)	Variance (V)	F-ratio (F)	Pure-sum (S_p)	Percent (%)
S	3	154.48	51.53	56.73	151.75	61.30
C	1	10.78	10.78	11.87	9.87	03.99
T	1	73.12	73.12	80.50	72.21	29.17
Error	10	9.08	0.91			05.54
Total	15	247.57				100.00

Table 5.18: ANOVA table for WC-12Co coated SS 304

Factor	D.o.f	Sum of squares (S)	Variance (V)	F-ratio (F)	Pure-sum (S_p)	Percent (%)
S	3	172.22	57.41	137.26	170.96	57.19
C	1	49.28	49.28	117.84	48.86	16.34
T	1	73.27	73.27	175.18	72.85	24.37
Error	10	4.18	0.42			2.10
Total	15	298.96				100.00

Table 5.19: ANOVA table for WC-12Co coated SS 202

Similarly analysis of variance results are given in Table 5.17, 5.18 and 5.19 for WC-12Co coated and Table 5.20, 5.21 and 5.22 for Ni-Cr_2O_3 coated Mild steel, SS 304 and SS 202 materials respectively, results obtained from this analysis are in good agreement with taguchi analysis results

Factor	D.o.f	Sum of squares (S)	Variance (V)	F-ratio (F)	Pure-sum (S_p)	Percent (%)
S	3	182.46	60.82	69.45	179.82	62.00
C	1	24.46	24.46	27.94	23.58	08.13
T	1	74.34	74.34	84.90	73.46	25.33
Error	10	8.76	0.88			04.54
Total	15	290.02				100.00

Table 5.20: ANOVA table for Ni-20Cr_2O_3 coated Mild steel

Factor	D.o.f	Sum of squares (S)	Variance (V)	F-ratio (F)	Pure-sum (S_p)	Percent (%)
S	3	190.02	63.34	105.59	188.22	59.03
C	1	28.54	28.54	47.58	27.94	08.76
T	1	94.29	94.29	157.19	93.69	29.38
Error	10	5.99	0.60			02.83
Total	15	318.86				100.00

Table 5.21: ANOVA table for Ni-20Cr_2O_3 coated SS 304

Factor	D.o.f	Sum of squares (S)	Variance (V)	F-ratio (F)	Pure-sum (S_p)	Percent (%)
S	3	182.27	60.75	100.05	180.44	60.92
C	1	34.17	34.17	56.26	33.56	11.33
T	1	73.68	73.68	121.34	73.07	24.67
Error	10	6.07	0.61			03.08
Total	15	296.19				100.00

Table 5.22: ANOVA table for Ni-20Cr_2O_3 coated SS 202

Influence of three different parameters speed, concentration and time for uncoated materials is shown in Fig. 5.10, percentage contribution for each of the parameter shows the domination of factors on the erosion wear. As for SS 304 uncoated material influence of speed is more and for Mild steel influence of speed is less, this implies that Mild steel material is more suitable for the slurry transportation at different speed limits. Similarly for SS 202 uncoated material effect of slurry transportation is minimum and for Mild steel is maximum, this implies SS 202 is more preferable for slurry transportation at higher concentrations than other materials. Also Mild steel is more preferable for long life of pipe but with this material higher slurry transportation is not preferably possible because of more influence of concentration on this material. Error noticed in ANOVA results if not more than 1% for uncoated materials this ensures the preciseness of the erosion result analysis.

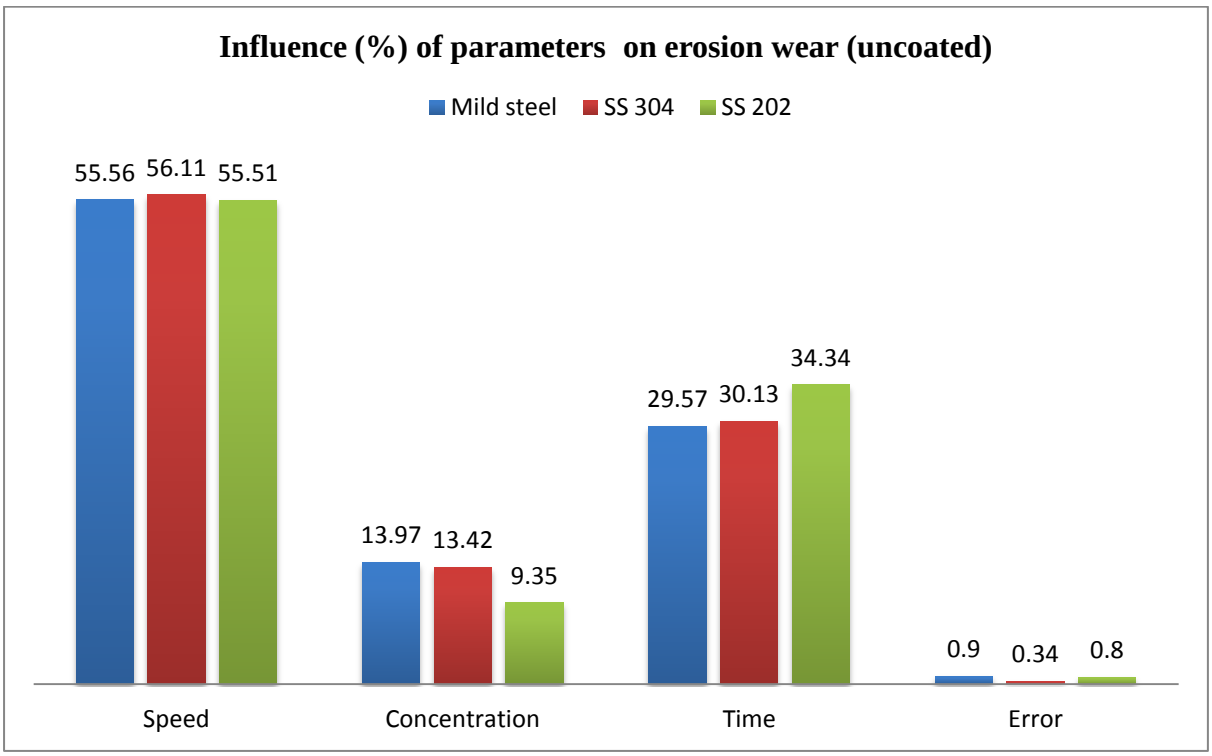

Fig. 5.10: Influence (%) of parameters on erosion wear (uncoated materials)

ANOVA analysis results for WC-12Co and Ni-20Cr_2O_3 coated Mild steel, SS 304 and SS 202 is shown in Fig. 5.11 and Fig. 5.12 respectively, it is noticed that effect of speed is minimum in case of WC-12Co coated SS 202 and Ni-20Cr_2O_3 coated SS 304 and maximum for WC-12Co coated SS 304 and Ni-20Cr_2O_3 Mild steel.

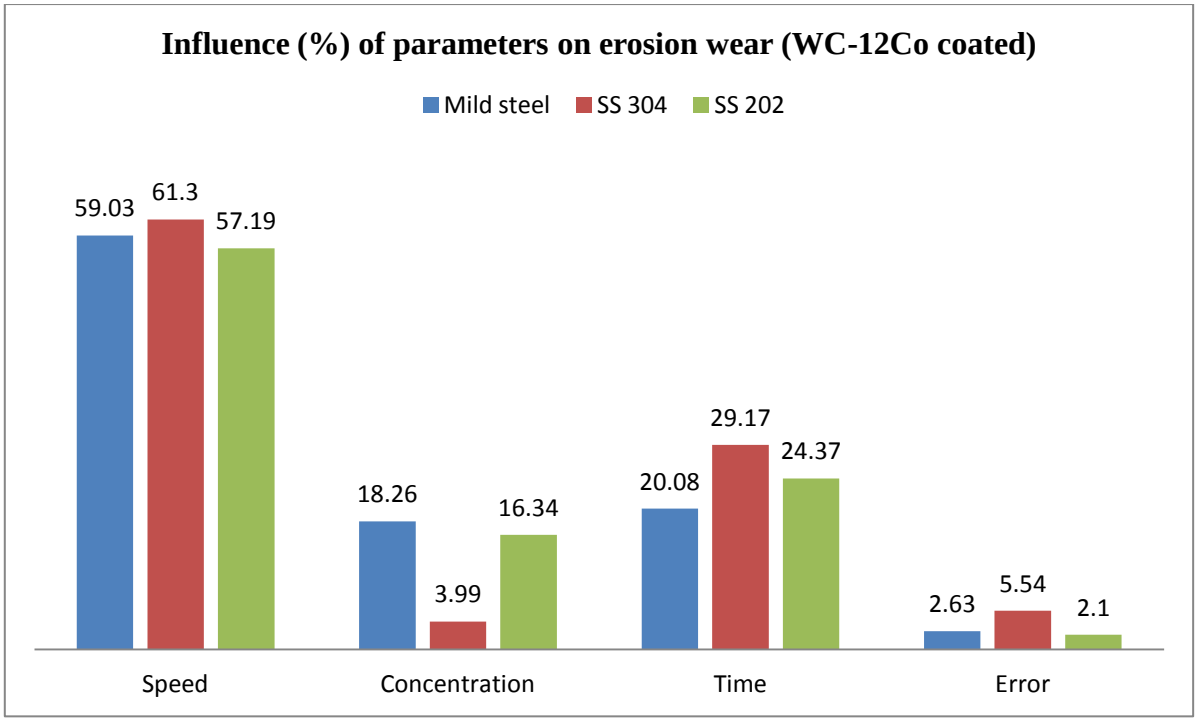

Fig. 5.11: Influence (%) of parameters on erosion wear (WC-12Co coated materials)

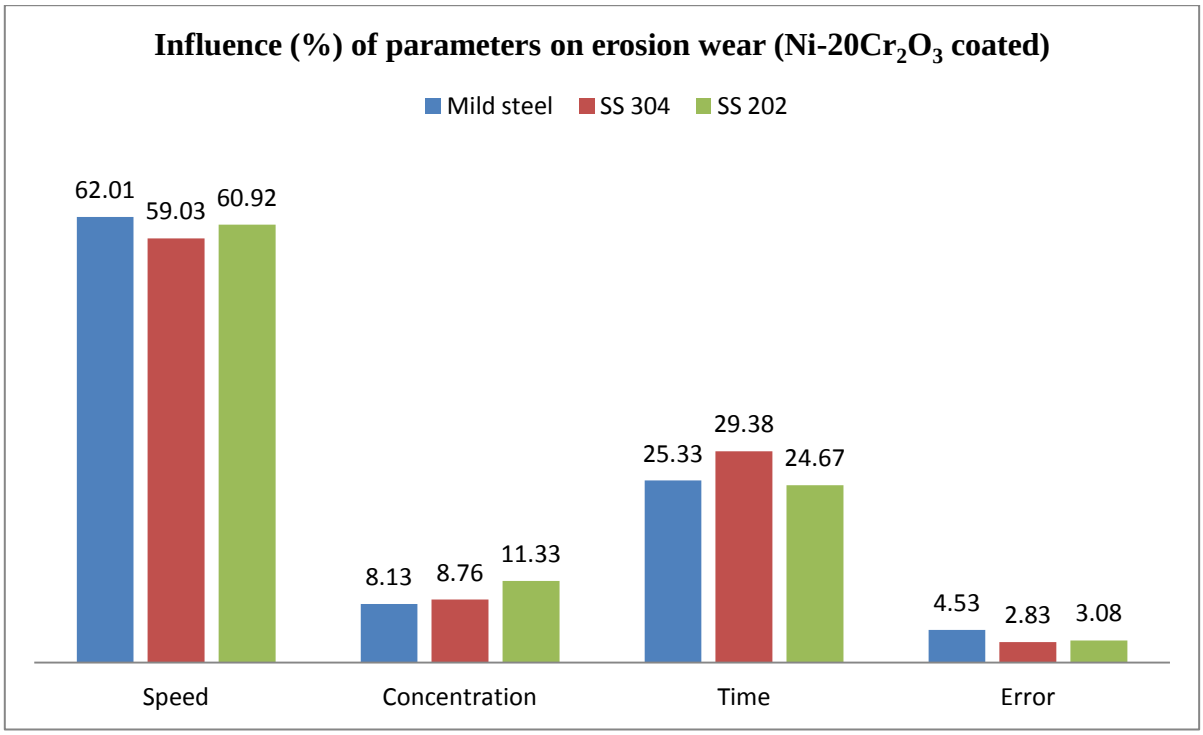

Fig. 5.12: Influence (%) of parameters on erosion wear (Ni-20Cr_2O_3 coated materials)

Effect of slurry concentration is maximum for WC-12Co coated Mild steel and Ni-20Cr_2O_3 coated SS 202 and minimum for WC-12Co coated SS 304 and Ni-20Cr_2O_3 coated Mild steel, that is coatings with minimum influence of concentration are more preferable for slurry

transportation at higher concentration because chances of erosion wear are less under minimum influence circumstances. Similarly WC-12Co coated Mild steel and Ni-20Cr_2O_3 coated SS 202 have more service life under the constraints of small speed and less slurry transportation conditions.

CHAPTER 6

CONCLUSIONS AND SCOPE FOR FUTURE WORK

6.1 CONCLUSIONS

Investigations of the parameters affecting the erosion wear of slurry pipeline materials and coatings has been carried out in the present work and weight loss result obtained are further investigated with the taguchi approach to study the percentage influence of parameters on the erosion wear. WC-12Co, Ni-20Cr_2O_3 coated and uncoated materials Mild steel, SS 304 and SS 202 are used to study erosion wear and bottom ash slurry is taken as erodent medium, slurry pot tester is used to conduct the erosion tests. Speed exponent and slurry concentration exponent that are calculated in present experimental results are also compared with past research works. High velocity oxy-fuel process is used to deposit coatings on Mild steel, SS 304 and SS 202 materials

1. SS 202 shows better erosion resistance under all the circumstances and is followed by erosion resistance of SS 304 and Mild steel.
2. Excellent improvement in hardness is reported in case of WC-12Co coated materials as compared to Ni-20Cr_2O_3 coated materials.
3. WC-12Co coating shows considerable improvement in erosion wear resistance of all the three substrate materials SS 202, SS 304 and Mild steel to 2.29 ± 0.24, 5.52 ± 0.89 and 6.74 ± 0.95 times respectively. Whereas Ni-20Cr_2O_3 coating improves erosion wear resistance of SS 202, SS 304 and Mild steel to 1.35 ± 0.12, 1.87 ± 0.20 and 3.58 ± 0.49 times respectively.
4. Brittle wear mechanism has noticed in WC-12Co coatings and ductile wear mechanism has noticed in Ni-20Cr_2O_3 coatings.
5. Speed exponent and concentration exponent values for all the materials are found in good agreement with previous research works.
6. By adapting taguchi analysis it has been seen that influence of speed is more on the erosion wear of all the materials and coatings and followed by time and concentration parameters, results are validated with respect to analysis of variance method.

6.2 SCOPE FOR FUTURE WORK

The study needs more systematic approach and attention to deal with pipeline material erosion wear problems, different type of erosion tester can be used to determine the improvement in erosion wear results. Fly ash can be mixed with bottom ash to evaluate the particle diameter exponent values. Coating parameters can be more optimized to improve the coating hardness and other coating materials can be used to improve the erosion wear resistance. Each experiment can be repeated for two or three times for getting more precise results.

REFERENCES

[1] Truscott, G. F. (1975) A Literature Survey on Wear on Pipelines. *BHRA Fluid Engineering*, TN 1295.

[2] Gupta, R.; Singh, S.N.; Sehadri, V. (1995) Prediction of Uneven Wear in a Slurry Pipeline on the Basis of Measurements in a Pot Tester. *Wear*, 184: 169-178.

[3] Schwetzke, R.; Kreye. H. (1999) Microstructure and Properties of Tungsten Carbide Coatings Sprayed with Various High-Velocity Oxygen Fuel Spray Systems. *Journal of Thermal Spray Technology*, 8(3): 433-439.

[4] Stokes, J.; Looney, L. (2004) Residual Stress in HVOF Thermally Sprayed Thick deposits. *Surface and Coatings Technology*, 177-178: 18-23.

[5] Kilu, P.; Hussainova, I.; Veinthal, R. (2005) Solid Particle Erosion of Thermal Sprayed Coatings. *Wear*, 258: 488-496.

[6] Desale, G.R.; Gandhi, B.K.; Jain, S.C. (2006) Effect of Erodent Properties on Erosion Wear of Ductile Type Materials. *Wear*, 261: 914-921.

[7] Picas, J.A.; Forn, A.; Matthaus, G. (2006) HVOF Coatings as an Alternative to Hard Chrome for Pistons and Valves. *Wear*, 261: 477-484.

[8] Sidhu, H.S.; Sidhu, B.S.; Prakash, S. (2006) Mechanical and Microstructural Properties of HVOF Sprayed WC-Co and Cr_3C_2-NiCr Coatings on the Boiler Tube Steels Using PLG as the Fuel Gas. *Journal of Materials Processing Technology*, 171: 77-82.

[9] Sidhu, H.S.; Sidhu, B.S.; Prakash, S. (2007), Solid Particle Erosion of HVOF Sprayed NiCr and Stellite-6 Coatings. *Surface and Coatings Technology*, 202: 232-238.

[10] Wang, Y.; Yang, Y.; Yan, M.F. (2007) Microstructures, Hardness, and Erosion Behavior of Thermal Sprayed and Heat Treated NiAl Coatings with Different Ceria. *Wear*, 263: 371-378.

[11] Cho, T.Y.; Yoon, J.H.; Kim, K.S.; Song, K.O.; Joo, Y.K.; Fang, W.; Zhang, S.H.; Youn, S.J.; Chun, H.G.; Hwang, S.Y. (2008) A Study on HVOF Coatings of Micron and Nano WC-Co powders. *Surface and Coatings Technology*, 202: 5556-5559.

[12] Bolleli, G.; Lusvarghi, L.; Barletta, M. (2009) HVOF-Sprayed WC-CoCr Coatings on Al Alloy: Effect of the Coating Thickness on the Tribological Properties. *Wear*, 267: 944-953.

[13] Cho, T.Y.; Yoon, J.H.; Cho, J.Y.; Joo, Y.K.; Kang, J.H.; Zhang, S.; Chun, H.G.; Hwang, S.Y.; Kwon, S.C. (2009) Surface Properties and Tensile Bond Strength of HVOF Thermal Spray Coatings of WC-Co Powder onto the Surface of 420J2 Steel and the Bond Coats of Ni, NiCr, and Ni/NiCr. *Surface and Coatings Technology*, 203: 3250-3253.

[14] Fang, W.; Cho, T.Y.; Yoon, J.H.; Song, K.O.; Hur, S.K.; Youn, S.J.; Chun, H.G. (2009) Processing Optimization, Surface Properties and Wear Behavior of HVOF Spraying WC-CrC-Ni Coating. *Journal of Materials Processing Technology*, 209: 3561-3567.

[15] Mishra, S.C.; Praharaj, S.; Satpathy, A. (2009) Evaluation of Erosion Wear of a Ceramic Coating with Taguchi Approach. *Journal of Manufacturing Engineering*, 4(2): 241-246.

[16] Shivamurthy, R.C.; Kamaraj, M.; Nagarajan, R.; Shariff, S.M.; Padmanabham, G. (2009) Slurry Erosion Characteristics and Erosive Wear Mechanisms of Co-Based and Ni-Based Coatings Formed by Laser Surface Alloying. *The Minerals, Metals and Materials Society*, 41A: 470-486.

[17] Wang, Q.; Chen, Z.H.; Ding, Z.X.; (2009) Performance of Abrasive Wear of WC-12Co Coatings Sprayed by HVOF. *Tribology International*, 42: 1046-1051.

[18] Zhang, S.H.; Cho, T.Y.; Yoon, J.H.; Li, M.X.; Shum, P.W.; Kwon, S.C. (2009) Investigation on Microstructure, Surface Properties and Anti-Wear Performance of HVOF Sprayed WC-CrC-Ni Coatings Modified by Laser Heat Treatment. *Material Science and Engineering B*, 162: 127-134.

[19] Babu, P.S.; Basu, B.; Sundararajan, G. (2010) Abrasive Wear Behavior of Detonation Sprayed WC-12Co Coatings: Influence of Decarburization and Abrasive Characteristics. *Wear*, 268: 1387-1399.

[20] Ramesh, M.R.; Prakash, S.; Nath, S.K.; Sapra, P.K.; Venkataraman, B. (2010) Solid Particle Erosion of HVOF Sprayed WC-Co/NiCrFeSiB Coatings. *Wear*, 269: 197-205.

[21] Kasem, A.A. (2011) Particle Size Effects on Slurry Erosion of 5117 Steels. *Journal of Tribology*, 133: 1-7.

[22] Srinivasulu, M.; Komaraiah, M.; Rao, C.S.K.P. (2011) Experimental Investigations on the Surface Roughness of AA6082 Flow Formed Tubes-A Taguchi Aproach. *International Conference on Emerging Trends in Mechanical Engineering*, Thapar University, Patiala, India, 24-26: 431-439.

[23] Goyal, D.K.; Singh, H.; Kumar, H.; Sahni, V. (2012) Slurry Erosion Behaviour of HVOF Sprayed WC-10Co-4Cr and Al_2O_3+13TiO_2 coatings on a Turbine Steel. *Wear*, 289: 46-57.

[24] Fly Ash Utilization (FAU) (2013), *Second Annual International Summit*, New Delhi, India.

[25] Thakur, L.; Arora, N. (2013) A Comparative Study on Slurry and Dry Erosion Behaviour of HVOF Sprayed WC-CoCr Coatings. *Wear*, 303: 405-411.

[26] Venter, A.M.; Oladijo, O.P.; Luzin, V.; Cornish, L.A.; Sacks, N. (2013) Performance Characterization of Metallic Substrates Coated by HVOF WC-Co. *Thin Solid Films*, 549: 330-339.

[27] Enayati, M.H.; Karimzadeh, F.; Jafari, M.; Markazi, A.; Tahivilian, A. (2014) Microstructural and Wear Characteristics of HVOF-Sprayed Nanocrystalline NiAl Coating. *Wear*, 309: 192-199.

[28] Goyal, D.K.; Singh, H.; Kumar, H.; Sahni, V. (2014) Erosive Wear Study of HVOF Spray Cr_3C_2-NiCr Coated CA6NM Turbine Steel. *Journal of Tribology*, 136: 1-11.

[29] Kumar, S.; Gandhi, B.K.; Mohapatra, S.K. (2014) Performance Characteristics of Centrifugal Slurry Pump with Multi-Sized Particulate Bottom and Fly Ash Mixtures. *Particulate Science and Technology*, 1-35.

[30] Murugan, K.; Ragupathy, A.; Balasubaraminian, V.; Sridhar, K. (2014) Optimizing HVOF Spray Process Parameters to Attain Minimum Porosity and Maximum Hardness in WC-10Co-4Cr Coatings. *Surface and Coatings Technology*, 247: 90-102.

[31] Oksa, M.; Auerkari, P.; Salonen, J.; Varis, T. (2014) Nickel-Based HVOF Coatings Promoting High Temperature Corrosion Resistance of Biomass-Fired Power Plant Boilers. *Fuel Processing Technology*, 125: 236-245.